ON THE TWO-DIMENSIONAL ATMOSPHERIC TURBULENCE RESPONSE OF AN AIRPLANE

By

David T. Sawdy
B.S., University of Wichita, 1960
M.S., University of Wichita, 1964

Submitted to the Engineering Mechanics Department and the Faculty of the Graduate School of the University of Kansas in partial fulfillment of the requirements for the degree of Doctor of Philosophy

ON THE TWO-DIMENSIONAL ATMOSPHERIC TURBULENCE RESPONSE OF AN AIRPLANE

by

David T. Sawdy
B.S., University of Wichita, 1960
M.S., University of Wichita, 1964

Submitted to the Engineering Mechanics Department and the Faculty of the Graduate School of the University of Kansas in partial fulfillment of the requirements for the degree of Doctor of Philosophy

Dissertation Committee:

_____
Chairman

_____

_____

TABLE OF CONTENTS

LIST OF FIGURES

FIGURE PAGE

FIGURE PAGE

ACKNOWLEDGMENTS

The author wishes to take this opportunity to express his appreciation to Professor Kenneth Lenzen and the University of Kansas for their part in making this dissertation possible. The author also wishes to express his appreciation to the National Aeronautics and Space Administration for its support of this research. Particular thanks are extended to Dr. John Duberg, Mr. I. E. Garrick, and Mr. Harry Runyan for their part in making the opportunity of conducting this project at Langley Research Center possible. The author wishes to thank Mr. Jerry Rainey and the members of the Aeroelasticity Branch for their help and Mr. Kermit Pratt for his encouragement and criticism of the investigation.

INTRODUCTION

The structural loads and accompanying stresses arising from the responses of airplanes to the velocities of the atmosphere during flight through turbulent air have been of concern throughout the history of airplanes. In fact, this was the subject of the first technical report published by the NACA in 1915. The effort required to develop gust load design methods may be appreciated from a chronological résumé presented in reference 8.

Experience has shown that the local air velocities are continuous and random in nature and definable only in a statistical sense. Consequently the responses of the airplane can only be known in a statistical sense. Of the methods of response calculations available to the designer, the spectral density approach is perhaps the best. This approach, in contrast with earlier methods, accounts for the continuous nature of turbulence, including the effects of repeated gust peaks of various intensities, sizes, and phasing. The spectral approach provides statistical descriptions of the dynamic responses from a combination of a power spectral description of the turbulent velocities and solutions of linear equations of motion of the airplane. The linear equations can be written to include elastic modes of vibration as well as the rigid-body modes of motion.

Inherent in the use of this approach of the problem are several important assumptions that must be employed. The intuitive concept that the atmosphere must be described by time and spatial averages that vary

with position and time, respectively, is amended by the assumption that it consists of "patches" of stationary (time-invariant averages) and homogeneous (spatially invariant averages) turbulence. For these patches, time and statistical averages are assumed to be equivalent, an assumption which compensates for the lack of an ergodic theorem in fluid mechanics. Also, the probability distribution of the homogeneous and stationary patches of turbulence has been shown to be nearly Gaussian which allows the spectral density function to give a complete statistical description of the random responses. Taylor's hypothesis is assumed to be valid. This hypothesis assumes that the turbulence pattern is essentially frozen until the airplane has passed through it; consequently, the time displacements are equivalent to longitudinal space displacements.

Another assumption concerns the existence and determination of a characteristic length in the atmosphere. The characteristic length of the atmosphere is assumed to be given by the scale of turbulence. This length appears as a parameter in the mathematical description of turbulence and serves as a useful indication of the influence of the turbulence environment on the response of an airplane. The scale of turbulence is a function of altitude for altitudes below 1,000 feet, and in this range there is evidence that its value is approximately equal to the altitude.

The most commonly used formulation of the spectral approach is the "one-dimensional analysis." This formulation of the problem is characterized by the assumption that the airplane responds only to variations of the gust velocity along the flight path. The spatial pattern of turbulence along the flight path is related to the response of the

airplane through the airplane's velocity and the use of Taylor's hypothesis. The response spectrum is related to the frequency response function and the gust spectrum by the classical input-output relation for a linear system responding to a random excitation. The frequency response function is the response of the airplane to a sinusoidal wave of downwash along the flight path that is constant along the span. The response spectrum provides statistical parameters for the response. These are the mean-square value (the area under the response spectrum) and the average number of mean crossings per unit time (proportional to the second moment of the area under the response spectrum). The one-dimensional gust response analysis has been and continues to be the most frequently used type of analysis. The reason for this is that it has been used with outstanding success when applied to existing airplanes operating at altitudes higher than 1,000 feet.

It is a general consensus of opinion, however, that the one-dimensional analysis may not be sufficient to analyze airplanes with large spans flying at altitudes of 1,000 feet or less. In such cases, an analysis that accounts for the spanwise variation of the gust velocities can be used. Several formulations of this type of analysis, called a "two-dimensional analysis," have been present in the technical literature for some time. Although each formulation expresses the response in the form of a spectral density function, they are considerably different with respect to the distinct elements of the response problem. These elements are:

(a) The statistical description of the atmosphere.

(b) The calculation of the aerodynamic forces associated with the turbulence field.

(c) The calculation of the frequency response functions.

(d) The mathematical form of the input-output relation used to calculate the response.

These elements are not independent; in fact, the latter three are strongly dependent upon the form of the first element. This will be shown in the following discussion of previous work on the two-dimensional gust response problem.

Liepmann in reference 28 presented one of the earliest studies of the influence of a two-dimensional turbulence field on the gust response of an airplane. The influence of the spanwise variation of the gust velocities was analyzed by describing the atmosphere by a two-dimensional gust spectrum which represents the atmosphere as a superposition of an infinite number of sinusoidal waves of shearing motion of all orientations and wavelengths. The response characteristics of the airplane are described by the two-dimensional frequency response function, which represents the response of an airplane to a downwash field described by a sinusoidal wave along the flight path and a sinusoidal wave along the span. The input-output relation for this formulation expresses the response spectrum as the integral of the product of the square of the modulus of the frequency response function and the gust spectrum where the integration is performed with respect to the spanwise frequency variable. Liepmann applied this formulation to the calculation of the mean square value of the lift on a rigid wing. The frequency response

function was computed using simple-strip analysis aerodynamic theory, and was used to investigate the limiting cases of the mean-square value of the lift for large and small values of the span which provided closed-form expressions for the integrals. For the case of a small value of the span, the expression is shown to be the same as the one-dimensional.

In references 25 and 26, Diederich presented a different formulation of the two-dimensional response problem. This formulation differs from that of Liepmann by the description of the spanwise variation of the gust velocities. The atmosphere is described by a correlated gust spectrum that analyzes the spanwise variation as a spanwise correlation of the gust velocities. The significance of this change is reflected in the calculation of the frequency response function and the input-output relation. The spanwise correlated frequency response function is the response of the airplane to a downwash distribution described by a sinusoidal wave along the flight path and a spanwise impulse function along the wing. The input-output relation relates the response spectrum to a spatial convolution of the product of the gust spectrum and the frequency response function. In reference 25 the formulation was applied to the calculation of the mean-square value of the lift. The limiting case for small values of the span is shown to give the same result as Liepmann. In reference 26, Diederich used a modified-strip analysis and reciprocal flow relations to calculate the responses of a rigid and flexible mathematical model to a two-dimensional turbulence field. Diederich presents the result that the ratio of two-dimensional to one-dimensional rigid-body acceleration mean-square value approaches unity as the ratio of the span to scale of turbulence approaches zero.

The principal feature of this formulation is that it requires the calculation of an unsteady pressure distribution on a wing of finite aspect ratio to a downwash distribution described by an impulse function. This calculation has not been done in closed form and is very difficult to perform numerically. Diederich avoids this difficulty by the incorporation of a lift distribution that must be calculated by wing reciprocal flow relations and modified-strip analysis. This difficulty of the calculation of the lift distribution places a practical limitation on the formulation, especially for the flexible modes; consequently, it is not easily applied to an analysis with many degrees of freedom.

Houbolt in reference 27 used the turbulence description of Diederich to formulate the two-dimensional problem. Otherwise, the formulation differs from Diederich in that the problem is analyzed by dividing the wing into streamwise strips and replacing the spatial convolution in the input-output relation with a double summation. This analysis was applied to the calculation of the response of a cantilevered wing to two-dimensional turbulence. The effect of a spatial tuning of the flexible modes with the lift distributions is calculated and shown to be more significant for the highest wing modes. This formulation has a severe aerodynamic limitation because a lift distribution is required that represents the response to a downwash distribution described by an impulse function along the span. This lift distribution can only be treated practically by two-dimensional unsteady aerodynamic theory, and is limited to the use of a simple-strip analysis.

Etkin in reference 31 used the formulation of Liepmann to calculate the response of a lifting surface to a two-dimensional downwash expanded in terms of a Taylor's series. This expansion enabled him to utilize the familiar stability derivatives to calculate the frequency response function which is the summation of the responses of each of the downwash terms in the series. The analysis was applied to the response of a flat plate in unsteady two-dimensional incompressible flow, and gave a good approximation of the Sear's function for values of reduced frequency less than one. This formulation has a built-in frequency limitation due to the dropping of the higher order terms of the expansion; a limitation that would be too restrictive for a large airplane with poorly damped elastic modes.

The literature survey discussed above revealed that with the exception of one method these formulations are not well suited for incorporating refined aerodynamic force calculations for flexible airplanes. The excepted method by Liepmann appeared to be suitable, but had applied only to the determination of the mean-square lift on a rigid wing. The present study explores the feasibility of extending Liepmann's formulation to the general problem of determining motion and load responses of a flexible airplane flying in a two-dimensional turbulence field.

The object of this dissertation is to develop a practical and accurate two-dimensional gust response analysis. Liepmann's formulation has several advantages over the previously mentioned formulations. First, it formulates the generalized gust forces by calculating the

response of a lifting surface to a downwash distribution described by a sinusoidal wave along the flight path and a sinusoidal wave along the span. Thus, it avoids the aerodynamic difficulties inherent in Houbolt's formulation and does not require the lift distribution associated with the reciprocal flow relations of Diederich. The major feature of the formulation is its aerodynamic versatility. The response of the lifting surface can be calculated either directly in terms of a pressure distribution by using an unsteady lifting-surface aerodynamic theory, or in terms of an unsteady lift distribution calculated by a modified-strip analysis that includes unsteady finite span induction effects. This formulation calculates the frequency response function directly and does not have an upper frequency limitation as severe as Etkin's formulation.

The relationship between the response spectrum and the product of the two-dimensional frequency response function and the two-dimensional gust spectrum is an integration with respect to the spanwise frequency variable. This form of the input-output relation provides a clear insight to the weighting influence of the gust spectrum on the response function, in a manner analogous to the one-dimensional analysis. In addition, the effect of the aspect ratio of the wing on the response spectrum is clearly shown, an effect inherently missing in the one-dimensional analysis. This formulation, however, has a limitation; viz., a truncation error in the response spectrum. This limitation exists because in the numerical evaluation of the response spectrum the integration can be performed only to a finite upper limit.

A survey of literature on the theory of turbulent fluid flow revealed that no one source provided a complete presentation of the general theory of isotropic, homogeneous turbulent flow with regard to general effects of atmospheric turbulence on the response of airplanes. Since the determination of a two-dimensional description of atmospheric turbulence was necessary for this study, those aspects of the existing information pertinent to the multidimensional description of atmospheric turbulence have been assembled and presented herein for sake of completeness in Chapter One. A brief review of the general theory of isotropic, homogeneous turbulent flow is presented and the multidimensional Von Karman and Dryden representations given. Also presented is a discussion of the assumptions necessary to use current mathematical descriptions for an input to a mathematical model representing an airplane.

Chapter Two presents the different forms of the input-output relation for the two-dimensional gust analysis used by various investigators. Herein the different mathematical formulations are compared and their relationships are discussed.

The three forms of the input-output relation are discussed with regard to their merits and disadvantages in Chapter Three. The two-dimensional formulation is presented and its principal elements are described. The principal elements are the calculation of the frequency response function, the weighting influence of the two-dimensional gust spectrum, and the effect of the truncation error on the response spectrum. The two-dimensional generalized gust forces are formulated in terms of lifting-surface aerodynamic theory and the equations of motion are developed.

Chapter Four presents an application of the two-dimensional gust response analysis to a mathematical model of an airplane in the form of a trend study. The analysis is used to predict the longitudinal motion and load responses of an airplane to a two-dimensional vertical gust velocity field. Results in the form of response spectra and statistical parameters are presented and compared with corresponding results of a one-dimensional analysis. Consideration is given to the effects of a finite aspect ratio on the variation of the statistical parameters with span to scale of turbulence ratio. Also, the effect of truncation error on the response spectra is examined.

LIST OF SYMBOLS

A_{ij}, A_i'	dimensionless coefficients (see appendix C)
AR	aspect ratio
b	span of lifting surface
B_{ij}, B_i'	dimensionless coefficients (see appendix C)
$BB_i(\Omega_2^*), BB'(\Omega_2^*)$	dimensionless coefficients (see appendix C)
$BM(k,\Omega_2,y)$	two-dimensional bending moment frequency response function at station y
$\hat{BM}(k,\Omega_2^*)$	two-dimensional normalized wing-root bending moment frequency response function
c	semichord of lifting surface
$\bar{c}$	reference semichord
$c\ell_\alpha$	section lift-curve slope
$\frac{cc\ell_\alpha}{\bar{c}C_{L_\alpha}}$	normalized steady-state lift distribution
C(k)	Theordorson function
C_{L_α}	total lift-curve slope
D_i	dimensionless coefficients (see appendix C)
E	modulus of elasticity, lb/in^2
$E[\ ]$	statistical average
$E(\ )$	energy density function
f(r)	nondimensional correlation function
g(r)	nondimensional correlation function
$G(y,\eta)$	Green's function for local lift

$h(r)$	nondimensional correlation function
$h(t)$	time system impulse response function
$h(t,y)$	time-spatial system impulse response function
$H(\omega)$	one-dimensional frequency response function
$\hat{H}(\omega,y)$	spatial correlated one-dimensional frequency response function
$H(\omega,\Omega_2)$	two-dimensional frequency response function
$I(y^*)$	bending stiffness distribution
I_R	reference bending stiffness
$J_n(k)$	integer order Bessel function of first kind
k	reduced frequency
$k(r)$	nondimensional correlation function
$K(k)$	circulation function
$\ell(y,t)$	unsteady lift distribution
$\ell^G(y,k,\Omega_2^*)$	two-dimensional unsteady lift distribution
$\ell_i^M(y,k)$	unsteady lift distribution due to the ith mode
L	scale of turbulence
$m(y)$	mass distribution
$m^*(y)$	normalized mass distribution
M_a	total airplane mass
M_R	reference mass
$M_\mu(\ )$	nth order joint characteristic function
M_{1j}	generalized mass
N_o	number of mean crossings per unit time with positive slope

$\hat{N}_o$	normalized number of mean crossings per unit time with positive slope
p	pressure
$p(t)$	response of a linear system
$p(u_1, \ldots, u_n)$	nth order joint probability density function
$\Delta p^M(x,y,\omega)$	differential pressure distribution due to ith mode
$\Delta p^G(x,y,\omega,\Omega_2)$	differential pressure distribution due to two-dimensional downwash field
$q(r)$	nondimensional correlation function
q_i	ith generalized coordinate associated with ith mode of motion or deformation
$\hat{q}_i$	ith nondimensional normalized generalized coordinate
$Q_i^G(\omega,\Omega_2)$	two-dimensional generalized gust force
$\hat{Q}_i^G(k,\Omega_2^*)$	nondimensional generalized gust force
$Q_{ij}^M(\omega)$	generalized motion force due to ith mode
$\hat{Q}_{ij}^G(k)$	nondimensional generalized motion force due to ith mode
$Q_{ij\ldots p}^{(m)}(\underline{r},t)$	m-order n-point velocity product mean value
Q_s	symmetrical aerodynamic influence matrix
r	magnitude of spatial separation vector
r_i	ith component of spatial separation vector
$\underline{r}$	spatial separation vector
$R_e\{\ \}$	designates real part of complex quantity
$R_p(\tau)$	response correlation function
$R_w(t_2+\tau-t_1, y_2-y_1)$	two-dimensional correlation function of downwash

$R_{ij}(\underline{r})$	double correlation tensor component
s	nondimensional time $\frac{t}{\frac{c}{U}}$
S	area of lifting surface
t	time
T	period of time average
$T_{ijk}(\underline{r})$	triple correlation tensor component
u	longitudinal gust velocity component
u_i	ith component of fluctuation velocity vector
$\underline{u}$	fluctuation velocity vector
U	flight path speed
v	lateral gust velocity component
w	vertical gust velocity component; downwash
w_g	magnitude of vertical gust velocity component
$W(\Omega)$	work density function
$W_{ijk}(\underline{\Omega})$	triple spectral tensor component
x	flight path coordinate
y	lateral coordinate
y*	normalized lateral coordinate
$Y_n(k)$	integer order modified Bessel function of first kind
z	vertical coordinate
$z(k,\Omega_2^*)$	two-dimensional normalized plunge displacement frequency response function
$\dot{z}(k,\Omega_2^*)$	two-dimensional normalized plunge velocity frequency response function

$\ddot{z}(k,\Omega_2^*)$	two-dimensional normalized plunge acceleration frequency response function
$\ddot{z}_s$	sharp-edge gust acceleration
α	angle of attack
γ	normalized steady-state lift curve slope distribution
Γ	gamma function
$\Gamma(r_2)$	autoconvolution function of γ
δ	impulse function
$\epsilon(k)$	truncation error
η	spanwise variable
η^*	normalized spanwise variable
λ	mass parameter
μ	inertial distribution
ν	kinematic viscosity
ξ_i	ith mode of motion or deformation
ρ	density
τ	time lag
ϕ	one-dimensional spectrum
$\phi_D(k)$	normalized one-dimensional Dryden spectrum
$\phi_{we}(\omega)$	effective one-dimensional spectrum
$\hat{\phi}$	cross-spectrum
$\hat{\phi}_{ij}(\omega,r_2)$	correlated spectrum
Φ	two-dimensional spectrum
$\Phi_D(k,\Omega_2^*)$	normalized two-dimensional Dryden spectrum
$\Phi_{ij}(\underline{\Omega})$	spectral tensor component

ω	circular frequency, rad/sec
ω_i	natural frequency of ith mode
Ω	magnitude of spatial frequency
Ω_i	ith component of spatial frequency vector
$\underline{\Omega}$	spatial frequency vector
Ω_2	lateral spatial frequency component
Ω_2^*	nondimensional lateral spatial frequency component
Ω_o	reference spatial frequency

Superscripts and Subscripts

*	normalized quantity; complex conjugate
^	nondimensional quantity
e	effective

A dot over a symbol represents differentiation with respect to time

A bar under a symbol represents a vector quantity

A bar over a symbol represents a time average

Magnitudes of quantities are denoted by the symbol $| \; |$

CHAPTER ONE

MATHEMATICAL DESCRIPTION OF ATMOSPHERIC TURBULENCE

The purpose of this investigation is to prepare an analysis which can predict the dynamic response of airplanes to atmospheric turbulence. A basic principle of system analysis states that the response of a linear system can be determined if the input and input-output relation are known. Clearly, an adequate mathematical model of the earth's atmosphere is required.

Experience has shown that the motion of the atmosphere must be mathematically described as a random process. A theory for the specific case of homogeneous and isotropic turbulent flow has been developed (refs. 1 through 6 and 9 through 18). This theory has produced several mathematical representations of turbulence, two of which have been successfully used to describe atmospheric turbulence. A detailed presentation of the derivation of these two representations is given in appendix A.

The use of the two mathematical representations for describing the atmosphere's motion requires consideration of the conditions under which these representations are to be used. In these representations the atmosphere is described as a continuous, homogeneous, stationary and isotropic random process. These conditions are satisfied by the atmosphere in a localized area for short periods of time. In addition, for these representations to be used for the input to an airplane, Taylor's hypothesis must be valid. This enables the flight path displacement coordinate

to be related to the time coordinate through the airplane's velocity. For conventional airplanes under normal circumstances, Taylor's hypothesis has been shown to be valid.

1.1 General Formulation

The atmosphere will be assumed to be a continuous medium. This assumption is reasonable because of the role that viscosity plays in damping small scale, high frequency motion of a fluid. It also allows that the motion and physical properties of the atmosphere are subject to the governing laws of a continuous fluid.

The motion of the atmosphere is given by the instantaneous velocity which is assumed to be the sum of a steady velocity and a zero-mean turbulent fluctuation velocity, denoted $\underline{u}(\underline{x},t)$. The turbulent fluctuation velocity is mathematically described by a random vector field which is a function of time and spatial coordinates. The magnitude of the components of $\underline{u}(\underline{x},t)$; u, v, w are usually rather small, at least small compared to the speed of sound, which allows the incompressible form of the continuity and Navier-Stokes equations to be used.

$$\nabla \cdot \underline{u} = 0 \tag{1}$$

$$\frac{\partial \underline{u}}{\partial t} + \underline{u} \cdot \nabla \underline{u} = -\frac{1}{\rho} \nabla p + \nu \nabla^2 \underline{u} \tag{2}$$

The mathematical description of atmospheric turbulence is provided by the solutions of equations (1) and (2) which satisfy prescribed initial and boundary conditions. The boundary conditions are specified by the statistical properties of the motion with respect to position,

while the initial conditions are specified by the statistical properties with respect to time. For the limited extent of the atmosphere which may be assumed to be homogeneous, the boundary conditions specify that the motion be statistically uniform. The initial conditions specify that at some instant $\underline{u}(\underline{x},t)$ is a random function of position which must conform to given probability laws. Then if $\underline{u}(\underline{x},t)$ is specified statistically at one instant, through equations (1) and (2) which determine the way in which any particular velocity distribution changes with time, the random velocity field is statistically determinate (ref. 6).

The statistical uniformity specified by the boundary conditions implies that the joint-probability distribution of the values of $\underline{u}(\underline{x},t)$ for any set of points in space-time, $\underline{u}(\underline{x}_1 + \underline{y}, t_1 + \tau)$, $\underline{u}(\underline{x}_2 + \underline{y}, t_2 + \tau)$, . . ., $\underline{u}(\underline{x}_n + \underline{y}, t_n + \tau)$ is independent of the space vector y and time difference τ. Turbulent flow which is assumed to have this joint-probability distribution is called homogeneous and stationary.

The validity of this assumption for atmospheric turbulence depends on the extent of the atmosphere that is being considered. Intuitively, the consideration of the effects of climate, weather and terrain on the atmosphere's motion may be used to place a quantitative limit on the extent of the atmosphere that should be considered homogeneous. The atmosphere as a whole must be considered to be nonhomogeneous. However, that there do exist small "patches" of the atmosphere which may be considered homogeneous has been shown in reference 8. The sizes of the

patches have no defined limits, they may vary from many miles in clear air to several thousand feet in thunderstorms.

The description of atmospheric turbulence is given by the statistical description of the turbulent fluctuation velocity. It is a premise of probability theory that a random function such as $\underline{u}(\underline{x},t)$ is determined statistically by the complete set of joint-probability distributions of the values of $\underline{u}(\underline{x},t)$ at any n values of $\underline{x}$ and t,n having any integral value. These joint-probability density functions can be expressed in terms of a nth-order joint-characteristic function $M_u(i\underline{\alpha}_1, \ldots, i\underline{\alpha}_n)$ by a multiple n-dimensional Fourier transform.

$$p(\underline{u}_1,\ldots,\underline{u}_n) = \left(\frac{1}{2\pi}\right)^n \int_{-\infty}^{\infty} \cdots \int_{-\infty}^{\infty} M_u(i\underline{\alpha}_1,\ldots,i\underline{\alpha}_n) \; e^{-i(\underline{\alpha}_1 \cdot \underline{u}_1 + \ldots + \underline{\alpha}_n \cdot \underline{u}_n)} d\underline{\alpha}_1 \ldots d\underline{\alpha}_n \qquad (3)$$

The characteristic function is defined as the statistical average of $\exp(i\underline{\alpha}_1 \cdot \underline{u}_1 + \ldots + i\underline{\alpha}_n \cdot \underline{u}_n)$, reference 7. A series expansion of the joint characteristic function in terms of the joint-moments may be obtained through the use of power-series expansions of the exponentials in the integral expression, equation (3). Interchanging orders of integration and summation, the mean-value velocity products are defined as the statistical average of the joint-moments. The joint-characteristic function can be expressed in terms of the mean-value velocity products

$$M_u(i\underline{\alpha}_1,\ldots,i\underline{\alpha}_n) = \prod_{j=1}^{n} \left[\sum_{m=0}^{\infty} \frac{(i)^m}{m!} E\left[(\underline{\alpha}_j \cdot \underline{u}_j)^m\right] \right]$$

Therefore, the joint-probability density functions are related to the complete set of mean-value velocity products provided the inverse Fourier transform of equation (3) exists. The set of mean-value velocity products consists of components which are the statistical average of the product of m components of the velocities at n different points.

$$Q^{(m)}_{ij\ldots p}(\underline{r},t) = E\left[u_i(\underline{x}_1,t_1)u_j(\underline{x}_2,t_2)\ldots u_p(\underline{x}_m,t_m)\right]$$

The configuration formed by those n of the points $\underline{x}_1, \underline{x}_2, \ldots, \underline{x}_m$ that are different is specified by the $3(n-1)$ dimensional vector $\underline{r}$. Since each of the m velocities transform under change of coordinate system like a first order tensor and since this property is retained after the linear operation of taking a statistical average has been made, the 3^m scalar components, $Q^{(m)}_{ij\ldots p}(\underline{r},t)$ form an m-order Cartesian tensor.

It has been shown by using the governing equations of motion that $Q^{(m)}_{ij\ldots p}(\underline{r},t)$ for the value of $n = 2$ is sufficient to describe homogeneous and isotropic turbulence, reference 6. This case is for velocity components taken at two points and has the name correlation tensor. Only two correlation tensors are shown to be important, these are the double correlation tensor, $m = 2$ whose components are

$$R_{ij}(\underline{r},t_o) = Q^{(2)}_{ij}(\underline{r},t_o) = E\left[u_i(\underline{x}_1,t_o)u_j(\underline{x}_2,t_o)\right] \tag{4}$$

and the triple correlation tensor, $m = 3$ whose components are

$$T_{ijk}(\underline{r},t_o) \equiv Q^{(3)}_{ijk}(\underline{r},t_o) = E\left[u_i(\underline{x}_1,t_o)u_j(\underline{x}_1,t_o)u_k(\underline{x}_2,t_o)\right] \tag{5}$$

The time t_o appears in equations (4) and (5) to establish that the statistical average is taken at a constant time, t_o. Thus, the symbolization of time will not appear in any of the following expressions for the components of the correlation tensors.

The statistical description of atmospheric turbulence is also given by a mathematical expression called the spectral tensor, whose components are related to the components of the correlation tensor through a Fourier transform pair.

$$\Phi_{ij}(\underline{\Omega}) = \frac{1}{\pi^3} \int_{-\infty}^{\infty} R_{ij}(\underline{r}) e^{-i(\underline{\Omega} \cdot \underline{r})} d\underline{r} \tag{6}$$

$$W_{ijk}(\underline{\Omega}) = \frac{1}{\pi^3} \int_{-\infty}^{\infty} T_{ijk}(\underline{r}) e^{-i(\underline{\Omega} \cdot \underline{r})} d\underline{r} \tag{7}$$

The vector $\underline{\Omega}$ is called the wave number vector and defines the location of a point in wave number space which is related to the correlation vector $\underline{r}$ through the above transform.

The condition for the existences of the spectral tensor is

$$\int_{-\infty}^{\infty} R_{ij}(\underline{r}) d\underline{r} < \infty$$

$$\int_{-\infty}^{\infty} T_{ijk}(\underline{r}) d\underline{r} < \infty$$

Batchelor in reference 9 has shown that the integrals do exist when the velocity components are chosen such that their mean is zero. J. Kampe de Feriet in reference 17 has presented the properties of the spectral tensor components in equation (10). Some of these properties are:

a) $\Phi_{ij}(\underline{\Omega})$ is a continuous and complex function of $\underline{\Omega}$.

b) $\Phi_{ij}(\underline{\Omega})$ has Hermitian symmetry.

c) The diagonal components $\Phi_{ii}(\underline{\Omega})$ are real, positive and bounded functions of $\underline{\Omega}$.

1.2 Requirements for Airplane Response Calculations

The mathematical model of turbulence is sufficiently described by the correlation tensors. Unfortunately, for homogeneous turbulence this description has little value because of the complex structure of the correlation tensor. This complexity may be appreciated by considering the expression for the components of the double correlation tensor, which contains 31 terms (ref. 6, p. 44). The complexity of the tensor correlations may be lessened by assuming that the turbulent velocity field has some statistical symmetry. The assumption of isotropic symmetry provides the simplest expressions for the correlation tensor. Isotropy requires that the statistical description of $\underline{u}(\underline{x},t)$ be invariant under rotations and reflections of the reference coordinate system. A less restrictive assumption is that the turbulence is axisymmetric. The statistical description of axisymmetric turbulence is invariant for rotations about a given vertical vector and for reflections of the configuration of the vector argument in any point.

Measurements of atmospheric turbulence indicate that its statistical properties are essentially invariant in all directions in a given horizontal plane, but do vary with altitude, reference 8. These measurements are the basis for assuming that in general the atmosphere may be considered to have axisymmetric statistical properties, which implies that an airplane in level flight would experience the same turbulence environment regardless of heading. Furthermore, these measurements are the basis for justifying the assumption that the turbulence encountered by the airplane in a horizontal plane at a given altitude has isotropic statistical properties.

Being able to justify the use of isotropic symmetry in a horizontal plane is very important because the present descriptions of turbulence are limited to isotropic symmetry. Isotropic theory has provided mathematical functions for the components of the correlation tensors which are the solutions of the equations of motion given by equations (1) and (2). This theory is the result of extensive research on the description of isotropic turbulence in fluid flow, references 1 through 6 and 9 through 18. A detailed discussion of the theory of isotropic turbulence and the resulting mathematical representations are presented in Appendix A. Having justified the use of isotropic symmetry to describe atmospheric turbulence in a horizontal plane, attention is now turned to the justification of using it to describe atmospheric turbulence as an input to an airplane response analysis.

In general, turbulence velocities are space and time dependent. For purposes of airplane response, the variation is assumed to be space

dependent, and invariant with the time of traverse by an airplane. This model is a result of Taylor's hypothesis. Taylor in reference 1 introduced the assumption that if the velocity of the airstream is very much greater than the turbulent velocity, the spatial pattern of turbulent motion is carried past a fixed point by the mean wind speed without any essential change. Lin in reference 16 has investigated this hypothesis and found that for wind tunnel turbulence the criteria for its validity is

$$\frac{\overline{u_1^2}}{U^2} << 1 \tag{8}$$

Applying this to the case of the airplane flying through the atmosphere results in a requirement that the speed of the airplane must be much greater than the root-mean-square of the turbulent velocity. This insures that the gust pattern of the atmosphere will remain essentially the same, or "frozen" until the airplane has traversed the given body of air. For the flight conditions of the airplanes considered in this investigation, Taylor's hypothesis will be assumed to be valid.

Taylor's hypothesis provides an equivalence of space and time averages through the speed of the airplane in the direction of flight. However, the correlation tensors are described in terms of statistical averages and their relations to time or spatial averages must be considered, references 17 and 18. From a statistical viewpoint, a statistical average, for example, equation (4), is the only mathematically rigorous average that should be used in the formulation of the theory of isotropic turbulent flow. The statistical average is taken over an

ensemble of sample of turbulent velocity functions. An example of this average is given by the double correlation tensor.

$$R_{ij}(\underline{r},t_o) = \iint_{-\infty}^{\infty} u_i u_j p(u_i,u_j)du_i du_j \tag{9}$$

Unfortunately, statistical averages cannot be measured; instead time or spatial averages must be used. A consequence of Taylor's hypothesis is that the turbulent velocities are independent of time and that a spatial average must be used to formulate the gust response problem. The spatial average in terms of the double correlation tensor is

$$R_{ij}(\underline{r},t_o) = \lim_{V_B \to \infty} \frac{1}{V_B} \int_{V_B} u_i(\underline{x},t_o)u_j(\underline{x} + \underline{r},t_o)d\underline{x} \tag{10}$$

For the spatial displacement along the flight path, the double correlation tensor may be formulated by a time average of the turbulent velocities.

$$R_{ij}(\tau) = \lim_{T \to \infty} \frac{1}{2T} \int_{-T}^{T} u_i(t)u_j(t + \tau)dt \tag{11}$$

The average is performed with respect to a time that is related to the spatial displacement through airplane's velocity.

Some relation between the three types of averages is needed to establish a completely rational theory of turbulence. In classical mechanics this relation is provided by an ergodic theorem which states the equivalence of all three averages. Unfortunately in fluid mechanics, no ergodic theorem has yet been provem. However, it has been assumed in

past work and in this investigation that all three types of averages, and consequently the double correlation tensors given by equations (9), (10), and (11) are equivalent.

The last assumption concerned with the justification of using isotropic theory to describe atmospheric turbulence is that of dimensionality. The concept of dimensionality is concerned with the necessity of accounting for each gust velocity component's dependence on each spatial coordinate. A measure of the dependence of a gust velocity component on a spatial coordinate is given by comparing the characteristic length of the airplane with the characteristic length of turbulence.

The characteristic length of atmosphere turbulence is given by the scale of turbulence. This length was introduced by Taylor in reference 1 and is used as a parameter in the mathematical descriptions of atmospheric turbulence. Its value is a function of altitude for the range of altitude below 1,000 feet for which there is evidence that its value is approximately equal to the altitude. The scale of turbulence is physically interpreted by Houbolt in reference 8, to be a rough measure of the largest distance that two points in a turbulent flow can be separated before the correlation between gust velocities becomes zero. It is a useful measure of the development of the inertial transfer of energy of turbulent flow (see Appendix A).

When a characteristic length of the airplane is small compared to the scale of turbulence, the gust velocities are nearly invariant with

respect to the spatial coordinate considered. This is shown by examining the influence of the vertical variation of the gust velocities on the response of an airplane. The conventional airplane is usually small in the vertical direction and for this case the correlation of the gust velocities over this direction is nearly unity. Thus the airplane is insensitive to changes of $\underline{u}(\underline{x},t)$ in the vertical direction.

The influence of the spanwise variation of the gust velocities on the gust response of an airplane is measured by comparing the span with the scale of turbulence. When the span is large the effect of the spanwise variation of the gust velocities can be significant. When the span is small, the effect of the spanwise variation of the gust velocities is small.

For the case of an airplane that is small in the vertical direction and has a large span, the turbulence description is two-dimensional, that is, it varies only in the horizontal plane of flight. For an airplane that is small in the vertical direction and has a small span, the turbulence description is usually considered to be one-dimensional, that is, it varies only along the flight path.

1.3 Mathematical Representations

The most commonly used expressions for the representation of atmospheric turbulence are the Dryden and Von Karman spectral density functions which are named after their developers. A detailed derivation of these spectra in multidimensional form and their corresponding correlation functions are presented in Appendix A. The one- and two-dimensional

spectra for a vertical gust velocity component are used in the response calculations in this investigation and are presented here

DRYDEN

$$\Phi_{33}(\Omega_1) = \frac{L}{\pi}\overline{w^2}\,\frac{1 + 3(L\Omega_1)^2}{\left[1 + (L\Omega_1)^2\right]^2} \tag{12}$$

$$\Phi_{33}(\Omega_1,\Omega_2) = \frac{3L^2\overline{w^2}}{\pi}\,\frac{(L\Omega_1)^2 + (L\Omega_2)^2}{\left[1 + (L\Omega_1)^2 + (L\Omega_2)^2\right]^{5/2}} \tag{13}$$

VON KARMAN

$$\Phi_{33}(\Omega_1) = \frac{L\overline{w^2}}{\pi}\,\frac{1 + \frac{8}{3}\left(\frac{\Omega_1}{\Omega_o}\right)^2}{\left[1 + \left(\frac{\Omega_1}{\Omega_o}\right)^2\right]^{11/6}} \tag{14}$$

$$\Phi_{33}(\Omega_1,\Omega_2) = \frac{16\overline{w^2}}{9\Omega_o^2\pi}\,\frac{\left(\frac{\Omega_1}{\Omega_o}\right)^2 + \left(\frac{\Omega_2}{\Omega_o}\right)^2}{\left[1 + \left(\frac{\Omega_1}{\Omega_o}\right)^2 + \left(\frac{\Omega_2}{\Omega_o}\right)^2\right]^{7/3}} \tag{15}$$

The arguments Ω_1 and Ω_2 of the spectra denote components of the wave number space while the scale of turbulence L, reference wave number Ω_o, (see Appendix A), and the mean square value of the vertical gust velocity

$\overline{w^2}$ are mathematical parameters that must be determined. A detailed discussion of the experimental determination of L and $\overline{w^2}$ is presented in reference 8.

CHAPTER TWO

FORMULATION OF THE INPUT-OUTPUT RELATION

The formulation of a gust response analysis requires not only the mathematical description of the two physical quantities involved, the dynamic characteristics of the airplane and the turbulence of the atmosphere, but also the mathematical relationship between them. This mathematical relationship is called the input-output relation. The mathematical form of the input-output relation depends upon the formulation of the analysis and the multidimensional form of the turbulence description. For the two-dimensional gust analysis, four forms of the input-output relation are developed in Appendix B. These forms are discussed with respect to their mathematical structure and the efforts of previous investigators to analyze two-dimensional gust response of airplanes.

The formulation of the gust response analysis governs the complexity of the mathematical model of an airplane flying through a turbulence field. The most general case of formulation is the three-dimensional which requires that the airplane be described as a system which is sensitive to changes of gust velocity in all three coordinate directions. While this formulation is conceptually more desirable than either the one- or two-dimensional cases, in practice it does not appear to be necessary and its use involves needless complexity.

The complexity of the model may be substantially reduced by reducing the dimensionality of the formulation. This is done by considering the airplane to be sensitive to changes in the gust velocity along the flight path only. The airplane may be regarded to be a lifting point or

line concurrent with the line of flight. The validity of this one-dimensional formulation is dependent upon the comparison of the span of the airplane with the scale of turbulence. The one-dimensional gust analysis has been developed and extensively used. It will be used in Appendix B to provide the basis for the development of the two-dimensional formulation and it also provides a reference for comparison with the two-dimensional analysis.

The mathematical model of an airplane flying through the atmosphere can be made more realistic by allowing the airplane to respond only to variations of the gust velocity in the plane of its equilibrium position. This equilibrium position is specified to be the x-y plane with respect to a rectangular x, y, z coordinate system chosen such that the mean values of the respective gust velocity components, u, v, w are zero. This model is visualized to be an airplane represented as an unrestrained elastic planar lifting surface flying with the steady velocity U along the negative x axis, and through a continuously varying two-dimensional gust field.

2.1 Two Dimensional Correlation Relation

The mathematical form of the description of atmospheric turbulence governs the form of the input-output relation. One description of isotropic turbulence is given by the correlation function which through the input-output relation expresses the response in the form given by equation (B12):

$$R_p(\tau) = \int_{-b/2}^{b/2} \int_{-\infty}^{\infty} h(t_1,y_1)h(t_2,y_2)R_w(t_2 + \tau - t_1, y_2 - y_1)dt_1dt_2dy_1dy_2 \tag{16}$$

The dynamic characteristics of the airplane are described by the impulse

response function h(t,y), which is the response to a downwash represented by a unit time-spatial impulse

$$w(x,y,t) = \delta\left(t - \frac{x}{U}\right)\delta(y - y_1) \tag{17}$$

The impulse response function h(t,y) is an aerodynamic influence function which relates the desired response, e.g. lift or stress, to the downwash by relating the pressure at one point y_1 on the wing to the past history of the downwash intensity at another point on the wing y_2. For Gaussian turbulence, the spectral density function of the response is needed to obtain the necessary statistical parameters of the response. Although this spectrum could be obtained by taking a Fourier transform of $R_p(\tau)$ it can be calculated directly by using the proper form of input-output relation.

2.2 Cross-Spectrum Relation

The spectral density function of the response is given by two different forms of the input-output relation equations (B14) and (B19). One of these describes the input in terms of the spatial cross-spectral density function $\hat{\phi}_w(\omega,r_2)$ which is related to the correlated spectral density function for vertical gust velocity by equation (B16). This relation is

$$\phi_p(\omega) = \int_{-b/2}^{b/2}\int_{-b/2}^{b/2} \hat{H}(\omega,y_1)\hat{H}^*(\omega,y_2)\hat{\phi}_w(\omega,r_2)dy_1dy_2 \tag{18}$$

The dynamic characteristics of the airplane are given by the frequency response function $\hat{H}(\omega,y)$ which is the response to a downwash represented by a sinusoidal wave of frequency ω and a spatial impulse function.

$$w(x,y,t) = e^{i\omega(t-x/U)}\delta(y - y_1) \tag{19}$$

The frequency response function $\hat{H}(\omega,y)$ is an influence function which relates the desired response to the downwash by relating the pressure at any point y on the wing due to a traveling wave of downwash of length $2\pi U/\omega$ at another point on the wing y_1. Diederich in reference 25 discussed the calculation of $\hat{H}(\omega,y)$. He considered two separate cases, one for the total loads of an airplane, the other for local loads and their distribution.

Diederich first discussed the case for total loads, in particular the total lift and rolling moment. For these loads the influence function was identified with a specific lift distribution on the wing in reverse flow by using the reciprocity theorems of linearized lifting-surface theory. Using this theory and the assumption that the lift distribution of an oscillating wing is essentially independent of frequency, Diederich wrote the influence function for total loads in the form

$$\hat{H}(\omega,y) = H(\omega)\gamma(y) \tag{20}$$

The function $H(\omega)$ is the one-dimensional frequency response function and was calculated from modified strip analysis aerodynamic theory. The function $\gamma(y)$ is the steady-state lift distribution for a uniform downwash distribution. The use of equation (20) enables the input-output relation given by equation (18) to be written

$$\phi_p(\omega) = |H(\omega)|^2 \phi_{we}(\omega) \tag{21}$$

The spectral density function $\phi_{we}(\omega)$ is called an averaged spectrum. It is averaged in the sense that the cross-spectrum of the downwash is integrated with respect to the steady state lift distribution $\gamma(y)$

$$\phi_{we}(\omega) = \frac{1}{b} \int_0^b \Gamma(r_2)\hat{\phi}_w(\omega,r_2)dr_2 \tag{22}$$

through the function $\Gamma(r_2)$ which is the autoconvolution of $\gamma(y)$

$$\Gamma(r_2) = \frac{2}{b} \int_{-b/2}^{b/2 - r_2} \gamma(y)\gamma(y + r_2)dy$$

The expressions for the total loads given by equations (21) and (22) are used in reference 26 to calculate the effect of spanwise variation of the vertical gust velocity on the vertical acceleration and rolling acceleration of an airplane. It is shown that the mean-square value of the vertical acceleration response to the averaged spectrum is substantially reduced for high values of b/L and aspect ratio. The mean-square value of the rolling acceleration response to a vertical gust velocity is shown to become significant for moderate values of b/L.

For the local lift of the wing the influence function $\hat{H}(\omega,y)$ is difficult to analyze. This function defines the contribution of one station on the wing to the lift at another station and thus represents a Green's function for the unsteady spanwise lift distribution which can not be identified with an easily calculated lift distribution on the wing in reverse flow. Diederich in reference 25 presents a method to calculate the local response influence functions. This method is a generalization of a method used in steady flow and is also based on the separation of the unsteady and spatial parts of the function. The local lift is

$$\ell(y,t) = \frac{1}{b} \int_{-\infty}^{\infty} h(t_1)dt_1 \frac{1}{b} \int_{-b/2}^{b/2} G(y,\eta)w(t - t_1,\eta)d\eta \qquad (23)$$

This function is used to determine the required influence functions for the calculations of the spectral density function of the response. Diederich used modified-strip-analysis aerodynamic theory for the calculation of $H(\omega)$, the Fourier transform of $h(t)$. The function $G(y,\eta)$ is the Green's function that relates the local lift to the local downwash distribution.

In reference 26, Diederich assumed the local lift given by equation (23) can be calculated by summing the contributions to the lift from each natural mode. This modal approach enabled the influence function to be written

$$\hat{H}(\omega,y) = \sum_{i=1}^{N} H_i(\omega)\gamma_i(y) \qquad (24)$$

and the input-output relation becomes

$$\phi_p(\omega) = \sum_{i=1}^{N} \sum_{j=1}^{N} R_e\left\{H_i(\omega)H_j^*(\omega)\right\} \phi_{we_{ij}}(\omega) \qquad (25)$$

The averaged spectrum is given in terms of the spatial cross spectrum

$$\phi_{we_{ij}}(\omega) = \frac{1}{b} \int_0^b \Gamma_{ij}(r_2)\hat{\phi}_w(\omega,r_2)dr_2$$

and the function $\Gamma_{ij}(r_2)$ which is the autoconvolution of $\gamma_i(y)$

$$\Gamma_{ij}(r_2) = \frac{2}{b} \int_{-b/2}^{b/2 - r_2} \gamma_i(y)\gamma_j(y + r_2)dy$$

With these expressions Diederich shows that the mean-square values of the root bending moment of a rigid and flexible wing on an airplane free to move vertically vary from the mean square values calculated from a one-dimensional analysis.

Houbolt in reference 27 has presented an alternate method of finding the spectral density function of the response. He used the concept of equation (B6) which describes the spectral density function of the response in terms of the spectral density function $\Phi_{w_{nm}}(\omega)$

$$\Phi_p(\omega) = \sum_{n=1}^{N} \sum_{m=1}^{N} H_n(\omega) H_m^*(\omega) \Phi_{w_{nm}}(\omega) \tag{26}$$

This function is defined by equation (B7) and is related to the isotropic correlation spectral density function by equation (B9). Using the axis-symmetric property of the input spectrum given by equation (B10), the response is

$$\Phi_p(\omega) = \Phi_{w_{11}}(\omega) \left[\sum_{n=1}^{N} H_n(\omega) H_n^*(\omega) \right] + 2\Phi_{w_{12}}(\omega) R_e \left[\sum_{n=1}^{N-1} H_n(\omega) H_{n+1}^*(\omega) \right] \tag{27}$$

$$+ \cdots + 2\Phi_{w_{1N}}(\omega) R_e \left[H_n(\omega) H_N^*(\omega) \right]$$

The frequency response function $H_n(\omega)$ is the response to a downwash which is a sinusoidal wave of frequency ω and is constant over the spanwise element.

$$w_n(x,t) = e^{i\omega(t-x/U)} \tag{28}$$

The function $H_n(\omega)$ is the aerodynamic influence function that relates the lift at one designated station to the downwash at another station interval n. Houbolt used strip analysis aerodynamic theory to analyze the response of a cantilever beam to a random input. His results show the high occurrence of a spatial tuning of the deformation modes with the lift distributions, which results in the higher modes being excited more than the lower modes.

2.3 Two-Dimensional Spectrum Relation

The second form of the input-output relation which describes the response in terms of a spectral density function is

$$\phi_p(\omega) = \int_0^\infty |H(\omega,\Omega_2)|^2 \Phi_w(\omega,\Omega_2) d\Omega_2 \tag{29}$$

This expression relates the response to the two-dimensional spectral density function which is related to the corresponding function of isotropic turbulence for vertical gusts by equation (B21). The dynamic response characteristics of the airplane are given by the two-dimensional frequency response function $H(\omega,\Omega_2)$ which is the response to a downwash field represented by two sinusoidal waves

$$w(x,y,t) = e^{i\omega(t-x/U)} e^{i\Omega_2 y} \tag{30}$$

The two-dimensional response function $H(\omega,\Omega_2)$ is an influence function which relates the response to the downwash by relating the pressure to a sinusoidal wave along the flight path of wave length $2\pi U/\omega$ and to a wave in the lateral direction of wave length $2\pi/\Omega_2$.

This form of the input-output relation has been used by Etkin in references 31 and 32 to formulate the dynamic response of an airplane to

turbulence. Etkin approximated the downwash field by a two-dimensional Taylor's series expansion about the airplane center of gravity. This expansion enables the downwash field to be represented by the superposition of several relatively simple spatial distributions, each of which varies periodically. These distributions are called equivalent gust mode shapes which provide the boundary conditions for determining the aerodynamic response function. Thus $H(\Omega_1, \Omega_2)$ is found to be the summation of the responses to the equivalent gust modes. The expansion of the frequency response function is placed in the input-output relation and the spatial frequency component is integrated over finite limits of Ω_2. The total mean square value of the response is calculated by summing the mean-square values for each term of the expansion. Etkin applied this theory to the normal force and moment response of a flat plate with unsteady two-dimensional aerodynamic theory. With this procedure he obtained the Sear's function for both the moment and normal force for values of reduced frequency up to 1.0.

CHAPTER THREE

FORMULATION OF THE TWO-DIMENSIONAL GUST RESPONSE ANALYSIS

The formulation of the two-dimensional gust response analysis has been presented in the form of three different input-output relations. Although the mathematical structure of each relation is different, all three of them express the statistical properties of the response in terms of the input and the dynamic characteristics of the airplane. Having described the motion of atmospheric turbulence, the use of one of these relations requires only the calculation of the dynamic characteristics of the airplane.

3.1 Discussion of Previous Work on the Formulation of the Two-Dimensional Gust Response Problem

The first form of input-output relation given by equation (16) has little practical value, because the influence function $h(t,y)$ is difficult to calculate. This difficulty exists because presently used methods of obtaining pressure distributions on the finite span of a wing in unsteady flow usually require numerical methods which do not lend themselves to the analysis of downwash distributions represented by impulse functions. This form has the additional disadvantage of relating the influence function to the input spectrum through a time and spatial convolution. Furthermore, the description of the response is a correlation function which in itself does not easily permit the calculation of all the required statistical parameters of the response. For these reasons, this form of the input-output relation is useful for conceptual purposes only.

Since for a Gaussian process the spectrum of the response does permit the calculation of all the required statistical parameters, obtaining it directly would be a better method. The spectrum of the response can be calculated from either one of the two forms of the input-output relation. One of these forms is given by equation (18), a form which expresses the dynamic characteristics of the airplane in terms of the influence function $\hat{H}(\omega,y)$. This function is also difficult to calculate because the downwash distribution in the lateral coordinate is represented by an impulse function. Another undesirable feature is the spatial convolution which must be performed to calculate the spectrum of the response.

Diederich's formulation of the problem in terms of the influence function $\hat{H}(\omega,y)$ is given by equation (21). Evidence that the spatial and frequency parts may be separated is indicated by Pratt in reference 35 for rigid body motion. He shows that for the rigid-body plunge mode, the spanwise lift distributions are essentially independent of the frequency of oscillation. This is shown to be true for swept and straight wings in compressible flow. The steady-state lift distributions are calculated for rigid-body modes by using the reciprocity theorems of lifting-surface theory.

The formulation expressed by equation (21) was used by Coleman in reference 34 to correct flight test data for the effects of spanwise variations in the vertical gust velocity. The experimental normal acceleration frequency response functions were calculated by two different methods. When the correction was applied to these response functions they showed a better agreement over a frequency range that extended from the short period frequency up to the first elastic mode.

For the inclusion of elastic modes in the analysis, Diederich's formulation becomes complex. In general, the lift distributions are difficult to calculate. They are not easily identified with corresponding reverse flow conditions and have to be calculated directly. The modal analysis given by equation (25) would be difficult to incorporate for an analysis with many degrees of freedom.

For the large flexible airplane, Diederich assumes that the modal approach is an inadequate formulation of the response analysis. He develops an analysis which is based on the use of a local lift distribution that is used to form an influence function which is needed to calculate the motion and load responses. Since neither this formulation nor the modal approach have been applied to an airplane for which experimental response data is available, the validity of this assumption is not known.

Houbolt in reference 27 formulates the problem by replacing the spatial convolution by a double summation. His formulation requires the generalized coordinates to be calculated for N number of intervals taken on the lifting surfaces. The lift distributions required for the calculation of $H_n(\omega)$ are difficult to obtain for an unrestrained airplane with many elastic degrees of freedom. Also a large number of intervals should be taken to assure a reasonable degree of accuracy for the analysis.

Etkin in reference 31, avoided the mathematical difficulties associated with the downwash represented by a spatial impulse function by using the expression for the downwash given by equation (30). This expression, presented by Ribner in reference 30 defines the downwash to be the superposition of an infinite number of inclined sinusoidal waves of shearing

motion. Using equation (29) for the input-output relation, Etkin's expansion of the downwash field results in the response becoming the summation of the responses of the individual derivative terms of the expansion. He has shown that only the second-order derivative terms need be retained to include the aeroelastic effects of the lowest flexible modes on the response. The response to the zero-order and first-order derivative terms of the expansion are the classical aerodynamic stability derivatives. The second-order derivative terms contain the aeroelastic effect of the local lift and its distribution. The response to the downwash expansion has a frequency limitation associated with the dropping of the third-and higher-order terms. The lower limiting value of the wave lengths $2\pi/\Omega_1$, $2\pi/\Omega_2$ which are adequately represented is twice the corresponding airplane dimension (length or span). This formulation has a built-in frequency limitation that would be too restrictive for a large airplane with poorly damped elastic modes.

3.2 Presentation of the Two-Dimensional Gust Response Analysis

The purpose of this investigation is to develop an analysis that accurately accounts for the contributions of the structural modes to the motion and load responses of a large flexible airplane. The analysis is formulated by using the exact expression for the two-dimensional frequency response function. With this function and the two-dimensional isotropic gust spectrum, the input-output relation of equation (29) is used to calculate the response spectrum. Three aspects of the analysis will be discussed. These are: 1) the calculation of the frequency response

function, 2) the relation between the function and the input spectrum, and 3) the integration of the product to obtain the response spectrum.

The two-dimensional frequency response function $H(\omega,\Omega_2)$ is an aerodynamic function that relates the response through the local lift and its distribution to the downwash field. Mathematically it is a complex function whose real and imaginary parts are represented by surfaces. The intersection of these surfaces with a plane through the ω axis produces two curves which are the real and imaginary parts, respectively, of the one-dimensional frequency response function. The calculation of $H(\omega,\Omega_2)$ is an extension of the work of Pratt who in reference 33 used the lifting surface aerodynamic theory of reference 39 to calculate one-dimensional frequency response function.

The major feature of this formulation is the versatility concerning the use of aerodynamic theory used in the calculation of the two-dimensional frequency response function. This formulation can utilize lifting-surface theory as well as strip-analysis theory. The presentation of the formulation is given in a form which incorporates lifting-surface theory. An example of this theory is given in references 38 and 39.

The airplane will be regarded to be an unrestrained flexible planar lifting surface whose equilibrium position is given by the coordinate system presented in the previous chapter. The vertical deviation of the airplane from its equilibrium position is specified by the coordinate z. Assuming the deviations to be small, the governing equations of motion can be linearized. The superposition principle can then be used to express the deviation in the form of the summation of the natural modes of motion

and deformation ξ_i and the generalized coordinates q_i.

$$z = \sum_{i=1}^{N} \xi_i q_i$$

The generalized coordinates are the solutions of the linear governing equations of motion for the airplane subjected to a two-dimensional gust field given by equation (30). These equations are

$$-\omega^2 \sum_{j=1}^{N} M_{ij} q_j(\omega,\Omega_2) + \omega_i^2 M_{ii} q_i(\omega,\Omega_2) = \sum_{j=1}^{N} Q_{ij}^{M}(\omega) q_j(\omega,\Omega_2) + Q_i^{G}(\omega,\Omega_2) \qquad (31)$$

The equations of motion have inertial coupling terms present in the form of the generalized mass terms M_{ij} which are the integration of the weighted inertial distribution $\mu(x,y)$ over the surface S.

$$M_{ij} = \iint_S \mu(x,y)\xi_i(x,y)\xi_j(x,y)dx\,dy \qquad (32)$$

The generalized forces are given by two terms: the forces due to the airplane motion $Q_{ij}^{M}(\omega)$ and the forces due to the gust velocity field $Q_i^{G}(\omega,\Omega_2)$. The generalized motion forces are dependent only on the modal displacements and velocities of the airplane.

$$Q_{ij}^{M}(\omega) = \iint_S \xi_i(x,y)\Delta p_j^{M}(x,y,\omega)dx\,dy \qquad (33)$$

These forces provide both an aeroelastic coupling and damping to the airplane. The differential pressure distribution $\Delta p_i^{M}(x,y,\omega)$ is found by applying the boundary conditions in the form of the modal shapes and

slope to the lifting-surface aerodynamic theory. An example of the boundary conditions for several rigid body and flexible modes is given in reference 33.

The generalized gust forces are

$$Q_i^G(\omega,\Omega_2) = \iint_S \xi_i(x,y)\Delta p_i^G(x,y,\omega,\Omega_2)dx\ dy \tag{34}$$

The pressure distribution $\Delta p_i^G(x,y,\omega,\Omega_2)$ is calculated by applying the boundary conditions in the form of equation (30) to the lifting-surface aerodynamic theory. These generalized downwash forces and consequently the equations of motion differ from the one-dimensional case by the functional dependence of Ω_2. By setting $\Omega_2 = 0$ the generalized coordinates are calculated for a one-dimensional gust analysis from equation (31).

Once the generalized coordinates are calculated, the motion response of the airplane is known. The two-dimensional coordinates are used to calculate the two-dimensional frequency response functions for the motion and load responses. The motion frequency response functions are calculated directly from the generalized coordinates, while the load response functions are calculated by summing the forces on the airplane. These forces are due to the motions of the airplane, the inertia forces, and the applied external forces due to the gust velocity.

The square of the modulus of the two-dimensional frequency response functions is used to weight the input spectrum. This product (integrand of equation (29)) is a two-dimensional response spectrum that is represented by a surface. The volume under the surface is the mean-square value of the response. The influence of the scale of turbulence on the

response spectrum is shown by relating the nondimensional arguments of the input spectrum and of the square of the modulus of the frequency response function. These relations are

$$L\Omega_1 = k\frac{L}{\bar{c}} \tag{35}$$

$$L\Omega_2 = \Omega_2^* \frac{2L}{b} \tag{36}$$

The one-dimensional effect of the input spectrum is given by the ratio of the scale of turbulence to the reference semichord $\bar{c}$. This ratio is the measure of the effect of the size of the chord on the gust response of an airplane. The measure of the two-dimensional effect of the input spectrum is given by the ratio of the scale of turbulence and the semispan of the airplane. This ratio, b/L, is the measure of the effect of the size of the span on the gust response of the airplane.

The response to two-dimensional turbulence requires that both the one-dimensional and two-dimensional parameters be considered. These parameters are not independent. For a given airplane geometry they are related through the aspect ratio AR

$$\frac{L}{\bar{c}} = \frac{AR}{\frac{b}{2L}} \tag{37}$$

The nondimensional form of equation (29) is

$$\phi(k) = \int_0^\infty \left|H(k,\Omega_2^*)\right|^2 \Phi_w(k,\Omega_2^*)\,d\Omega_2^* \tag{38}$$

This relation requires that the integration of the two-dimensional response spectrum be carried out for all positive values of Ω_2^*. The numerical

calculation of the response spectra requires that a finite upper limit of integration be used in equation (38). The error introduced in the calculation of the truncated response spectrum is dependent on the behavior of the square of the modulus of the response, the values of b/L, and the integration limit. The effect of the error is to make the truncated response spectrum less than the true response spectrum. To evaluate this error with any degree of certainty, each two-dimensional response spectrum must be examined separately.

Having calculated the response spectra the familiar statistical parameters obtained from the response spectrum can be obtained from the truncated response spectrum. These parameters are:

The response mean-square value

$$\overline{p^2} = \int_0^\infty \phi_p(\omega)d\omega \tag{39}$$

The response root-mean-square value

$$\sqrt{\overline{p^2}} = \left[\int_0^\infty \phi_p(\omega)d\omega\right]^{1/2} \tag{40}$$

The average number of corssings of the mean with positive slope per unit time

$$N_o = \frac{1}{2\pi} \frac{\left[\int_0^\infty \omega^2\phi_p(\omega)d\omega\right]^{1/2}}{\left[\int_0^\infty \phi_p(\omega)d\omega\right]^{1/2}} \tag{41}$$

CHAPTER FOUR

PRESENTATION OF THE TREND STUDY RESPONSE CALCULATIONS

The two-dimensional gust response analysis was formulated in the previous chapter. This analysis is used to predict the longitudinal response of an airplane to a two-dimensional vertical gust velocity field. The analysis is applied to two mathematical models of an airplane, both of which are described in detail in Appendix C. Results for the acceleration and bending moment responses are calculated for both models using two strip-analysis aerodynamic theories. These results in the form of response spectra and statistical parameters given by equations (39) and (41) are compared to the corresponding results of a one-dimensional analysis. The truncation errors for the acceleration and bending moment response spectra are evaluated.

The major elements of the two-dimensional gust response analysis presented in the previous chapter were: the aerodynamic representation of the generalized forces; the weighting of the frequency response function with the gust spectrum; and the truncation error. The objective of this chapter is to emphasize the two-dimensional effects of the latter two elements. This is done in the form of a trend study which shows the effect of the two-dimensional scale parameter b/L and the truncation error on the one-dimensional response spectra.

4.1 Description of the Mathematical Model

The airplane is represented by an unswept tapered wing and a lumped mass fuselage. It is restrained against all motion and deformation except rigid-body vertical motion and wing vertical bending deformation. The

two models considered in the calculations are rigid and elastic. The rigid-model has only a plunging mode while the elastic model includes two wing elastic vertical bending modes as well.

Lagranges equations of motion are used to calculate the frequency response functions. The nondimensional form of the equations of motion given by equation (31) are expressed in terms of nondimensional generalized coordinates $\hat{q}_i$, mass parameter λ, generalized forces $\hat{Q}^M_{ij}$, $\hat{Q}^G_i$ and reduced frequency k.

$$(k_i^2 - k^2)\lambda\hat{q}_i - \sum_{j=1}^{N} \hat{q}_j\hat{Q}^M_{ij} = 2\hat{Q}^G_i \tag{42}$$

The generalized mass terms are calculated by equation (32) using orthogonal free-free symmetric wing bending modes, normalized such that the mass terms have the values

$$M_{ij} = \begin{cases} M_a & i = j \\ 0 & i \neq j \end{cases}$$

which in nondimensional form are

$$\lambda = \frac{2M_a}{C_{l_\alpha}\rho S\bar{c}} \tag{43}$$

4.2 Description of the Aerodynamic Representations of the Generalized Forces

For the trend study the nondimensional generalized forces are calculated by using strip-analysis aerodynamic theory. This theory provides a clear manner of expressing the influence of the spatial frequency on the unsteady lift distributions of the wing. The price of this visualization is a theory which does not correct the unsteady lift distribution for finite aspect ratio.

Strip-analysis is concerned only with the spanwise lift distribution on the wing. This distribution is found by calculating the local lift on each of a number of streamwise strips on the wing. The local lift per unit strip width is assumed to be proportional to the local angle of attack. The generalized forces are formulated in terms of the unsteady lift distributions for two-dimensional incompressible flow. These distributions are discussed in detail in Appendix C.

The generalized aerodynamic forces due to motions are:

$$\hat{Q}^{M}_{ij} = k^2 A_{ij} - 2iC(k)B_{ij}$$

The terms A_{ij} and B_{ij} are nondimensional coefficients which represent the contributions of the unsteady apparent mass and circulatory distributions respectively. The function C(k) is the well known Theordorsen function for incompressible two-dimensional flow. The nondimensional coefficients are defined in Appendix C.

The strip-analysis formulation of the generalized gust forces requires that the contribution of the spanwise frequency distribution of the downwash be treated as an angle of attack distribution which is independent of reduced frequency. This requirement allows the unsteady part of the local lift to be calculated separately from the remaining spatial part of the generalized forces. Thus, the generalized gust forces are

$$\hat{Q}^{G}_{i} = K(k)BB_{i}(\Omega^{*}_{2})$$

The unsteady part of the generalized gust force K(k) is called the circulation function. It represents the response of a lifting chord to a traveling sinusoidal wave acting along the flight path. The incompressible two-dimensional flow expression of K(k) is given in Appendix C.

The contribution of the spanwise frequency distribution is given by $BB_i(\Omega_2^*)$. This term is the response of the lifting surface to a sinusoidal wave acting along the span.

$$BB_i(\Omega_2^*) = \frac{1}{4} \int_{-1}^{1} \gamma(y^*) e^{i\Omega_2 y^*} \xi_i(y^*) dy^*$$

The function γ is a symmetrical normalized lift curve slope distribution which is used to weight the symmetrical modes ξ_i. Expanding the exponential function in terms of trignometric functions, $BB_i(\Omega_2^*)$ is expressed in terms of a real and imaginary function. The imaginary part of $BB_i(\Omega_2^*)$ is an odd function because of the sin $(\Omega_2^* y^*)$ term. This part of $BB_i(\Omega_2^*)$ vanishes when the integration over the even limits is performed. Thus $BB_i(\Omega_2^*)$ is a real function for symmetrical modes and it is given by

$$BB_i(\Omega_2^*) = \frac{1}{2} \int_{0}^{1} \gamma(y^*) \cos(\Omega_2^* y^*) \xi_i(y^*) dy^* \qquad (44)$$

The generalized coordinates are calculated by solving the set of simultaneous equations given by equation (42). These coordinates are used to calculate the two-dimensional frequency response function. The motion frequency response functions are calculated directly from the generalized coordinates. The load frequency response functions are cal-

culated by summing the inertial forces and aerodynamic forces due to the airplane motions and the gust field.

The bending moment frequency response function is calculated by taking the moment of the total load distribution on the wing. The wing-root bending moment is

$$\left[\frac{\bar{c}\lambda}{UM_a\frac{b}{2}}\right]\frac{BM(k,\Omega_2^*)}{W_G} = K(k)BB'(\Omega_2^*) + \frac{1}{2}\sum_{i=1}^{N}\left[k^2A_i' - 2ikC(k)B_i' + 2\lambda k^2D_i\right]\hat{q}_i \qquad (45)$$

The nondimensional coefficients A_i, B_i, and D_i are the contributions of the apparent mass, velocity and inertial forces respectively. These coefficients are defined in Appendix C. The term $BB'(\Omega_2^*)$ represents the moment of the gust force distribution on the wing.

$$BB'(\Omega_2^*) = \frac{1}{2}\int_0^1 \gamma(\eta^*)e^{i\Omega_2^*\eta^*}\,\eta^*\,d\eta^*$$

It is a complex function whose imaginary part represents the rolling excitation of the wing of a symmetrical elastic mode. For symmetric bending moment responses the imaginary part is neglected and $BB'(\Omega_2^*)$ is

$$BB'(\Omega_2^*) = \frac{1}{2}\int_0^1 \gamma(\eta^*)\cos(\Omega_2^*\eta^*)\eta^*\,d\eta^* \qquad (46)$$

Equation (38) is used to calculate the response spectrum in terms of the two-dimensional frequency response functions. The frequency response function is weighted by the normalized two-dimensional Dryden vertical gust velocity spectrum. This spectrum is derived by using the nondimensional argument relations given by equations (35) and (36) and the input spectrum

given by equation (13).

$$\Phi_D(k,\Omega_2^*) = \frac{3AR}{\pi\left(\frac{b}{2L}\right)^2} \frac{(L\Omega_1)^2 + (L\Omega_2)^2}{\left[1 + (L\Omega_1)^2 + (L\Omega_2)^2\right]^{5/2}} \tag{47}$$

The normalized one-dimensional Dryden vertical gust spectrum is derived by using equation (35) and the input spectrum given by equation (12).

$$\Phi_D(k) = \frac{1}{\pi\left(\frac{L}{c}\right)} \frac{1 + 3(L\Omega_1)^2}{\left[1 + (L\Omega_1)^2\right]^2} \tag{48}$$

This spectrum is used to weight the square of the modulus of the one-dimensional frequency response function to obtain the response spectrum.

$$\Phi(k) = |H(k)|^2 \Phi_D(k) \tag{49}$$

4.3 Spanwise Variation Effect of the Vertical Gust Velocity on the Longitudinal Response of an Airplane

The spanwise variation effect is measured by comparing the responses calculated by the two-dimensional analysis with the corresponding response calculated by the one-dimensional analysis. From equation (47) the response spectra calculated from the two-dimensional analysis is shown to depend explicitly on the parameter b/L. This parameter involves the scaling of the airplane with respect to the turbulence of the atmosphere. A change in the value of b/L may be considered as either a change in the size of the airplane with respect to the turbulence or vice versa. The geometric scaling relation is given by equation (37). The proper geometric scaling for the airplane and turbulence configuration is maintained provided that the same value of aspect ratio is used for all values of b/L.

Other scaling parameters must be considered to assure that the different airplane and turbulence configurations are dynamically similar. This similarity is maintained by keeping the forces of each configuration properly scaled.

Holding the mass parameter constant maintains the proper ratio of airplane and fluid inertial forces. Similarly, the elastic and aerodynamic force ratios are held constant. These force ratios are combined to form the mechanical vibration constant. This scaling parameter provides the natural frequencies for dynamically similar airplanes. Provided that the mass, stiffness, and lift distributions are the same for all configurations, dynamically similar mode shapes are calculated. Thus, the corresponding generalized mass and force terms in equation (42) provide equations of motion for dynamically similar configurations.

The ratio of mass between the wing and airplane is varied to measure the effect of mass distribution on the two-dimensional analysis response spectra. The total mass of the airplane and mass distribution of the wing is held constant. Mode shapes to be used in the generalized mass and force terms of the equations of motion are calculated for each value of mass ratio considered.

The motion and load responses are calculated for both the rigid and elastic models. For each of the models the responses are calculated by using simple-strip analysis and modified-strip analysis aerodynamic theories. The normalized lift curve slope distribution for the simple strip analysis is equal to the distribution of the normalized chord of the wing. The two-dimensional incompressible value of 2π is used for the total lift curve slope C_{l_α}.

The motion frequency response function of the rigid body model is calculated from equation (42) for a value of N = 1. The solution of this equation is the rigid-body plunge displacement. The plunge displacement for a given value of reduced frequency is proportional to the spatial frequency part of the generalized gust force. The spatial frequency distribution function $BB_1(\Omega_2{}^*)$ is given by equation (44) for the rigid-body plunge mode $\xi_1 = 1$ and is plotted as a function of $\Omega_2{}^*$ in figure 1. The function has its maximum value for $\Omega_2{}^* = 0$, and decays to ten percent of this value for a value of $\Omega_2{}^*$ corresponding to one and a quarter waves on the semispan.

The plunge velocity and plunge acceleration for a given value of k are also proportional to $BB_1(\Omega_2{}^*)$. The plunging acceleration frequency response function is calculated and normalized by the "sharp edge" gust acceleration.

$$\ddot{z}(k,\Omega_2^*) = \frac{-k^2\lambda\hat{q}_1}{2BB_1(0)}$$

The square of the modulus of $\ddot{z}(k,\Omega_2{}^*)$ is plotted for selected values of k against $\Omega_2{}^*$ in figure 2. These curves exhibit the decay and periodic properties of the function $BB_1(\Omega_2{}^*)$. For low values of $\Omega_2{}^*$, the variation of $|\ddot{z}(k,\Omega_2{}^*)|^2$ with $\Omega_2{}^*$ is essentially constant. The values of $|\ddot{z}(k,\Omega_2{}^*)|^2$ for this range of values of $\Omega_2{}^*$ are the same as the one-dimensional frequency response function for corresponding values of k.

Using equations (38) and (47) the plunge acceleration response spectrum is calculated. Figure 3 presents the acceleration spectrum for a value of b/L = 0.5. The acceleration response spectrum calculated from a one-

dimensional analysis is also shown for comparison. These two response spectra show a constant percentage difference for low values of reduced frequency. For large values of k, the two-dimensional analysis spectrum is attenuated more than the one-dimensional analysis spectrum. Figure 4 shows the higher attenuation of the two-dimensional analysis response spectrum on a linear plot. The area of the two-dimensional analysis acceleration spectrum is about 15 percent less than the area of the one-dimensional analysis spectrum. The reduction in mean-square value and $\hat{N}_o$ of the acceleration response for this and other values of b/L is shown in figure 5.

Figure 5 shows that the two-dimensional analysis response parameters do not approach the one-dimensional response parameters for values of b/L near zero. Diederich's results (reference 26), in contrast, indicate that the ratio of the two-dimensional to one-dimensional rigid body acceleration mean square value does approach unity as b/L approaches zero. The variation of the ratio of the response parameters with b/L can be explained by examining the effect of the aspect ratio on the product of the input spectrum and frequency response function.

The rigid-body acceleration response spectrum is given in terms of the gust spectrum and the frequency response function for a rectangular wing formulated by simple strip theory.

$$\phi(k) = \frac{k^2}{k^2 + \frac{4}{\lambda^2}} \int_0^\infty \left| \frac{\sin \Omega_2^*}{\Omega_2^*} \right|^2 \Phi_D(k,\Omega_2^*) d\Omega_2^* \qquad (50)$$

The behavior of the response spectrum is examined for two limiting cases of the gust spectrum. The limiting form is specified by whether the value of k is less than or greater than $\frac{b/2L}{AR}$. For values of $k < \frac{b/2L}{AR}$ the gust spectrum is given by

$$\Phi_D(k,\Omega_2^*) \approx \frac{3AR\,\frac{b}{2L}}{\pi} \frac{(\Omega_2^*)^2}{\left[\left(\frac{b}{2L}\right)^2 + (\Omega_2^*)^2\right]^{5/2}} \tag{51}$$

The roll-off point of the spectrum is given by the value of b/2L. For a value of b/2L = .25, figure 3 shows the response spectrum calculated by the two-dimensional analysis differs from the one-dimensional response spectrum by a constant ratio. As shown in figure 6, decreasing the value of b/2L to .025 decreases the weighting influence of the frequency response function; consequently, the response spectra calculated by both analysis are the same for all values of $k < .004$.

For values of $k > \frac{b/2L}{AR}$, the gust spectrum is

$$\Phi_D(k,\Omega_2^*) \approx \frac{3AR\,\frac{b}{2L}}{\pi} \frac{1}{\left[(kAR)^2 + (\Omega_2^*)^2\right]^{3/2}} \tag{52}$$

For these values of k, the roll-off point is independent of b/2L. This can be seen by comparing the values of k in figures 3 and 6 for which the two-dimensional attenuation of the response spectra begins. Unless the value of kAR = 0, the response spectrum calculated by the two-dimensional analysis is attenuated by the frequency response function for all values of b/2L. For the value of AR = 0 the response spectra calculated by both analysis are same, a result to be expected since the one-dimensional analysis

response spectrum is independent of aspect ratio. Thus the ratio of the response parameters do not approach unity for small values of b/L if the aspect ratio is greater than zero. The reduction of the ratio of the response parameters is also dependent on the value of the mass parameter. The ratio of two-dimensional to one-dimensional response parameters decreases as the mass parameter decreases.

An evaluation of the stress responses in the wing is made by calculating the wing bending moment response. The wing-root bending moment is calculated by using equation (45) for a value of N = 1. This bending moment frequency response function is normalized by the "sharp edge" gust bending moment.

$$B\hat{M}(k,\Omega_2^*) = \frac{K(k)BB'(\Omega_2^*)}{BB'(0)} + \frac{1}{2}\left[k^2A_1' - 2ikC(k)B_1' + 2\lambda k^2D_1\right]\frac{\hat{q}_1}{BB'(0)}$$

The bending moment response is dependent on the moment of the gust force distribution as well as its distribution. For small values of Ω_2^*, the bending moment frequency response function has the characteristics of the one-dimensional frequency response function. It is proportional to the acceleration response and approaches a value of zero for decreasing k. Figure 7 shows that for increasing values of Ω_2^* this trend is no longer seen. This distinct behavior of the two-dimensional bending moment frequency response function is dependent on the value of k.

For low values of k, the influence of the inertial forces on the response is negligible. The velocity forces are proportional to the gust forces through the generalized coordinate $\hat{q}_1$. The moment of the spatial frequency part of the gust force is given by equation (46). The variation

of $BB'(\Omega_2^*)$ with Ω_2^* is shown in figure 1. The phasing between gust forces and the displacement is such that the bending moment response is proportional to the difference of $BB_1(\Omega_2^*)$ and $BB'(\Omega_2^*)$. The bending moment is for values of Ω_2^* near zero. However, for large values of Ω_2^*, the bending moment increases. For example, for a value of $k = .0001$, the bending frequency response function modulus squared has a peak which is five orders of magnitude greater than its $\Omega_2^* = 0$ value.

The two-dimensional analysis bending moment has a response spectrum which is quite different from the one-dimensional analysis spectrum. The variation of the response spectrum with k is constant for small values of reduced frequency. This deviation from the one-dimensional analysis is shown in figure 8. It is a result of the peaking behavior of the frequency response function for low values of k. Another deviation for large values of k is shown to be an attenuation of the two-dimensional analysis spectrum. Of these two deviations only the attenuation for large values of k is significant. The effect of the attenuation on the response statistical parameters is shown in figure 9. The spectrum calculated by the two-dimensional analysis gives a 20 percent reduction of mean square value for a value of $b/L = .5$. The variation with b/L of the reduction in mean-square value and $\hat{N}_o$ given by the two-dimensional analysis is presented in figure 10.

The variation of the bending moment mean-square value of $\hat{N}_o$ with mass ratio is shown in figures 11 and 12 respectively. When most of the weight of the airplane is in the fuselage, a substantial reduction in bending moment is given by the two-dimensional analysis. The reduction decreases

for increasing values of mass ratio. A significant point to be made is that $\hat{N}_o$ is increased for large values of mass ratio by the two-dimensional analysis. The trend of the mean-square value and $\hat{N}_o$ is due to the fact that for a one-dimensional analysis the inertial load distribution of a flying wing is nearly the same as that of the motion and gust forces. The inertial load distribution tends to cancel the motion and gust forces on the wind and results in a decrease of the bending moment. For the two-dimensional analysis, the gust forces are not cancelled by the inertial forces and therefore, the bending moment does not vanish for values of mass ratio near unity.

The influence of elastic wing bending modes on the two-dimensional response analysis is shown by calculating the bending moment response for the flexible model. The two-dimensional frequency response function is calculated from equation (45) for a value of N = 3. The spatial frequency variation of the flexible bending moment response differs from the rigid-body response by the presence of the terms $BB_2(\Omega_2^*)$ and $BB_3(\Omega_2^*)$. These functions represent the flexible wing bending modal contributions to the bending moment response and are presented in figure 13. The maximum value for each function occurs at a value of Ω_2^* for which the variation of the function $\cos(\Omega_2^* y^*)$ with y^* approximates the respective mode shape. Figure 14 shows that the variation of the flexible bending moment response with Ω_2^* for small values of k is the same as the rigid-body response. For increasing values of k the contribution of the functions $BB_2(\Omega_2^*)$ and $BB_3(\Omega_2^*)$ becomes significant. This is shown by the peaks in the frequency response function for the k values of .15 and .52. These values of k represent the natural reduced frequencies of the first and second wing

bending modes, respectively. The peaking influence of the elastic modes on the frequency response function is called "spatial resonance" by Houbolt in reference 27.

The bending moment response spectra calculated from the one- and two-dimensional response analyses are shown in figure 15. The influence of the spatial resonance effect appears in the highest wing bending mode. The spectrum peak corresponding to this mode for the two-dimensional analysis is approximately four times higher than the peak for the one-dimensional analysis. While this spatial resonance effect has little influence on the mean-square value of the response it does effect the response $\hat{N}_o$. This is shown by the comparison of the response spectra calculated by both analyses which is presented in figure 16. The mean-square value of the flexible bending moment response calculated by the two-dimensional analysis is 78 percent of that calculated by the one-dimensional analysis. The variation of the reduction in mean-square value and $\hat{N}_o$ with b/L is presented in figure 17. The reduction of $\hat{N}_o$ is less for the flexible model than that for the rigid model. This is a result of the spatial resonance of the flexible model. The variation of the mean-square value and $\hat{N}_o$ for both the one- and two-dimensional analyses with mass ratio is shown in figure 18 and 19, respectively. The variation of mean-square value is similar to the variation of the mean-square value calculated by the rigid model analysis. The variation of the flexible model $\hat{N}_o$ is less than the variation of rigid model $\hat{N}_o$.

A more realistic mathematical model of the two-dimensional response problem is formulated by using a modified-strip-analysis aerodynamic theory.

The prominent feature of this theory is that the spanwise lift distribution has a value of zero at the wing tip. The lift-curve slope distribution is calculated by using a steady-state lifting line theory. For the calculations a lift-curve slope distribution for a wing of aspect ratio 6, taper ratio 1/2 and total lift-curve slope 4.321 is used. This distribution is calculated from a matrix formulation of the Weissinger L-method presented in reference 45 and is discussed in detail in Appendix C.

The effect of using the modified-strip analysis for the calculation of the generalized forces is shown in figure 20. The function $BB_2(\Omega_2^*)$ differs little from $BB_2(\Omega_2^*)$ calculated by simple-strip theory. The function $BB_3(\Omega_2^*)$ is different than the simple-strip analysis function for small values of Ω_2^*. The effect of using the modified-strip analysis is also seen in the flexible bending moment frequency response function. The peaks of the function shown in figure 21 illustrates two effects of the modified analysis. The first effect is the decrease in aerodynamic damping which is a result of the loss of wing tip contributions to the generalized motion forces. The second effect is an increase of the spatial resonance of the elastic modes.

The response spectra also reflect the effects of the modified analysis. The peak in the spectra of the second flexible wing mode calculated by the two-dimensional analysis is roughly 15 times greater than the peak calculated by the one-dimensional analysis. The increase in spatial resonance effect and the decrease in aerodynamic damping are shown in figure 22. The increase of the influence of the elastic modes on the bending moment response spectra occurs at such high values of reduced frequency that its

effect on the response statistical parameters is negligible. This is shown in figure 23. The variations of $\overline{BM^2}$ and $\hat{N}_o$ with b/L and mass ratio for the modified-strip analysis have the same trends as the variations calculated by the simple-strip analysis and consequently are not shown.

4.4 Truncation Error

The numerical integration of equation (38) can be performed only to some finite upper limit which produces a truncation error. The effect of the finite upper limit (a value of 3π is used in the trend study calculations) on the response statistical parameters is explained in this section.

A rough measure of the effect of truncation on the response spectra is evaluated by examining the effect of truncating the integral of the gust spectrum. The two-dimensional Dryden gust spectrum given by equation (47) is integrated over Ω_2^* to an upper limit of $\Omega_2^* = 3\pi$ for a value of b/L = 0.5. The truncated spectra and its mean-square value are compared to the one-dimensional Dryden gust spectrum given by equation (48). The effect of truncation is significant only for large values of k, for example at a value of k = 1, the truncated spectrum is 83.9 percent less than the exact spectrum. The deviation of the truncated spectrum at high values of k is not reflected in the mean-square value. The mean-square value of the truncated spectrum differs from the one-dimensional value by 0.8 percent.

Weighting the gust spectrum with the frequency response function attenuates the spectrum for high values of k and reduces the effect of truncation on the response spectrum. The truncation error for rigid-body acceleration response is examined by doing a closed form integration of

equation (38). The generalized gust force for an untapered wing is calculated by simple-strip theory. The frequency response function is assumed to be independent of k, i.e.

$$H(k,\Omega_2^*) = \frac{\sin \Omega_2^*}{\Omega_2^*}$$

Using this relation and equation (38) the truncation error is

$$\epsilon(k) = \int_{\Omega_2^*}^{\infty} \left| \frac{\sin \Omega_2^*}{\Omega_2^*} \right|^2 \Phi_D(K,\Omega_2^*) d\Omega_2^* \tag{53}$$

Equation (53) is difficult to evaluate in closed form. Because of this difficulty the truncation error is examined for two limiting cases of the gust spectrum. For case one the effect of truncation on the response spectrum for small values of k is considered. The values of k for which this case applies is $k < \frac{b/2L}{AR}$ and the gust spectrum is given by equation (51). The effect of truncation on the response spectrum is not significant, less than one percent of the error under the truncated spectrum, provided that values of b/2L are very much less than the upper limit of integration.

The second case examines the effect of truncation on the response spectrum for large values of k. The values of k for which case two applies is $k > \frac{b/2L}{AR}$ and the gust spectrum is given by equation (52). The effect of truncation on the response spectrum is dependent upon the value of the roll-off point of the gust spectrum. For low values of the roll-off point, i.e., $kAR \ll \pi$, the asymtotic expression of equation (52) is

$$\Phi_D(k,\Omega_2^*) \approx \frac{3AR\left(\frac{b}{2L}\right)}{\pi} \frac{1}{(\Omega_2^*)^3} \tag{54}$$

This expression of the gust spectrum is substituted into equation (53) and integrated. The value of the truncation error is given by equation (C37) in Appendix C. The truncation error was evaluated for values of the upper limit of Ω_2^* that ranged from 2.0 to 10.0 and values of b/L from 0.05 to 0.5. This study showed that the truncation error is largest for high values of b/L and low values of the integration upper limit. For the values of k for which equation (54) applies, i.e., $.04 < k << .5$, the truncation error is less than 5 percent of the area under the truncated spectrum for a value of b/L = .5 and a value of upper limit of 2.0.

For high values of the roll-off point, i.e., $kAR > \pi$, the gust spectrum becomes

$$\Phi_D(k,\Omega_2^*) \approx \frac{3\left(\frac{b}{2L}\right)}{\pi k^3 (AR)^2} \tag{55}$$

The percentage truncation error for this range of k values is given by equation (C38) in Appendix C. The percentage error was evaluated for values of the upper limit that ranged from 2.0 to 10.0, and values of b/L from 0.05 to 0.5. A maximum percentage error of 14.4 percent was calculated for a value of upper limit of 2.

An evaluation of the effect of truncation is made for the flexible bending moment. The frequency response function shown in figure 21 has a large variation with Ω_2^* for values of Ω_2^* near 3π. The mean-square value of the response is calculated for the response spectra for values of the upper limit of Ω_2^* that range from 3π to 2.5. The variation of the mean square value with the upper limit of Ω_2^* is shown in figure 24. This study shows that no appreciable error (less than 1 percent of the 3π value)

occurs above a value of upper limit of $\Omega_2^* = 6.0$. The mean-square value for an upper limit of $\Omega_2^* = 2.5$ differs by 6.3 percent from the value for an upper limit of $\Omega_2^* = 3\pi$. The variation of $\hat{N}_o$ with upper limit of Ω_2^* shows the same trend as the mean-square value. $\hat{N}_o$ for an upper limit limit of $\Omega_2^* = 2.5$ differs by 8.2 percent from the value of an upper limit of $\Omega_2^* = 3\pi$.

DISCUSSION

An analysis is formulated that predicts the motion and load responses of an airplane to a turbulence field that varies along the span as well as along the line of flight. A major feature of this formulation of the two-dimensional gust response problem is its aerodynamic versatility. The generalized aerodynamic forces can be calculated either by an unsteady lifting surface theory or an unsteady modified-strip analysis that includes unsteady finite span induction effects.

The analysis was applied to mathematical models of a rigid and a flexible airplane in the form of a trend study. Results of this study indicate that the influence of spanwise variation of the vertical gust velocity on the longitudinal motion and load responses can be significant for a large flexible airplane flying at altitudes of 1,000 feet or less.

With one important exception the results of the present procedure are generally similar to those of past investigations. The trend study results of this formulation show the rigid-body acceleration response predicted by a one-dimensional analysis to be a conservative estimate for large values of span to scale of turbulence ratio. Also, a conservative estimate of the rigid-body bending moment exists for various values of wing to fuselage mass ratio.

The exception to similarity to past results is that the conservative estimate of rigid-body acceleration exists for small values of span to scale of turbulence ratio. This difference is due to the influence of the aspect ratio on the weighting of the frequency response function with the

gust spectrum. This result is in contrast with results of earlier investigations that have shown the one-dimensional analysis to be a limiting case of the two-dimensional analysis. This study has shown that the limiting case exists only for a value of aspect ratio equal to zero, which points out the fact that the effect of aspect ratio is inherently missing in the one-dimensional analysis.

Both the rigid and flexible bending moment responses are shown to be different than the one-dimensional analysis responses. This difference is seen at both low and high values of reduced frequency. Only the difference at high frequencies is shown to be significant. For the model of the flexible airplane, a spatial tuning of the lift distribution with the elastic deformation modes is shown to result in a significant amount of amplification of the bending moment response spectra. The natural frequencies of the elastic modes were so high and widely separated, however, that the spatial resonance of the modes did not significantly affect the values of the response statistical parameters.

An important objective of the trend study was to evaluate the effect of the truncation error on the response spectra. This error is a consequence of the numerical integration of the input-output relation being performed to a finite upper limit. The error was evaluated for both rigid-body acceleration and flexible bending moment responses. It was found that the truncation error was small for values of upper limit of integration that are greater than a limit that represents a full wave of downwash along the semispan. Furthermore, this error is not a serious limitation to this formulation of the gust response problem. The only

practical limitation imposed by the truncation is the loss of resolution of the downwash description for higher values of integration upper limit. The trade-off between the effect of truncation error and resolution is largely a matter of the ability to use more control points along the semi-span in the aerodynamic force calculations.

Since this investigation did not deal with an application of the formulation to a large flexible airplane, further work in this area may be desirable. Specifically, the effects of sweep, flexibility, compressibility, and a rigid-body pitching degree of freedom should be ascertained on the basis of a comparison of calculated and flight test results.

REFERENCES

1. Taylor, G. I.: Statistical Theory of Turbulence. Parts I-IV. Turbulence - Classic Papers on Statistical Theory, S. K. Friedlander and Leonard Topper, eds. Interscience Publications, Inc. (New York), C. 1961, pp. 18-76.

2. Von Karman, T. and Howarth, L.: On the Statistical Theory of Isotropic Turbulence. Turbulence - Classic Papers on Statistical Theory, S. K. Friedlander and Leonard Topper, eds. Interscience Publications, Inc. (New York), C. 1961, pp. 76-100.

3. Dryden, H. L.: A Review of the Statistical Theory of Turbulence. Turbulence - Classic Papers on Statistical Theory, S. K. Friedlander and Leonard Topper, eds. Interscience Publications, Inc. (New York), C. 1961, pp. 115-150.

4. Von Karman, T.: Progress in the Statistical Theory of Turbulence. Turbulence - Classic Papers on Statistical Theory, S. K. Friedlander and Leonard Topper, eds. Interscience Publications, Inc. (New York), C. 1961, pp. 162-174.

5. Dryden, H. L., Schubauer, G. B., Mock W. C., Jr., and Skramstad, H. K.: "Measurements of Intensity and Scale of Wind-Tunnel Turbulence and their Relation to the Critical Reynolds Number of Spheres." NACA Report 581, 1937.

6. Batchelor, G. K.: The Theory of Homogeneous Turbulence. Cambridge Press, C. 1959.

7. Davenport, W. B., Jr. and Root, W. L.: An Introduction to the Theory of Random Signals and Noise. McGraw-Hill, c. 1958.

8. Houbolt, J. C., Steiner, R., and Pratt, K. G.: "Dynamic Response of Airplanes to Atmosphere Turbulence Including Flight Data on Input and Response." NASA Technical Report R-199, 1964.

9. Batchelor, G. K.: "Energy Decay and Self-Preserving Correlation Functions in Isotropic Turbulence." Quarterly of Applied Mathematics, c. 1948, 6, pp. 97.

10. Batchelor, G. K.: "The Application of the Similarity Theory of Turbulence to Atmosphere Diffusion." Quarterly Journal Royal Meteorological Society, c. 1950, 76, pp. 133.

11. Heisenberg, W.: "On the Theory of Statistical and Isotropic Turbulence." Proceedings of the Royal Society of London, c. 1948, A, 195, pp. 402.

12. Von Karman, T. and Lin, C. C.: On the Concept of Similarity in the Theory of Isotropic Turbulence. Turbulence - Classic Papers on Statistical Theory, S. K. Friedlander and Leonard Topper, eds. Interscience Publications, Inc. (New York), c. 1961, pp. 179-196.

13. Coburn, N.: Vecotr and Tensor Analysis. Macmillan Co. (New York), c. 1955.

14. S. Chardrasekhar, F. R. S.: "On Heisenberg's Elementary Theory of Turbulence." Proceedings of the Royal Society of London 1949 A, 200, pp. 20.

15. Proudman, I.: "A Comparison of Heisenberg's Spectrum of Turbulence with Experiment." Proceedings of the Cambridge Philosphical Society 1951, 47, pp. 158.

16. Lin, C. C.: "On Taylor's Hypothesis and the Acceleration Terms in the Navier - Strokes Equations." NAVORD Report 2306, 1952.

17. J. Kampe de Feriet: "Spectral Tensor of Homogeneous Turbulence." NAVORD Report 1136, 1949.

18. Pai, Shih-I: Viscous Flow Theory II - Turbulence Flow, D. Van Nostrand, Inc., c. 1957.

19. Erdelyi, Magnus, Oberhettinger, Tricomi: Tables of Integral Transforms. Vol. I, McGraw - Hill, New York, c. 1954.

20. Hodgman: Standard Mathemetical Tables. Chemical Rubber Co., Cleveland, Ohio, 11th Edition, c. 1957.

21. Hildebrand: Advanced Calculus for Applications, Prentice Hall, c. 1964.

22. Abramowitz and Stegan: Handbook of Mathematical Functions. Dover Co., c. 1965.

23. Gradshteyn and Ryzhik: Tables of Integrals, Series, and Products. Academic Press, London, c. 1965.

24. Bisplinghoff, R., Ashley, H., and Halfman, R.: Aeroelasticity. Addison - Wesley Co., Cambridge, Massachusetts, c. 1955.

25. Diederich, F.: "The Response of an Airplane to Random Atmospheric Disturbances." NACA TR 1345, 1958.

26. Diederich, F.: "The Dynamic Response of a Large Airplane to Continuous Random Atmospheric Disturbances." Journal of Aeronautical Sciences, Vol. 23, No. 10, October 1956, pp. 917-930.

27. Houbolt, J.: "On the Response of Structures Having Multiple Random Inputs." Jahrb. 1957 der WGL, Friedr, Vieweg and Son (Braumschweig), pp. 296-305.

28. Liepmann, H.: "Extension of the Statistical Approach to Buffeting and Gust Response of Wings of Finite Span." Rep. No. SM - 15172, Douglas Aircraft Co., Inc., February 1954.

29. Liepmann, H.: "On the Application of Statistical Concepts to the Buffeting Problem." Journal of the Aeronautical Sciences, Vol. 19, No. 12, December 1952, pp. 793.

30. Ribner, H.: "Spectral Theory of Buffeting and Gust Response; Unification and Extension." Journal of the Aeronautical Sciences. Vol. 23, No. 12, December 1956, pp. 1075-1077, 1118.

31. Etkin, B.: "A Theory of the Response of Airplanes to Random Atmospheric Turbulence." Journal of the Aeronautical Sciences, Vol. 26, No. 7, July 1959, pp. 409-420.

32. Etkin, B.: "Theory of the Flight of Airplanes in Isotropic Turbulence - Review and Extension." AGARD Report No. 373, April 1961.

33. Bennett, F. and Pratt, K.: "Calculated Responses of a Large Swept-wing Airplane to Continuous Turbulence with Flight - Test Comparison." NASA TR R-69, 1960.

34. Coleman, T., Press, H., and Meadows, M.: "An Evaluation of the Effects of Flexibility on Wing Strains in Rough Air for a Large Swept-wing Airplane by Means of Experimentally Determined Frequency - Response Functions with an Assessment of Random - Process Techniques Employed." NASA TR R-70, 1960.

35. Murrow, H., Pratt, K., and Drischler, J.: An Application of a Numerical Technique to Lifting - Surface Theory for Calculations of Unsteady Aerodynamic Forces Due to Continuous Sinusoidal Gusts on Several Wing Planforms at Subsonic Speeds. NASA TN D-1501, February 1963.

36. Bisplinghoff, R., Ashley, H.: Principles of Aeroelasticity, Wiley Co., New York, c. 1962.

37. Etkin, B.: Dynamics of Flight, Wiley Co., New York, c. 1959.

38. Watkins, C., Runyan, H., and Woolston, D.: "On the Kernal Function of the Integral Equation Relating the Lift and Downwash Distribution of Oscillating Finite Wings in Subsonic Flow." NACA TR 1234, 1955.

39. Watkins, C., Woolston, D., and Cunningham, H.: "A Systematic Kernal Function Procedure for Determining Aerodynamic Forces on Oscillating or Steady Finite Wings at Subsonic Speeds." NASA TR R-48, 1959.

40. Heaslet, M. and Speiter, J.: "Reciprocity Relations in Aerodynamics." NACA TR 1119, 1953.

41. Yates, C.: "Modified - Strip - Analysis Method for Predicting Wing Flutter at Subsonic to Hypersonic Speeds." Journal of Aircraft, Vol. 3, No. 1, January - February 1966.

42. Fung, Y.: The Theory of Aeroelasticity, Wiley Co., New York, c. 1955.

43. Reissner, E.: "Effect of Finite Span on the Airload Distributions for Oscillating Wings." NACA TN 1194, March 1947.

44. Theodorsen, T.: "General Theory of Aerodynamic Instability and the Mechanism of Flutter." NACA TR 496, 1934.

45. Diederich, F. and Zlotnick, M.: "Calculated Spanwise Life Distributions, Influence Functions, and Influence Coefficients for Unswept Wings in Subsonic Flows." NACA TR 1228, 1953.

46. Barmby, J., Cunningham, H., and Garrick, I.: "Study of Effects of Sweep on the Flutter of Cantilever Wings." NACA TR 1014, 1948.

47. Hsu, P. T.: "Some Recent Developments in the Flutter Analysis of Low-Aspect-Ratio Wings." Proceedings of the IAS National Specialists Meeting on Dynamics and Aeroelasticity, Institute of Aerospace Sciences, (New York), c. 1958, pp. 27-36.

APPENDIX A

THE DESCRIPTION OF HOMOGENEOUS AND ISOTROPIC TURBULENT FLUID FLOW

This appendix presents the mathematical description of homogeneous and isotropic turbulent fluid flow. A brief presentation of the principles and assumptions concerning isotropic and homogeneous turbulent flow theory is made and the resulting correlation functions and spectral density functions are presented.

A.1 General Development

The kinematics and dynamics of isotropic and homogeneous turbulence were developed by Von Karman and Howarth, who in reference 2 used the work of Reynolds and Taylor to develop a general theory of isotropic turbulent flow. Von Karman and Howarth generalized Taylor's concept of the correlation function to three dimensions. The result of this generalization was the time averages of the products of two, $\overline{u_i u_j}$ and three, $\overline{u_i u_j u'_k}$ velocity components taken at two different points $\underline{x}$ and $\underline{x}'$. They showed that for homogeneous turbulence these averages form the components of two tensors and are scalar functions of the separation of the two points. The property of isotropy was shown to give the tensors spherical symmetry which resulted in the vanishing of all but five of the velocity averages. The mean square values of the velocity components are equal and are independent of position.

$$\overline{u_i^2} = \overline{u_i'^2} = \overline{u^2} \tag{A1}$$

If statistical and time averages are equivalent then the time averages of the products of the velocity components of the double and triple correlation tensors (equations (4) and (5)) can be equated.

$$R_{ij}(\underline{r}) = \overline{u_i u_j'} \tag{A2}$$

$$T_{ijk}(\underline{r}) = \overline{u_i u_j u_k'} \tag{A3}$$

By either examining the structure of the time averages, reference 2, or using the mathematical properties of the isotropic correlation tensors, reference 6, the components of the double and triple correlation tensors can be shown to have the forms

$$R_{ij}(\underline{r}) = \overline{u^2}\left[\frac{f(r) - g(r)}{r^2} r_i r_j + g(r)\delta_{ij}\right] \tag{A4}$$

$$T_{ijk}(\underline{r}) = (\overline{u^2})^{3/2}\left[\frac{k(r) - h(r) - 2q(r)}{r^3} r_i r_j r_k + \delta_{ij} r_k \frac{h(r)}{r} + \delta_{ik} r_j \frac{q(r)}{r} + \delta_{jk} r_i \frac{q(r)}{r}\right] \tag{A5}$$

The scalar functions in the above expressions are the non-vanishing time averages of the products of the velocity components.

$$f(r) = (\overline{u^2})\overline{u_1 u_1'}$$

$$g(r) = (\overline{u^2})\overline{u_2 u_2'}$$

$$h(r) = (\overline{u^2})^{3/2}\,\overline{u_2^2 u_1'}$$

$$k(r) = (\overline{u^2})^{3/2}\,\overline{u_1^2 u_1'}$$

$$q(r) = (\overline{u^2})^{3/2}\,\overline{u_1 u_2 u_2'}$$

These scalar functions are not independent. This follows from the application of the continuity condition to the double and triple correlation tensors.

$$\frac{\partial R_{ij}(\underline{r})}{\partial r_i} = 0 \tag{A6}$$

$$\frac{\partial T_{ijk}(\underline{r})}{\partial r_k} = 0 \tag{A7}$$

These expressions furnish the following relations between the scalar functions.

$$g(r) = f(r) + \frac{r}{2} f'(r) \tag{A8}$$

$$k(r) = -2h(r) \tag{A9}$$

$$q(r) = -h(r) - \frac{r}{2} h'(r) \tag{A10}$$

The dynamical relations for the scalar functions are found by applying the momentum condition to the correlation tensors. The governing equations are the incompressible Navier-Stokes equations which in tensor notation are

$$\frac{\partial u_i}{\partial t} + u_j \frac{\partial u_i}{\partial x_j} = -\frac{1}{\rho} \frac{\partial p}{\partial x_i} + \nu \nabla_x^2 u_i \tag{A11}$$

The Laplacian operator ∇_x^2 is

$$\nabla_x^2 = \frac{\partial^2}{\partial x_1^2} + \frac{\partial^2}{\partial x_2^2} + \frac{\partial^2}{\partial x_3^2}$$

and p and ν denote pressure and viscosity respectively. The governing equations for the dynamics of the correlation functions are determined by multiplying equation (A11) by u_i and u_i' and adding the resulting time averages. Using equations (A2) and (A3) these equations in tensor notation become

$$\frac{\partial}{\partial t} R_{ij}(\underline{r}) - \frac{\partial}{\partial r_j}\left[T_{ijk}(\underline{r}) + T_{kji}(\underline{r})\right] = 2\nu \nabla^2 R_{ij}(\underline{r}) \tag{A12}$$

These equations may be reduced to a partial differential equation relating the scalar functions f(r) and h(r), through the use of equations (A4)-(A10).

$$\frac{\partial}{\partial t}(\overline{u^2} f) + 2(\overline{u^2})^{3/2}\left(\frac{\partial h}{\partial r} + \frac{4}{r} h\right) = 2\nu\, \overline{u^2}\left(\frac{\partial^2 h}{\partial r^2} + \frac{4}{r}\frac{\partial t}{\partial r}\right) \tag{A13}$$

This expression is called the Von Karman-Howarth equation. Although this equation has been solved only for the limiting cases of large and small Reynolds numbers, it has provided the mathematical basis for understanding turbulent flow. For large values of Reynolds numbers, Von Karman assumed that the scalar functions are independent of viscosity and preserve their shape. This concept of self-preserving correlation functions is based on the assumption that both f and h are functions of one variable, r/L only and that the scale of turbulence L changes with time. Batchelor in reference 9 has presented a concise and complete discussion of the self-preserving solutions of equation (A13).

The concept of self-preserving correlation functions has both mathematical and physical significance. Mathematically it provides a transformation that reduces equation (A13) to an ordinary differential equation.

Physically, the concept is an assumption which concerns the decay of the energy of turbulent flow.

Kolmogoroff, reference 9, used the concept of similarity in a local sense to produce a theory of energy dissipation. The term local implies that only small scale motion can be considered to be both isotropic and self-preserving. The extent of this local region is largely dependent on the Reynolds numbers of the flow. Kolmogoroff's theory was presented in the form of two similarly hypothesis which combine to supply the description of energy decay of small scale turbulence.

A.2 Energy Equation of Isotropic Flow

The local similarity theory of Kolmogoroff becomes important when applied to the energy equation of isotropic flow. This equation is derived by taking a three dimensional Fourier transform of equation (A12) and using equations (6) and (7). Contracting this equation and multiplying by $4\pi\Omega^2$ the governing equation for the decay of energy is

$$\frac{\partial}{\partial t} E(\Omega) + W(\Omega) = -2\nu\Omega^2 E(\Omega) \qquad (A14)$$

The function $E(\Omega)$ is called the energy density function. It represents the distribution of the total kinetic energy per unit mass of the fluid in wave number space. It is related to the spectral tensor by

$$E(\Omega) = \frac{\pi\Omega^2}{4} \Phi_{ii}(\underline{\Omega}) \qquad i \text{ summed} \qquad (A15)$$

The function $W(\Omega)$ is called the work density function. It represents the amount of energy transferred by the non-linear inertial terms contained in an element of wave number space. It is related to the transform of the triple correlation tensor by

$$W(\Omega) = \frac{\pi\Omega^2}{4} 2i\Omega_j W_{kjk}(\underline{\Omega}) \qquad k \text{ summed} \tag{A16}$$

The governing energy equation shows the generally accepted concept of energy decay:

a) The low wave numbers contain the bulk of the energy while viscous dissipation is negligible.

b) The low wave numbers furnish energy by the action of inertial forces to the higher wave number ranges where it is dissipated by viscosity.

This concept and the Kolmogoroff hypothesis, imply that the decay process can not be considered to be similar for all values of wave numbers.

A.3 Development of Multidimensional Spectra

The importance of the energy density function is that its definition, equation (A15), provides a relation between it and the energy spectral tensor. The form of the spectral density tensor is written

$$\Phi_{ij}(\underline{\Omega}) = A(\Omega)\Omega_i\Omega_j + B(\Omega)\delta_{ij} \tag{A17}$$

in terms of the scalar functions A and B with argument Ω. This result has been presented by Batchelor, reference 6 and Coburn reference 13. The scalar functions may be found by applying the continuity condition to

equation (A17)

$$\Omega_i \Phi_{ij}(\underline{\Omega}) = 0 \tag{A18}$$

and using equation (A15). Once the energy density function is known, $\Phi_{ij}(\underline{\Omega})$ may be found.

$$\Phi_{ij}(\underline{\Omega}) = \frac{2E(\Omega)}{\pi\Omega^4}(\Omega^2\delta_{ij} - \Omega_i\Omega_j) \tag{A19}$$

The components of the double correlation tensor and the spectral density tensor are expressed in terms of the scalar correlation functions $f(r)$ and $g(r)$ and the energy density function $E(\Omega)$ respectively. The definition of the scalar correlation functions provides an intepretation for the subscript notation of these tensors. The diagonal elements of the double correlation tensor represent either a longitudinal correlation $f(r)$ or a lateral correlation $g(r)$. By letting the subscripts $i = 1, 2, 3$ represent velocity components in the longitudinal (flight path), lateral, and vertical directions respectively, the diagonal terms of these tensors represent correlation functions and spectral density functions for the longitudinal, lateral and vertical components of the gust velocity. The off diagonal terms of the double correlation tensor and the spectral tensor represent cross-correlations and cross-spectral density functions bewteen the gust velocity components.

The correlation functions for one- and two-dimensions are found by letting the spatial separation distance be

$$r = r_1$$

$$r = \sqrt{r_1^2 + r_2^2}$$

respectively. The spectral density functions for one- and two-dimensions are found by integrating the corresponding higher dimensional spectral density function over the undesired wave number axis. For example,

$$\Phi_{ij}(\Omega_1,\Omega_2) = \int_0^\infty \Phi_{ij}(\underline{\Omega})d\Omega_3 \tag{A20}$$

$$\Phi_{ij}(\Omega_1) = \int_0^\infty \Phi_{ij}(\Omega_1,\Omega_2)d\Omega_2 \tag{A21}$$

For two-dimensional turbulence a correlated spectral density tensor exists whose components are

$$\hat{\Phi}_{ij}(\Omega_1,r_2) = \int_0^\infty \Phi_{ij}(\Omega_1,\Omega_2)\cos(\Omega_2 r_2)d\Omega_2 \tag{A22}$$

Several expressions describing the turbulent motion of a fluid have been developed. Only the expressions due to Dryden and Von Karman will be presented, however, additional expressions may be found by consulting references 4, 11, 14, and 15.

4.4 Von Karman Representation

Von Karman in reference 4 presented an expression for the description of isotropic turbulent flow in terms of the energy density function. He assumed that $W(\Omega)$ can be expressed in terms of $E(\Omega)$ and Ω. Then substituting this expression for $W(\Omega)$ into equation (A14), he considered two cases of flow. While both of these cases neglected the decay term, the first case neglected the viscous term. The solution for this case is

$$E(\Omega) \sim \Omega^{-5/3} \tag{A23}$$

which is the result of Kolmogoroff for large wave numbers, reference 9.

The second case was that of including the viscous terms and assuming that $E(\Omega)$ preserves its shape for small and intermediate values of wave numbers. This resulted in a solution of $E(\Omega)$ which involves integrals of $E(\Omega)$ but has the limiting form for small wave numbers

$$E(\Omega) \sim \Omega^{4} \tag{A24}$$

This expression agrees with the results of many authors for low wave numbers, reference 12. Von Karman proposed an interpolation form for $E(\Omega)$ which has equations (A23) and (A24) for its limiting forms.

$$E(\Omega) = \frac{55}{9} \frac{L}{\pi} \overline{u^2} \frac{\left(\frac{\Omega}{\Omega_o}\right)^4}{\left[1 + \left(\frac{\Omega}{\Omega_o}\right)^2\right]^{17/6}} \tag{A25}$$

The corresponding scalar correlation functions are

$$f(r) = \frac{2^{2/3}}{\Gamma\left(\frac{1}{3}\right)} (\Omega_o r)^{1/3} K_{1/3}(\Omega_o r) \tag{A26}$$

$$g(r) = \frac{2^{2/3}}{\Gamma\left(\frac{1}{3}\right)} (\Omega_o r)^{1/3} \left[K_{1/3}(\Omega_o r) - \frac{\Omega_o r}{2} K_{2/3}(\Omega_o r)\right] \tag{A27}$$

From these expressions the one-, two-, and three-dimensional correlation functions and spectra are

SPECTRAL DENSITY FUNCTIONS

THREE-DIMENSIONAL

$$\left.\begin{aligned}
\Phi_{11}(\underline{\Omega}) &= \frac{55}{9}\frac{\overline{Lu^2}}{\pi^2\Omega_o}\frac{\left(\frac{\Omega_2}{\Omega_o}\right)^2+\left(\frac{\Omega_3}{\Omega_o}\right)^2}{\left[1+\left(\frac{\Omega}{\Omega_o}\right)^2\right]^{17/6}} \\
\Phi_{22}(\underline{\Omega}) &= \frac{55}{9}\frac{\overline{Lu^2}}{\pi^2\Omega_o}\frac{\left(\frac{\Omega_1}{\Omega_o}\right)^2+\left(\frac{\Omega_3}{\Omega_o}\right)^2}{\left[1+\left(\frac{\Omega}{\Omega_o}\right)^2\right]^{17/6}} \\
\Phi_{33}(\underline{\Omega}) &= \frac{55}{9}\frac{\overline{Lu^2}}{\pi^2\Omega_o}\frac{\left(\frac{\Omega_1}{\Omega_o}\right)^2+\left(\frac{\Omega_2}{\Omega_o}\right)^2}{\left[1+\left(\frac{\Omega}{\Omega_o}\right)^2\right]^{17/6}}
\end{aligned}\right\} \qquad \text{(A28)}$$

TWO-DIMENSIONAL

$$\left.\begin{aligned}
\Phi_{11}(\Omega_1,\Omega_2) &= \frac{2\overline{u^2}}{3\pi\Omega_o^2}\frac{1+\left(\frac{\Omega_1}{\Omega_o}\right)^2+\frac{11}{3}\left(\frac{\Omega_2}{\Omega_o}\right)^2}{\left[1+\left(\frac{\Omega_1}{\Omega_o}\right)^2+\left(\frac{\Omega_2}{\Omega_o}\right)^2\right]^{7/3}} \\
\Phi_{22}(\Omega_1,\Omega_2) &= \frac{2\overline{u^2}}{3\pi\Omega_o^2}\frac{1+\frac{11}{3}\left(\frac{\Omega_1}{\Omega_o}\right)^2+\left(\frac{\Omega_2}{\Omega_o}\right)^2}{\left[1+\left(\frac{\Omega_1}{\Omega_o}\right)^2+\left(\frac{\Omega_2}{\Omega_o}\right)^2\right]^{7/3}} \\
\Phi_{33}(\Omega_1,\Omega_2) &= \frac{16\overline{u^2}}{9\Omega_o^2\pi}\frac{\left(\frac{\Omega_1}{\Omega_o}\right)^2+\left(\frac{\Omega_2}{\Omega_o}\right)^2}{\left[1+\left(\frac{\Omega_1}{\Omega_o}\right)^2+\left(\frac{\Omega_2}{\Omega_o}\right)^2\right]^{7/3}}
\end{aligned}\right\} \qquad \text{(A29)}$$

$$\hat{\Phi}_{33}(\Omega_1,r_2) = \frac{2^{1/6}\overline{u^2}}{\sqrt{\pi}\,\Omega_o\Gamma\left(\frac{1}{3}\right)}\left\{\frac{-(r_2\Omega_o)^{11/6}K_{1/6}\left(\Omega_o r_2\sqrt{1+\left(\frac{\Omega_1}{\Omega_o}\right)^2}\right)}{\left[1+\left(\frac{\Omega_1}{\Omega_o}\right)^2\right]^{11/12}}\right.$$

$$\left. + \frac{\left[1+\frac{8}{3}\left(\frac{\Omega_1}{\Omega_o}\right)^2\right](\Omega_o r_2)^{5/6}K_{5/6}\left(\Omega_o r_2\sqrt{1+\left(\frac{\Omega_1}{\Omega_o}\right)^2}\right)}{\left[1+\left(\frac{\Omega_1}{\Omega_o}\right)^2\right]^{17/12}}\right\} \qquad \text{(A31)}$$

$$\Omega_o = \frac{1}{L}\frac{\Gamma\left(\frac{1}{2}\right)\Gamma\left(\frac{5}{6}\right)}{\Gamma\left(\frac{1}{3}\right)} = \frac{1}{1.3389853L} \qquad \text{(A32)}$$

$$\Omega^2 = \Omega_1^2 + \Omega_2^2 + \Omega_3^2 \qquad \text{(A33)}$$

CORRELATION FUNCTIONS

TWO-DIMENSIONAL

$$\left.\begin{aligned}
R_{11}(r_1,r_2) &= \frac{2^{2/3}\overline{u^2}}{\Gamma\left(\frac{1}{3}\right)}\left[(\Omega_o r)^{1/3}K_{1/3}(\Omega_o r) - \frac{\Omega_o^{4/3}r_2^2 r^{-2/3}}{2}K_{2/3}(\Omega_o r)\right] \\
R_{22}(r_1,r_2) &= \frac{2^{2/3}\overline{u^2}}{\Gamma\left(\frac{1}{3}\right)}\left[(\Omega_o r)^{1/3}K_{1/3}(\Omega_o r) - \frac{\Omega_o^{4/3}r^{-2/3}r_1^2}{2}K_{2/3}(\Omega_o r)\right] \\
R_{33}(r_1,r_2) &= \frac{2^{2/3}\overline{u^2}}{\Gamma\left(\frac{1}{3}\right)}\left[(\Omega_o r)^{1/3}K_{1/3}(\Omega_o r) - \frac{\Omega_o r}{2}K_{2/3}(\Omega_o r)\right] \\
r^2 &= r_1^2 + r_2^2
\end{aligned}\right\} \qquad \text{(A34)}$$

ONE-DIMENSIONAL

$$\left.\begin{aligned}
\Phi_{11}(\Omega_1) &= \frac{2\overline{Lu^2}}{\pi}\,\frac{1}{\left[1+\left(\frac{\Omega_1}{\Omega_o}\right)^2\right]^{5/6}} \\
\Phi_{22}(\Omega_1) &= \frac{\overline{Lu^2}}{\pi}\,\frac{1+\frac{8}{3}\left(\frac{\Omega_1}{\Omega_o}\right)^2}{\left[1+\left(\frac{\Omega_1}{\Omega_o}\right)^2\right]^{11/6}} \\
\Phi_{33}(\Omega_1) &= \frac{\overline{Lu^2}}{\pi}\,\frac{1+\frac{8}{3}\left(\frac{\Omega_1}{\Omega_o}\right)^2}{\left[1+\left(\frac{\Omega_1}{\Omega_o}\right)^2\right]^{11/6}}
\end{aligned}\right\} \qquad \text{(A30)}$$

CORRELATED SPECTRA

$$\hat{\Phi}_{11}(\Omega_1,r_2) = \frac{2^{1/6}\overline{u^2}}{\sqrt{\pi}\,\Omega_o\Gamma\left(\frac{1}{3}\right)}\left\{-(\Omega_o r_2)^{11/6}\left[1+\left(\frac{\Omega_1}{\Omega_o}\right)^2\right]K_{1/6}\left(\Omega_o r_2\sqrt{1+\left(\frac{\Omega_1}{\Omega_o}\right)^2}\right)\right.$$
$$\left.+\frac{2(\Omega_o r_2)^{5/6}K_{5/6}\left(\Omega_o r_2\sqrt{1+\left(\frac{\Omega_1}{\Omega_o}\right)^2}\right)}{\left[1+\left(\frac{\Omega_1}{\Omega_o}\right)^2\right]^{5/12}}\right\}$$

$$\hat{\Phi}_{22}(\Omega_1,r_2) = \frac{2^{1/6}\overline{u^2}}{\sqrt{\pi}\,\Omega_o\Gamma\left(\frac{1}{3}\right)}\left\{\frac{\left(\frac{\Omega_1}{\Omega_o}\right)^2(\Omega_o r_2)^{11/6}K_{1/6}\left(r_2\Omega_o\sqrt{1+\left(\frac{\Omega_1}{\Omega_o}\right)^2}\right)}{\left[1+\left(\frac{\Omega_1}{\Omega_o}\right)^2\right]^{11/12}}\right.$$
$$\left.+\frac{(\Omega_o r_2)^{5/6}\left[1+\frac{8}{3}\left(\frac{\Omega_1}{\Omega_o}\right)^2\right]K_{5/6}\left(\Omega_o r_2\sqrt{1+\left(\frac{\Omega_1}{\Omega_o}\right)^2}\right)}{\left[1+\left(\frac{\Omega_1}{\Omega_o}\right)^2\right]^{17/12}}\right\} \qquad \text{(A31)}$$

ONE-DIMENSIONAL

$$\left.\begin{aligned} R_{11}(r_1) &= \frac{2^{2/3}\overline{u^2}}{\Gamma\left(\frac{1}{3}\right)}(\Omega_o r_1)^{1/3} K_{1/3}(\Omega_o r_1) \\ R_{22}(r_1) &= \frac{2^{2/3}\overline{u^2}}{\Gamma\left(\frac{1}{3}\right)}(\Omega_o r_1)^{1/3}\left[K_{1/3}(\Omega_o r_1) - \frac{\Omega_o r_1}{2} K_{2/3}(\Omega_o r_1)\right] \\ R_{33}(r_1) &= \frac{2^{2/3}\overline{u^2}}{\Gamma\left(\frac{1}{3}\right)}(\Omega_o r_1)^{1/3}\left[K_{1/3}(\Omega_o r_1) - \frac{\Omega_o r_1}{2} K_{2/3}(\Omega_o r_1)\right] \end{aligned}\right\} \quad (A35)$$

A.5 Dryden Representations

Dryden presented an expression for the description of turbulence in terms of a correlation function, which is expressed in terms of the exponential decay function. He found that this expression gave a good fit on experimentally measured correlation functions, reference 5, and spectral density functions, reference 3. These data were measured from turbulence which occurred behind a screen placed in a wind tunnel. Dryden has shown good agreement between the expression

$$f(r) = e^{-r/L} \quad (A36)$$

and experimental data for experimentally obtained values of L. Houbolt in reference 8 has presented an expression for the energy density function.

$$E(\Omega) = \frac{\overline{u^2} 8L}{\pi} \frac{(L\Omega)^4}{\left[1 + (L\Omega)^2\right]^3} \quad (A37)$$

The limiting form for small Ω is in accordance with previous theory, reference 12, and Von Karman's expression, equation (A24). The limiting form for large Ω is

$$E(\Omega) \sim \Omega^{-2} \tag{A38}$$

which is not in agreement with either the theory of decay or the expression of Von Karman, equation (A23). This is a result of the form of $f(r)$ given in equation (A36).

For this scalar function to be a solution of equation (A13), $f(r)$ must be similar for all values of r and Reynolds numbers. This in turn demands similarity of $E(\Omega)$ for all Ω which is incompatible with both physical reasoning and experimental results. Dryden discusses the form of $f(r)$, reference 5, and shows that its slope at $r = 0$ is $-1/L$. This does not agree with the properties of $f(r)$ which shows that its slope at $r = 0$ should be zero. This discrepancy has led Dryden to state that equation (A36) is not correct for values of r near zero.

The scalar correlation function $g(r)$ is found from equations (A36) and (A8).

$$g(r) = \left(1 - \frac{r}{2L}\right)e^{-r/L} \tag{A39}$$

From equations (A36), (A39), and (A37) the one-, two-, and three-dimensional correlation functions and spectra are

SPECTRAL DENSITY FUNCTIONS

THREE-DIMENSIONAL

$$\left.\begin{aligned}
\Phi_{11}(\underline{\Omega}) &= \frac{16L^5\overline{u^2}}{\pi^2}\,\frac{\Omega_2^2+\Omega_3^2}{\left(1+L^2\Omega_1^2+L^2\Omega_2^2+L^2\Omega_3^2\right)^3}\\
\Phi_{22}(\underline{\Omega}) &= \frac{16L^5\overline{u^2}}{\pi^2}\,\frac{\Omega_1^2+\Omega_3^2}{\left(1+L^2\Omega_1^2+L^2\Omega_2^2+L^2\Omega_3^2\right)^3}\\
\Phi_{33}(\underline{\Omega}) &= \frac{16L^5\overline{u^2}}{\pi^2}\,\frac{\Omega_1^2+\Omega_2^2}{\left(1+L^2\Omega_1^2+L^2\Omega_2^2+L^2\Omega_3^2\right)^3}
\end{aligned}\right\} \qquad (A40)$$

TWO-DIMENSIONAL

$$\left.\begin{aligned}
\Phi_{11}(\Omega_1,\Omega_2) &= \frac{L^2\overline{u^2}}{\pi}\,\frac{1+L^2\Omega_1^2+4L^2\Omega_2^2}{\left(1+L^2\Omega_1^2+L^2\Omega_2^2\right)^{5/2}}\\
\Phi_{22}(\Omega_1,\Omega_2) &= \frac{L^2\overline{u^2}}{\pi}\,\frac{1+4L^2\Omega_1^2+L^2\Omega_2^2}{\left(1+L^2\Omega_1^2+L^2\Omega_2^2\right)^{5/2}}\\
\Phi_{33}(\Omega_1,\Omega_2) &= \frac{3L^2\overline{u^2}}{\pi}\,\frac{L^2\Omega_1^2+L^2\Omega_2^2}{\left(1+L^2\Omega_1^2+L^2\Omega_2^2\right)^{5/2}}
\end{aligned}\right\} \qquad (A41)$$

ONE-DIMENSIONAL

$$\left.\begin{aligned}
\Phi_{11}(\Omega_1) &= \frac{2L\overline{u^2}}{\pi}\,\frac{1}{1+L^2\Omega_1^2} \\
\Phi_{22}(\Omega_1) &= \frac{L\overline{u^2}}{\pi}\,\frac{1+3L^2\Omega_1^2}{(1+L^2\Omega_1^2)^2} \\
\Phi_{33}(\Omega_1) &= \frac{L\overline{u^2}}{\pi}\,\frac{1+3L^2\Omega_1^2}{(1+L^2\Omega_1^2)^2}
\end{aligned}\right\} \qquad (A42)$$

CORRELATED SPECTRA

$$\left.\begin{aligned}
\hat{\Phi}_{11}(\Omega_1,r_2) &= \frac{L\overline{u^2}}{\pi}\left\{-\left(\frac{r_2}{L}\right)^2 K_o\left(\frac{r_2}{L}\sqrt{1+L^2\Omega_1^2}\right)\right. \\
&\qquad \left. + \frac{2r_2 K_1\left(\frac{r_2}{L}\sqrt{1+L^2\Omega_1^2}\right)}{L\sqrt{1+L^2\Omega_1^2}}\right\} \\
\hat{\Phi}_{22}(\Omega_1,r_2) &= \frac{L\overline{u^2}}{\pi}\left\{\frac{L^2\Omega_1^2\left(\frac{r_2}{L}\right)^2 K_o\left(\frac{r_2}{L}\sqrt{1+L^2\Omega_1^2}\right)}{\sqrt{1+L^2\Omega_1^2}}\right. \\
&\qquad \left. + \frac{(1+3L^2\Omega_1^2)\frac{r_2}{L}\,K_1\left(\frac{r_2}{L}\sqrt{1+L^2\Omega_1^2}\right)}{(1+L^2\Omega_1^2)^{3/2}}\right\} \\
\hat{\Phi}_{33}(\Omega_1,r_2) &= \frac{L\overline{u^2}}{\pi}\left\{\frac{-\left(\frac{r_2}{L}\right)K_o\left(\frac{r_2}{L}\sqrt{1+L^2\Omega_1^2}\right)}{(1+L^2\Omega_1^2)}\right. \\
&\qquad \left. + \frac{r_2}{L}\,\frac{(1+3L^2\Omega_1^2)K_1\left(\frac{r_2}{L}\sqrt{1+L^2\Omega_1^2}\right)}{(1+L^2\Omega_1^2)^{3/2}}\right\}
\end{aligned}\right\} \qquad (A43)$$

CORRELATION FUNCTIONS

TWO-DIMENSIONAL

$$\left.\begin{aligned} R_{11}(r_1,r_2) &= \overline{u^2}\left(1 - \frac{r_2^2}{2rL}\right)e^{-r/L} \\ R_{22}(r_1,r_2) &= \overline{u^2}\left(1 - \frac{r_1^2}{2rL}\right)e^{-r/L} \\ R_{33}(r_1,r_2) &= \overline{u^2}\left(1 - \frac{r}{2L}\right)e^{-r/L} \\ r^2 &= r_1^2 + r_2^2 \end{aligned}\right\} \qquad (A44)$$

ONE-DIMENSIONAL

$$\left.\begin{aligned} R_{11}(r_1) &= \overline{u^2}e^{-r_1/L} \\ R_{22}(r_2) &= \overline{u^2}\left(1 - \frac{r_1}{2L}\right)e^{-r_1/L} \\ R_{33}(r_1) &= \overline{u^2}\left(1 - \frac{r_1}{2L}\right)e^{-r_1/L} \end{aligned}\right\} \qquad (A45)$$

$$p(t) = \sum_{n=1}^{N} \int_{-\infty}^{\infty} h_n(t_1) w_n(t - t_1) dt_1 \tag{B2}$$

When the downwash inputs are the vertical gust velocities of homogeneous and stationary atmospheric turbulence, the description of the response is provided by the correlation function

$$R_p(\tau) = \overline{p(t)p(t + \tau)} = \sum_{n=1}^{N} \sum_{m=1}^{N} \int_{-\infty}^{\infty} \int_{-\infty}^{\infty} h_n(t_1) h_m(t_2) R_{w_{nm}}(\tau + t_2 - t_1) dt_1 dt_2 \tag{B3}$$

The cross-correlation function $R_{w_{nm}}$ is the spatial correlation of the nth and mth inputs which are assumed to have zero means and satisfy the limit of equation (10). The cross-correlation function is dependent only on the spatial separation of the nth and mth inputs, r_{nm} and the spatial separation r_1. For isotropic atmospheric turbulence, the assumption that Taylor's hypothesis is valid enables the time and spatial coordinates to be related through the airplane's velocity:

$$r_1 = U\tau \tag{B4}$$

APPENDIX B

DEVELOPMENT OF THE TWO-DIMENSIONAL INPUT-OUTPUT RELATIONS

The purpose of this Appendix is to derive the two-dimensional input-output relations which are discussed in Chapter Two and are used in the calculations.

The two-dimensional input-output relation is developed as an extension of one-dimensional theory. This extension is easily perceived by using the development of system analysis with multiple inputs. Consider the wing of an airplane to have N distinct downwash inputs $w_n(t)$ and a single response $p(t)$. Each one of the downwash inputs is assumed to act over a finite interval of the span Δy. If, in addition, the downwash input is assumed to be invariant in the lateral direction over Δy, the resulting response for that interval is given in terms of the downwash by

$$p_n(t) = \int_{-\infty}^{\infty} h_n(t_1) w_n(t - t_1) dt_1 \tag{B1}$$

The function $h_n(t)$ is the linear response of the airplane to the individual downwash $w_n(t)$ that is mathematically described to be a unit impulse at time t_1 and a constant over the spanwise interval Δy. Assuming the entire system to be linear, the superposition principle can be applied and the total response is

This relation and the assumption that time and statistical averages are equivalent allows the isotropic two-dimensional correlation function presented in Appendix A to be used for the cross-correlation function.

$$R_{w_{nm}}(\tau + t_2 - t_1) = R_{33}(r_1, r_{nm}) \tag{B5}$$

The statistical description of the response in the frequency domain is given by the Fourier transform of the correlation function, assuming the relation

$$\int_{-\infty}^{\infty} R_p(\tau)d\tau < \infty$$

is satisfied. Assuming that the Fourier transform of the right hand side of equation (B3) exists, the spectral density function of the response is

$$\phi_p(\omega) = \sum_{n=1}^{N} \sum_{m=1}^{N} H_n(\omega)H_m^*(\omega)\phi_{w_{nm}}(\omega) \tag{B6}$$

The frequency response functions $H_n(\omega)$ are the Fourier transforms of the impulse response functions $h_n(t)$. These functions $H_n(\omega)$ represent the complex amplitude of the response of the airplane to a sinusoidal downwash of unit amplitude which is constant over Δy and has frequency ω.

The spectral density function $\phi_{w_{nm}}$ is the spatial cross-spectral density function of the nth and mth inputs and it is the Fourier transform of $R_{w_{nm}}(\tau)$

$$\phi_{w_{nm}}(\omega) = \frac{1}{\pi} \int_{-\infty}^{\infty} R_{w_{nm}}(\tau) e^{-i\omega\tau} \, d\tau \tag{B7}$$

For isotropic atmospheric turbulence, the assumption that Taylor's hypothesis is valid provides an analogous relation to equation (B4)

$$\omega = U\Omega_1 \tag{B8}$$

This relation and the assumption that time and statistical averages are equivalent allows the isotropic two-dimensional correlation spectral density function presented in Appendix A to be used for the cross-spectral density function

$$\phi_{w_{nm}}(\omega) = \frac{1}{U} \hat{\phi}_{33}(\Omega_1, r_{nm}) \tag{B9}$$

For isotropic turbulence the cross-spectral density functions $\phi_{w_{nm}}(\omega)$ have the property that the only distinct spectra are

$$\phi_{w_{i,i+k}} \equiv \phi_{w_{i+k,i}} \equiv \phi_{w_{1,1+k}} \qquad \begin{cases} k = 0, \ . \ . \ ., N - i \\ i = 1, \ . \ . \ ., N - k \end{cases} \tag{B10}$$

This property allows the response spectral density function defined by equation (B6) to be written

$$\phi_{p}(\omega) = \phi_{w_{11}}(\omega)\left[\sum_{n=1}^{N} H_n(\omega)H_n^*(\omega)\right] + 2\phi_{w_{12}}(\omega)R_e\left[\sum_{n=1}^{N-1} H_n(\omega)H_{n+1}^*(\omega)\right]$$
$$+ \ldots + 2\phi_{1N}(\omega)R_e\left[H_n(\omega)H_N^*(\omega)\right]$$

A continuous two-dimensional input-output relation is obtained by applying the limit $N \to \infty$ and $\Delta y \to 0$ to equation (B2). The summation is replaced by an integration over the span and the downwash is now a function of the lateral coordinate and time. The total response is

$$p(t) = \int_{-b/2}^{b/2} \int_{-\infty}^{\infty} h(t,y)w(t - t_1,y)dt_1dy \qquad (B11)$$

This expression is the extension of the one-dimensional response analysis to include a continuous spanwise variation of the downwash. The function $h(t,y)$ represents the response of the airplane to a downwash represented mathematically by a time-space impulse function applied at time t_1 and at wing station y.

When the downwash input is the vertical gust velocity of a homogeneous and stationary atmospheric turbulence field, the description of the response is

$$R_p(\tau) = \iint_{-b/2}^{b/2} \iint_{-\infty}^{\infty} h(t_1,y_1)h(t_2,y_2)R_w(t_2 + \tau - t_1,y_2 - y_1)dt_1dt_2dy_1dy_2 \qquad (B12)$$

The cross-correlation function $R_w(t_2 + \tau - t_1, y_2 - y_1)$ is the spatial correlation of the inputs which are assumed to have zero means and satisfy the limit of equation (10). For isotropic atmospheric turbulence, the assumption that Taylor's hypothesis is valid enables equation (B4) to be used along with the assumption that time and statistical averages are equivalent to relate the isotropic two-dimensional correlation function presented in Appendix A to the cross-correlation function.

$$R_w(t_2 + \tau - t_1, |y_2 - y_1|) = R_{33}(r_1, r_2) \tag{B13}$$

The statistical description of the response in the frequency domain is

$$\phi_p(\omega) = \int_{-b/2}^{b/2} \int_{-b/2}^{b/2} \hat{H}(\omega, y_1)\hat{H}^*(\omega, y_2)\hat{\phi}_w(\omega, r_2)dy_1 dy_2 \tag{B14}$$

The spectral density function $\hat{\phi}_w(\omega, r_2)$ is the spatial cross-spectral density function of the inputs and it is the Fourier transform of $R_w(\tau, |y_2 - y_1|)$

$$\hat{\phi}_w(\omega, |y_2 - y_1|) = \frac{1}{\pi} \int_{-\infty}^{\infty} R_w(\tau, |y_2 - y_1|)e^{-i\omega\tau}\, d\tau \tag{B15}$$

For isotropic atmospheric turbulence, equation (B8) and the assumption that time and statistical averages are equivalent allows the isotropic

correlated spectral density function presented in Appendix A to be used for the cross-spectral density function.

$$\hat{\Phi}_w(\omega,|y_2 - y_1|) = \frac{1}{U}\hat{\Phi}_{33}(\Omega_1,r_2) \tag{B16}$$

The frequency response function $H(\omega,y)$ is the Fourier transform

$$\hat{H}(\omega,y) = \int_{-\infty}^{\infty} h(t,y)e^{-i\omega t}\,dt \tag{B17}$$

and it represents the complex amplitude of the response of the airplane to a downwash field which is expressed mathematically as the product of a spatial impulse function applied at y and a sinusoidal wave field of unit amplitude and frequency ω. The quantity $\hat{H}(\omega,y_1)\hat{H}^*(\omega,y_2)$ a complex quantity but the imaginary part can be ignored because in the spatial correlation of equation (B14), $\hat{\Phi}(\omega,|y_2 - y_1|)$ is an even function of $|y_2 - y_1|$.

An alternate form of the two-dimensional input-output relation is obtained by removing the spatial correlation of equation (B14). The convolution is removed by expressing the correlation spectral density function in terms of the two-dimensional spectral density function $\Phi_w(\omega,\Omega_2)$. These two spectra are related by a spatial Fourier transform

$$\hat{\Phi}_w(\omega,|y_2 - y_1|) = \frac{1}{2}\int_{-\infty}^{\infty} \Phi_w(\omega,\Omega_2)e^{i|y_2-y_1|\Omega_2}\,d\Omega_2 \tag{B18}$$

Using this expression in equation (B14) the input-output relation is

$$\Phi_p(\omega) = \frac{1}{2} \int_{-\infty}^{\infty} |H(\omega,\Omega_2)|^2 \Phi_w(\omega,\Omega_2) d\Omega_2 \tag{B19}$$

The function $H(\omega,\Omega_2)$ is a two-dimensional frequency response function that represents the complex amplitude of the response of the airplane to a two-dimensional downwash field represented by two sinusoidal waves of unit amplitude and frequencies ω and Ω_2. It is defined in terms of the frequency response function $\hat{H}(\omega,y)$ by

$$H(\omega,\Omega_2) = \int_{-\infty}^{\infty} \hat{H}(\omega,y) e^{-iy\Omega 2} \, dy \tag{B20}$$

For isotropic atmospheric turbulence, equation (B8) and the assumption that time and statistical averages are equivalent allows the isotropic two-dimensional spectral density function presented in Appendix A to be used for the two-dimensional spectral density function defined by the inverse Fourier transform of equation (B18).

$$\Phi_w(\omega,\Omega_2) = \frac{1}{U} \Phi_{33}(\Omega_1,\Omega_2) \tag{B21}$$

APPENDIX C

DESCRIPTION OF THE TREND STUDY MATHEMATICAL MODEL

The mathematical model of the airplane used for the trend study calculations will be presented in this Appendix. The expressions for the generalized forces and the frequency response functions are presented and the corresponding two-dimensional response spectra are calculated. From these spectra the truncation error is evaluated and the response statistical parameters are calculated.

C.1 Equations of Motion

The airplane is represented by an unswept tapered wing and a lumped mass fuselage. It is restrained against all motion and deformation except rigid-body vertical motion and wing vertical bending deformation. The total plunging displacement of any point of the airplane is given in terms of the sum of the products of the natural modes of motion and their associated generalized coordinates.

$$z = \sum_{i=1}^{N} \xi_i(x,y) q_i(t) \qquad (C1)$$

The generalized coordinates are calculated by solving Lagranges equations of motion, equation (31), for the plunging motion of the airplane subjected to a two-dimensional sinusoidally varying downwash field. The equations of motion are simplified by using weighted mode shapes that satisfy

$$\int_{-b/2}^{b/2} m(y)\xi_i(y)\xi_j(y)dy = \begin{cases} M_a & i = j \\ 0 & i \neq j \end{cases} \qquad (C2)$$

The orthogonality property of equation (C2) is satisfied by using free-free symmetrical vertical wing bending modes. These modes are normalized by weighting them by the mass distribution $m(y)$.

For the trend study calculations it is necessary to work with nondimensional parameters. This requires that the equations of motion be expressed in terms of nondimensional generalized coordinates, masses, and forces. The nondimensional reduced frequency parameter, k, is commonly used. It is related to the circular frequency by

$$k = \frac{\omega \bar{c}}{U} \qquad (C3)$$

From these relations the equations of motion written in terms of reduced frequency are

$$\left(\frac{U}{\bar{c}}\right)^2 (k_i^2 - k^2) M_a q_i(k, \Omega_2) = \sum_{j=1}^{N} Q_{ij}^M(k) q_j(k, \Omega_2) + Q_i^G(k, \Omega_2) \qquad (C4)$$

C.2 Generalized Forces

For the trend study the nondimensional generalized forces are calculated by strip-analysis aerodynamic theory. Strip analysis is concerned only with the spanwise lift distribution on the wing. This distribution is found by calculating the local lift on each of a number of streamwise strips on the wing. The local lift per unit strip width

is assumed to be proportional to the local angle of attack. For the case of simple-strip analysis, two-dimensional flow theory is applied to each individual strip. The vortex sheet on the wing is replaced by a single concentrated bound vortex which is located at the quarter-chord point. The boundary condition associated with the location of the vortex is the downwash at the three-quarter-chord point. The selection of the downwash at this point requires that the local lift-curve slope have the two-dimensional incompressible value 2π. This value of 2π is significant when unsteady flow is being considered. Each individual strip is considered to be an oscillating flat plate in two-dimensional incompressible flow. For a straight wing the unsteady lift of each strip is given by Theoderson in reference 44. This unsteady simple-strip analysis has been used by Barmby, Cunningham, and Garrick in reference 46 for flutter studies of both straight and unswept wings.

Yates, in reference 41, presents a modified unsteady strip-analysis theory. He modifies the unsteady simple-strip theory for finite span effects by letting the position of the aerodynamic center move from the quarter chord. This change of position of the aerodynamic center requires that the boundary condition be the downwash taken at a location on the chord other than the three-quarter-chord point. This modification of the simple-strip analysis is reflected only in the circulatory terms of the expression of the unsteady lift distribution. The modification of these terms is made by letting the local lift-curve slope have a value other than 2π and taking the effective angle of attack at some position other than the three-quarter-chord point. The value of the local-lift curve slope

c_{l_α} can be calculated from any suitable steady-state aerodynamic theory for finite wings. The value and location of the effective angle of attack is given in reference 41.

The generalized motion forces are formulated from the modified-strip analysis. The incompressible unsteady spanwise lift distribution for an unswept oscillating wing is

$$\ell_i^M(y,k) = \rho U^2 \left[\frac{\pi k^2}{2} \left(\frac{c}{\bar{c}} \right)^2 - ikc_{l_\alpha} \left(\frac{c}{\bar{c}} \right) C(k) \right] \xi_i \tag{C5}$$

The unsteady circulating term of the lift distribution is given by the two-dimensional incompressible Theodorsen function given in reference 44 in terms of the Bessel functions J_n and Y_n.

$$C(k) = \frac{-J_1(k) + iY_1(k)}{-(J_1(k) + Y_1(k)) + i(Y_1(k) - J_0(k))} \tag{C6}$$

The modified-strip analysis is used for the formulation of the generalized gust forces. The unsteady lift distribution resulting from a two-dimensional sinusoidal downwash field is given in terms of the local lift-curve slope and effective angle of attack. The value of the local lift-curve slope c_{l_α} can be calculated from any suitable steady-state aerodynamic theory for finite wings. The local angle of attack is the downwash normalized by the airplane velocity U.

$$\alpha = \frac{w_G}{U} e^{iks} e^{i\Omega_2 y} \tag{C7}$$

The downwash is taken at a point on the chord given by reference 41. The response of a rigid two-dimensional wing in incompressible flow to a one-dimensional sinusoidal downwash field is given in reference 24. Modifying this expression for finite span effects and the local angle of attack given by equation (C7), the incompressible unsteady lift distribution is

$$\ell^G(y,k,\Omega_2) = \rho U^2 c_{l_\alpha} c\, K(k) \frac{w_G}{U} e^{i\Omega 2y} \tag{C8}$$

The function $K(k)$ is called the circulation function and is given in reference 24.

$$K(k) = C(k)\left[J_o(k) - iJ_1(k)\right] + iJ_1(k) \tag{C9}$$

Substituting the lift distributions given by equations (C5) and (C8) into the expressions for the generalized forces given by equations (33) and (34), respectively, the generalized forces are

$$Q^M_{ij}(k) = \rho U^2 \int_{-b/2}^{b/2} \left[\frac{2\pi k^2}{4}\left(\frac{c}{\bar{c}}\right)^2 - ikc_{l_\alpha}\left(\frac{c}{\bar{c}}\right)C(k)\right]\xi_i \xi_j \, dy \tag{C10}$$

$$Q^G_i(k,\Omega_2) = \rho U^2 K(k) \frac{w_G}{U} \int_{-b/2}^{b/2} cc_{l_\alpha} \cos(\Omega_2 y)\xi_i \, dy \tag{C11}$$

The antisymmetrical term in the spatial frequency term is neglected because the integral of an odd function over a symmetric interval vanishes. These forces are written in terms of a normalized lift-curve slope distribution γ. The local lift-curve slope is normalized by the total

lift curve slope $C_{L\alpha}$ of the wing. The spanwise variable is normalized by the semispan and forces are expressed in terms of nondimensional coefficients.

$$Q^M_{ij}(k) = C_{L\alpha}\rho U^2 S \sum_{j=1}^{N} q_j\left(A_{ij}\frac{k^2}{2} - ikC(k)B_{ij}\right) \tag{C12}$$

$$Q^G_i(k,\Omega_2^*) = C_{L\alpha}\rho U^2 SK(k)\frac{w_G}{U}\,BB_i(\Omega_2^*) \tag{C13}$$

The nondimensional coefficients and variables are

$$A_{ij} = \frac{1}{2}\left(\frac{2\pi}{C_{L\alpha}}\right)\int_0^1 \left(\frac{c}{\bar{c}}\right)^2 \xi_i\xi_j\,dy^* \tag{C14}$$

$$B_{ij} = \frac{1}{2}\int_0^1 \gamma(y^*)\xi_i\xi_j\,dy^* \tag{C15}$$

$$BB_i(\Omega_2^*) = \frac{1}{2}\int_0^1 \gamma(y^*)\cos(\Omega_2^* y^*)\xi_i\,dy^* \tag{C16}$$

$$y^* = \frac{y}{\frac{b}{2}}$$

$$\Omega_2^* = \left(\frac{b}{2}\right)\Omega_2$$

$$\gamma = \frac{cc_{l\alpha}}{\bar{c}C_{L\alpha}}$$

The nondimensional equations are written in terms of the nondimensional generalized coordinate $\hat{q}_i$ by substituting the generalized forces given by equations (C10) and (C11) into equation (C4) and defining the mass parameter λ.

$$(k_i^2 - k^2)\lambda\hat{q}_i(k,\Omega_2^*) - \sum_{j=1}^{N} \hat{q}_j(k,\Omega_2^*)(k^2A_{ij} - 2ikC(k)B_{ij}) = 2K(k)BB_i(\Omega_2^*) \tag{C17}$$

$$\lambda = \frac{2M_a}{\rho C_{L\alpha}\bar{c}S} \tag{C18}$$

C.3 Frequency Response Functions

The frequency response functions needed to determine the desired response spectra are expressed in terms of the nondimensional generalized coordinates.

Two-Dimensional Analysis

The two-dimensional frequency response functions are calculated from the nondimensional generalized coordinates which are found to be solutions of the equations of motion given by equation (C17). The response functions calculated in this study are presented below.

Plunge Displacement

The nondimensional plunge displacement frequency response function is the nondimensional generalized coordinate for the rigid-body plunging mode of the airplane, $\xi_1 = 1$.

$$z(k,\Omega_2^*) = \frac{q_1(k,\Omega_2^*)}{\left(\frac{w_G}{U}\right)\bar{c}} \equiv \hat{q}_1(k,\Omega_2^*) \tag{C19}$$

Plunge Velocity

The plunging velocity frequency response function is normalized by the gust velocity magnitude and is calculated in terms of the plunge displacement.

$$\dot{z}(k,\Omega_2^*) = \frac{\dot{q}_1(k,\Omega_2^*)}{w_G} = ik\hat{q}_1(k,\Omega_2^*) \tag{C20}$$

Plunge Acceleration

The plunging acceleration frequency response function is normalized by the "sharp-edge gust" acceleration, which neglects the motion aerodynamic forces and considers only the response to the steady part of the gust forces.

$$\ddot{z}(k,\Omega_2^*) = \frac{\ddot{q}_1(k,\Omega_2^*)}{\ddot{z}_s} = -\frac{k^2\lambda\hat{q}_1(k,\Omega_2^*)}{2BB_1^*} \tag{C21}$$

The sharp-edge gust acceleration is

$$\ddot{z}_s = \frac{2BB_1^*}{\lambda}\left(\frac{U}{\bar{c}}\right)^2$$

Bending Moment

The wing bending moment frequency response function is found by taking the moment of the total load distribution on the wing. The total load distribution consists of the inertial, motion, and gust forces acting on the wing.

$$BM(k,\Omega_2^*,y) = \int_y^{b/2} \left[\ell G(k,\Omega_2^*,\eta) + \sum_{i=1}^{N} \left\{ \ell M_i(k,\eta) + \left(\frac{U}{c}\right)^2 k^2 \xi_i q_i m(\eta) \right\} \right] (\eta - y) d\eta \tag{C22}$$

The load distributions of the motion and gust forces are given by equations (C5) and (C8), respectively. The antisymmetric part of the gust forces is neglected since only the symmetric bending moment response is desired. The bending moment is rewritten in a manner similar to that used for the equations of motion. The nondimensional bending moment at the root, that is, $y = 0$ is

$$\left(\frac{\bar{c}\lambda}{UM\frac{b}{2}}\right)\frac{BM(k,\Omega_2^*,0)}{w_G} = K(k)BB' + \frac{1}{2}\sum_{i=1}^{N}\left[k^2 A_i' - 2ikC(k)B_i' + 2\lambda k^2 D_i\right]\hat{q}_i \tag{C23}$$

The dimensionless coefficients and variables are

$$A_i' = \frac{1}{2}\int_0^1 \frac{2\pi}{C_{L\alpha}}\left(\frac{c}{\bar{c}}\right)^2 \xi_i \eta^* d\eta^*$$

$$B_i' = \frac{1}{2}\int_0^1 \gamma(\eta^*)\xi_i \eta^* d\eta^*$$

$$D_i = \int_0^1 \gamma(\eta^*) m^* \eta^* d\eta^*$$

$$BB'(\Omega_2^*) = \frac{1}{2}\int_0^1 \gamma(\eta^*)\cos(\Omega_2^*\eta^*)\eta^* d\eta^*$$

$$\eta^* = \frac{\eta}{\frac{b}{2}}$$

$$m^* = \frac{m}{M_a}$$

The wing-root bending moment frequency response function is normalized by bending moment resulting from the steady-state gust forces, that is, for $k = 0$. This reference bending moment is found from equation (C23) for $k = \Omega^* = 0$.

$$\left(\frac{\bar{c}\lambda}{UM\,\frac{b}{2}}\right)\frac{BM(0,0,0)}{w_G} = BB'_0$$

The normalized nondimensional wing-root bending moment frequency response function is

$$\frac{\hat{BM}}{w_G}(k,\Omega_2^*,0) = \frac{K(k)BB'(\Omega_2^*)}{BB'(0)} + \frac{1}{2}\sum_{i=1}^{N}\left[k^2A'_i - 2ikC(k)B'_i + 2\lambda k^2 D_i\right]\frac{\hat{q}_i}{BB'(0)} \tag{C24}$$

One-Dimensional Analysis

The one-dimensional frequency response functions are related to the two-dimensional frequency response functions by setting $\Omega_2^* = 0$ in equations (C19), (C20), (C21), and (C24).

C.4 Response Spectra

The response spectra needed to determine the statistical parameters for the responses of the airplane are calculated.

Two-Dimensional Analysis

The two-dimensional response spectra are calculated by multiplying the normalized two-dimensional Dryden gust velocity spectrum by the square of the modulus of the two-dimensional frequency response functions given by equations (C19), (C20), (C21), and (C24). Integrating these spectra over finite limits of the spatial frequency Ω_2^*, a response spectrum is obtained from the two-dimensional analysis for each response variable.

$$\phi(k) = \int_0^{\Omega_2^*} \left|H(k,\Omega_2^*)\right|^2 \Phi_D(k,\Omega_2^*) d\Omega_2^* \tag{C25}$$

The normalized two-dimensional Dryden vertical gust velocity spectrum is

$$\Phi_D(k,\Omega^*) = \frac{3AR}{\pi\left(\frac{b}{2L}\right)^2} \frac{(L\Omega_1)^2 + (L\Omega_2)^2}{\left[1 + (L\Omega_1)^2 + (L\Omega_2)^2\right]^{5/2}} \tag{C26}$$

The arguments on the left and right hand side of the expression are related by equations (35) and (36).

$$L\Omega_1 = k\frac{L}{c}$$

$$L\Omega_2 = \Omega_2^* \frac{2L}{b}$$

One-Dimensional Analysis

The response spectra are obtained by multiplying the square of the modulus of the one-dimensional frequency response functions times the one-dimensional normalized Dryden gust velocity spectrum.

$$\phi(k) = |H(k)|^2 \phi_D(k) \tag{C27}$$

The normalized one-dimensional Dryden vertical gust velocity spectrum is

$$\phi_D(k) = \frac{1}{\pi\left(\frac{L}{c}\right)} \frac{1 + 3(L\Omega_1)^2}{\left[1 + (L\Omega_1)^2\right]^2} \tag{C28}$$

C.5 Statistical Parameters

The one-dimensional response spectra obtained from the two-dimensional analysis and the one-dimensional analysis are integrated over finite limits of reduced frequency to obtain the desired response statistical parameters.

Mean-Square Value

The mean-square value of the response was calculated by using equation (39).

$$\overline{(\quad)^2} = \int_0^k \phi(k)dk \tag{C29}$$

Root-Mean-Square Value

The root-mean-square value of the response was calculated by using equation (40).

$$\sqrt{\overline{(\quad)^2}} = \left[\int_0^k \phi(k)dk\right]^{1/2}$$

Number of Mean Crossings

The average number of mean crossings was calculated by using equation (41).

$$\hat{N}_o = \frac{N_o}{\left(\frac{U}{c}\right)} = \frac{1}{2\pi} \frac{\left[\int_0^k \phi(k)k^2dk\right]^{1/2}}{\left[\int_0^k \phi(k)dk\right]^{1/2}} \tag{C30}$$

C.6 Parameter Data

The scaling laws which govern the change of nondimensional parameters in the trend study calculations are presented.

Frequency Response Functions

The normalized nondimensional frequency response functions are developed in terms of nondimensional quantities. These quantities are dependent on the geometry, mass, stiffness, and aerodynamic properties of the airplane. A change in one or more of these properties must conform to scaling laws which provide the relations between the nondimensional forms of these properties. The quantities that govern the values of the frequency response functions are

a) Mode shapes $\xi_i(y^*)$

b) Normalized lift distribution $\gamma(y^*)$

c) Normalized mass distribution $m^*(y^*)$

The nondimensional coefficients used in equations (C17) and (C23) are constant for a change in the physical properties of the airplane provided

the mode shapes, normalized lift distribution, and normalized mass distribution are not changed.

The mode shapes are calculated from the governing equation of motion, reference 24.

$$\left[I^*(y^*)\xi''\right]'' - \frac{\left(\frac{b}{2}\right)^3 \omega_i^2 M_R}{EI_R} m^*(y^*)\xi = 0 \tag{C31}$$

The mode shapes are the same for any two different airplane configurations that have the same mass distribution, stiffness distribution $I^*(y^*)$ and mechanical vibration constant $\omega_i^2(b/2)^3 M_R/EI_R$. The mechanical vibration constant can be written in terms of the nondimensional parameters λ and k by using equations (C3) and (C18).

$$\frac{\omega_i^2\left(\frac{b}{2}\right)^3 M_R}{EI_R} = (\text{Constant})k^2\lambda C_{L\alpha} \frac{\left(\frac{b}{2}\right)^4}{I_R}\left(\frac{1}{2}\frac{\rho U^2}{E}\right) \tag{C32}$$

This relation shows that the natural reduced frequencies are the same for any two configurations that have the same values of:

d) Ratio of aerodynamic forces to elastic forces $1/2\ \rho U^2/E$

e) Mass parameter λ

f) Ratio of wing span to reference stiffness $(b/2)^4/I_R$

Equation (C18) shows that the mass parameter is inversely proportional to the total lift-curve slope and equation (C23) shows that the natural reduced frequencies are independent of $C_{L\alpha}$. For the trend study calculations the above parameters are held constant for a given value of the ratio of the wing mass to fuselage mass. The corresponding

natural mode shapes and reduced frequencies were calculated for different values of the ratio of wing mass to fuselage mass.

Response Spectra

The calculation of the two-dimensional response spectra requires the changing of the two-dimensional scale ratio $b/2L$. This in turn changes the one-dimensional scale ratio $L/\bar{c}$ in accordance with equation (37). For the trend study calculations the value of the aspect ratio is held constant. This constraint gives the proper geometry scaling for the airplane.

Stiffness Values

The values of the stiffness distribution, reference stiffness, and influence coefficients used in the trend study calculations are taken directly from example problem 2-1 in reference 24.

Mass Values

The mass distribution values for a wing mass to fuselage mass ratio of 0.585 and the value of reference mass is given in table I.

Mode Shapes and Frequencies

The calculated natural mode shapes and natural frequencies for a value of wing mass to fuselage mass ratio of 0.585 is given in table I.

Aerodynamics

Two strip-analysis aerodynamic theories are used to calculate the normalized lift distributions used in the trend study calculations.

Simple-Strip Analysis

Simple-strip analysis assumes that the local lift-curve slope of each section of the wing is constant and has the two-dimensional value of 2π. The lift distribution is then proportional to the normalized semichord relation.

$$\gamma(y^*) = \left(\frac{c}{\bar{c}}\right) = 1.3846135(1. - 0.55555556y^*) \tag{C33}$$

Modified-Strip Analysis

The normalized lift distribution for the modified-strip analysis is calculated from reference 45. This reference uses a matrix formulation of the Weissinger L-method of solving the three-dimensional steady flow equation. The solution of this equation is the values of the lift distribution $cc_l/\bar{c}C_{L\alpha}$ at selected semispan points. This distribution is dependent on the wing geometry and angle of attack distribution taken at the three-quarter-chord location. The symmetric distribution for a given angle of attack distribution $\{\alpha\}$ can be calculated from the presented values of the symmetric aerodynamic influence matrix

$$\left\{\frac{cc_l}{\bar{c}C_{L\alpha}}\right\} = \frac{1}{C_{L\alpha}}[Q_s]\{\alpha\}$$

The normalized lift distribution γ is defined in terms of a unit angle of attack distribution. The distribution γ is calculated in terms of the symmetric distribution $cc_l/\bar{c}C_{L\alpha}$ by the following relation.

$$\gamma = \frac{cc_l}{\bar{c}C_{L\alpha}} = \frac{AR}{2}[Q_s]\{\alpha = 1\} \tag{C34}$$

The symmetric influence matrix corresponding to an aspect ratio of 6, a taper ratio of 1/2, and a total lift-curve slope of 4.321 is used for the trend study calculations.

Coefficient Values

The values of the coefficients used in equations (C12) and (C23) for a value wing mass to fuselage mass ratio of 0.585 and values of $C_{L\alpha}$ of 2π and 4.321 are presented in table II.

C.7 Truncation Error

An analytical evaluation of the truncation error of the one-dimensional response spectra is made. The evaluation is made for the case of simple-strip analysis aerodynamic theory and the rigid-body plunge mode. For this case, the frequency response function is assumed to be independent of reduced frequency k, and has the form

$$H(k,\Omega_2^*) = \frac{\sin \Omega_2^*}{\Omega_2^*} \tag{C35}$$

Using this expression, the truncation error is formulated by comparing the one-dimensional response spectrum given by equation (C25) with the response spectrum given by equation (38).

$$\epsilon(k) = \int_a^\infty \left(\frac{\sin \Omega_2^*}{\Omega_2^*}\right)^2 \Phi_D(k,\Omega_2^*)d\Omega_2^* \tag{C36}$$

This expression is difficult to evaluate in closed form. Because of this difficulty, the truncation error is evaluated in closed form only for large values of k, that is, $k > (b/2L)/AR$. For these values

of k, the gust spectrum is approximated for two limiting values of the roll-off point.

For low values of the roll-off point, that is, $kAR << \pi$, the asymptotic expression of equation (52) is given by equation (54). Substituting this expression into equation (C36), the truncation error expressed in terms of the cosine integral function Ci(z) is,

$$\epsilon(k) = \frac{3AR}{\pi}\left(\frac{b}{2L}\right)\left\{\left| \frac{1}{8a^4} + \frac{\cos(2a)}{2}\left(\frac{1}{6a^2} - \frac{1}{4a^4}\right) + \frac{\sin(2a)}{2}\left(\frac{1}{6a^3} - \frac{1}{3a}\right) + \frac{Ci(2a)}{3}\right|\right\} \tag{C37}$$

For high values of the roll-off point, that is, $kAR > \pi$, the gust spectrum is given by equation (55). The gust spectrum is independent of Ω_2^* and a percentage error is calculated by normalizing equation (C36) by

$$\int_0^\infty \left(\frac{\sin \Omega_2^*}{\Omega_2^*}\right) d\Omega_2^* = \frac{\pi}{2}$$

The percentage truncation error in terms of the sine integral function Si(z) is

$$\frac{\epsilon(k)}{\frac{\pi}{2}} = 1 + \frac{1}{2a\pi} - \frac{1}{a\pi}\cos(2a) - \frac{2}{\pi}\,Si(2a) \tag{C38}$$

TABLE I.- TREND STUDY AIRPLANE CHARACTERISTICS

Airplane Parameters

Mass Parameters, λ	45.656
Aspect Ratio, AR	6.154
Taper Ratio	0.444
Reference Stiffness, EI_R, psi	6.8×10^{10}
Reference semichord, $\bar{c}$, inches	81.25
Reference Mass, M_R, slugs	1303.05

Mass Distribution and Mode Shapes

y^*	m^*	ξ_1	ξ_2	ξ_3
0	0.4151	1.0	-0.1586	0.1383
0.18	0.1441	1.0	-0.1177	-0.0362
0.372	0.2433	1.0	-0.0052	-0.1418
0.536	0.1002	1.0	0.2593	-0.3720
0.736	0.0811	1.0	0.5132	0.0415
0.916	0.0162	1.0	1.0	1.0

Reduced Frequencies of Orthogonal Modes

$k_1 = 0.0$

$k_2 = 0.156$

$k_3 = 0.525$

TABLE II.- TREND STUDY FORCE AND MOMENT COEFFICIENTS

Simple Strip Theory $C_{l_\alpha} = 2\pi$

$A_{11} = 0.5247$

$A_{12} = 0.2933$

$A_{13} = -0.0537$

$A_{22} = 1.280$

$A_{23} = 0.6732$

$A_{33} = 1.196$

$B_{11} = 0.5000$

$B_{12} = 0.4374$

$B_{13} = 0.0421$

$B_{22} = 1.756$

$B_{23} = 1.076$

$B_{33} = 1.607$

$A_1' = 0.1982$

$A_2' = 0.2991$

$A_3' = 0.0624$

$B_1' = 0.2179$

$B_2' = 0.4060$

$B_3' = 0.1455$

$D_1 = 0.1224$

$D_2 = 0.1174$

$D_3 = -0.0395$

Modified Strip Theory $C_{L_\alpha} = 4.321$

$A_{11} = 0.7629$

$A_{12} = 0.3961$

$A_{13} = -0.0076$

$A_{22} = 1.771$

$A_{23} = 1.012$

$A_{33} = 1.973$

$A_1' = 0.2882$

$A_2' = 0.4266$

$A_3' = 0.1074$

$B_1' = 0.2114$

$B_2' = 0.3305$

$B_3' = 0.0607$

TABLE II.- Concluded

Modified Strip Theory $C_{L_\alpha} = 4.321$

$B_{11} = 0.5000$	$D_1 = 0.1224$
$B_{12} = 0.3547$	$D_2 = 0.1174$
$B_{13} = -0.0301$	$D_3 = -0.0395$
$B_{22} = 1.262$	
$B_{23} = 0.6170$	
$B_{33} = 1.269$	

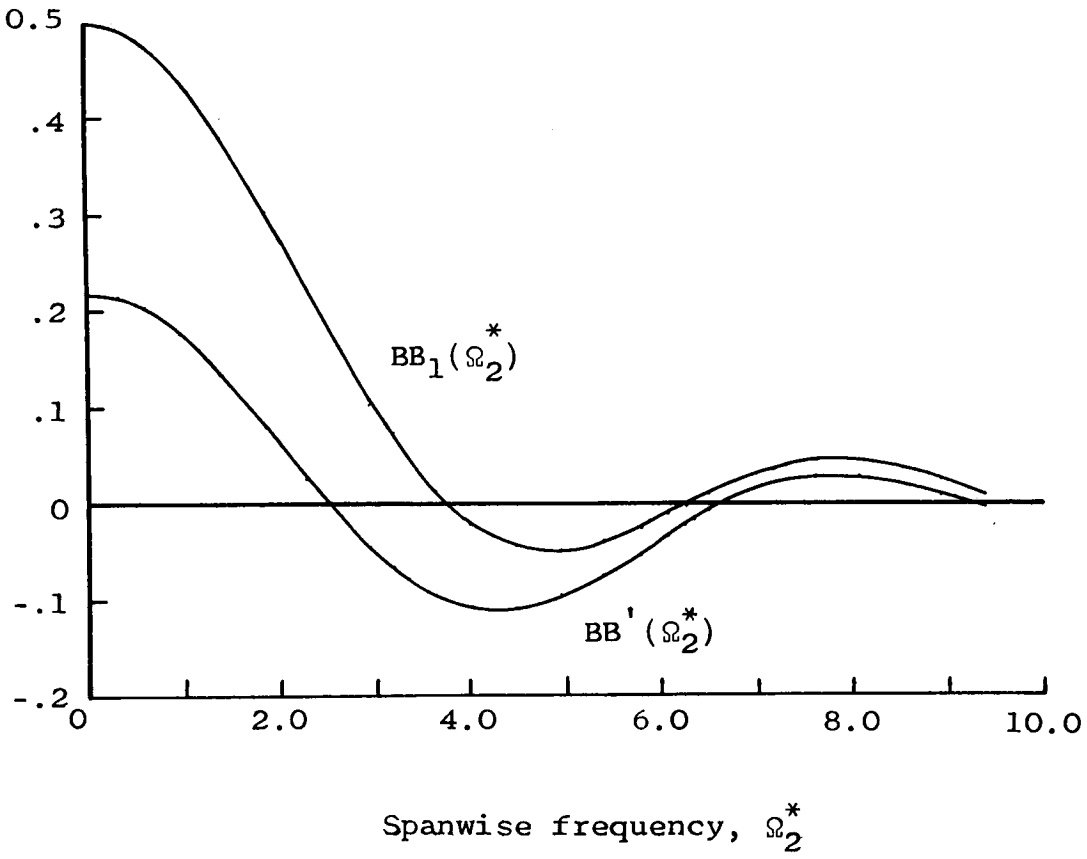

Figure 1.- Two-dimensional rigid body gust force variation with spanwise frequency.

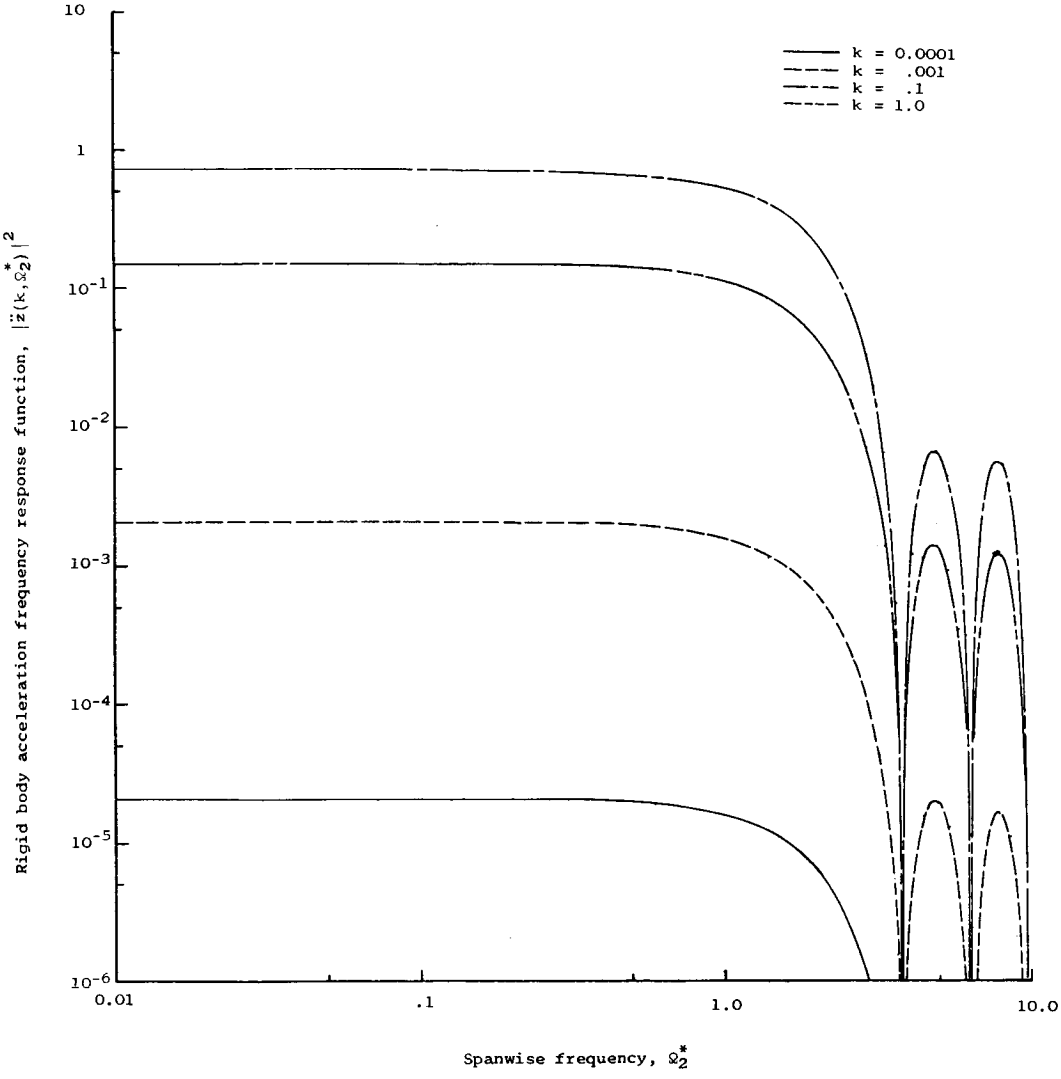

Figure 2.- Rigid body acceleration two-dimensional frequency response function variation with spanwise frequency.

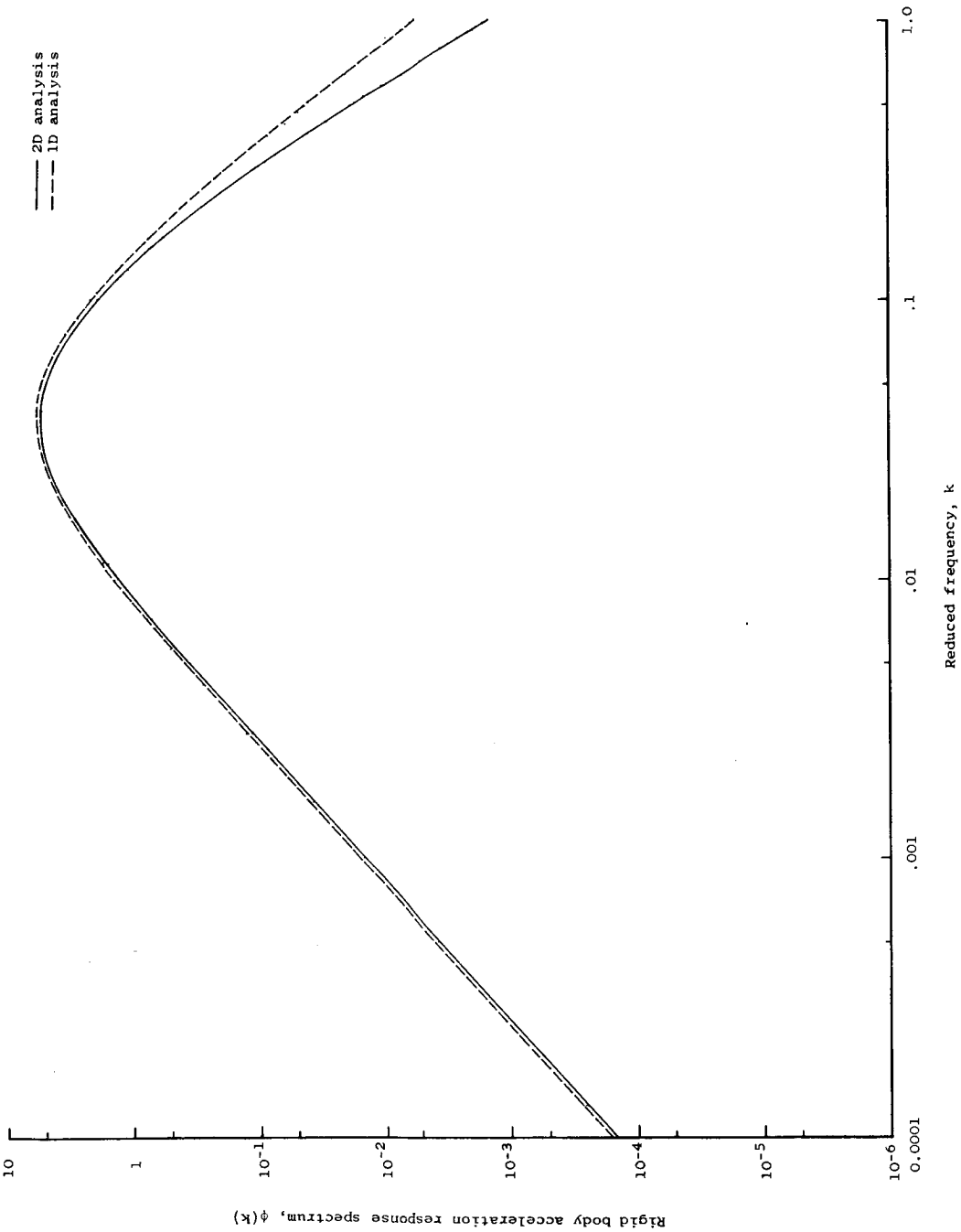

Figure 3.- Rigid body acceleration response spectra variation with reduced frequency (b/L = 0.5).

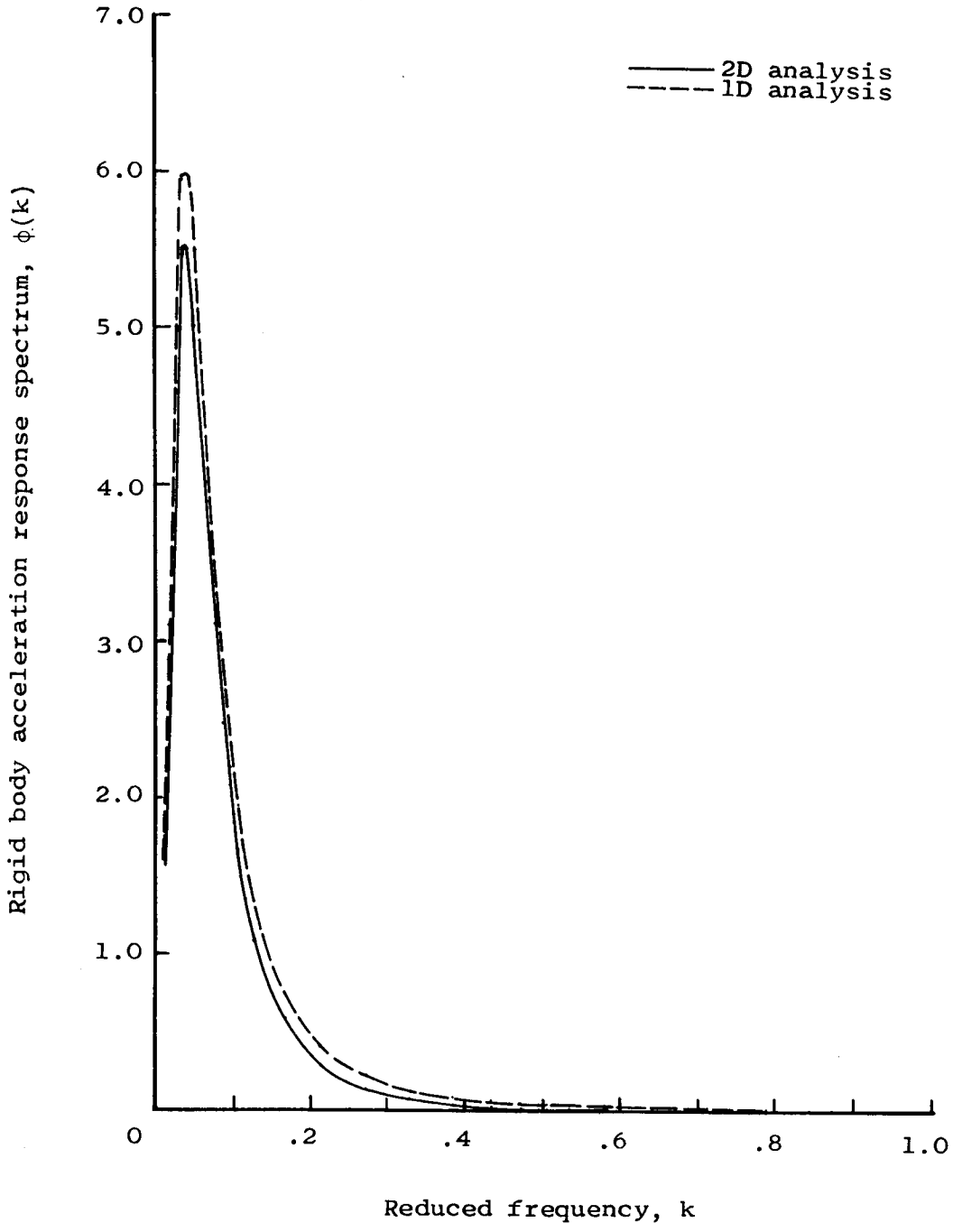

Figure 4.- Comparison of rigid body acceleration response spectra calculated by the one- and two-dimensional analyses (b/L = 0.5).

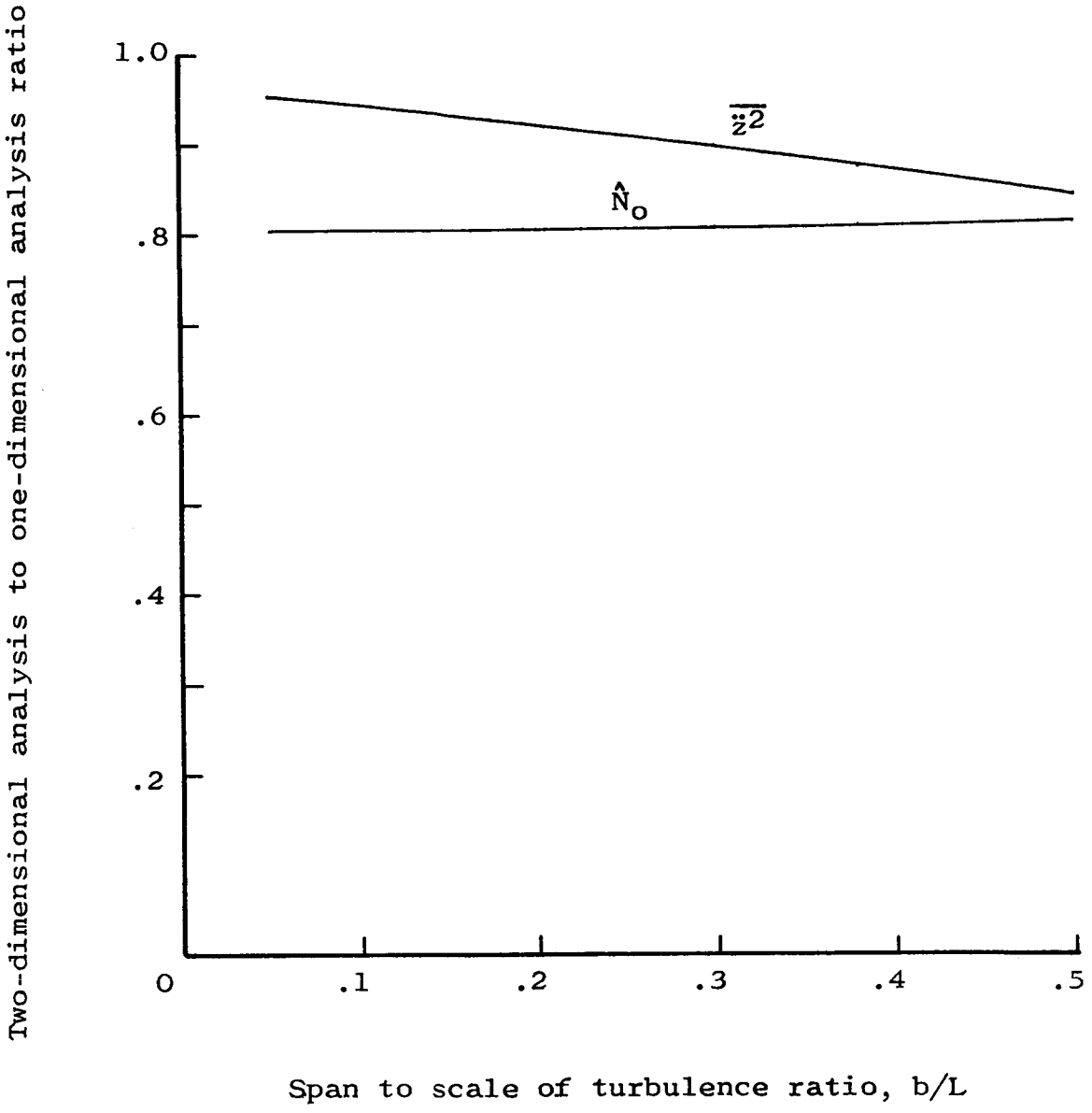

Figure 5.- Reduction of rigid body acceleration mean-square value and $\hat{N}_o$ given by two-dimensional analysis variation with b/L.

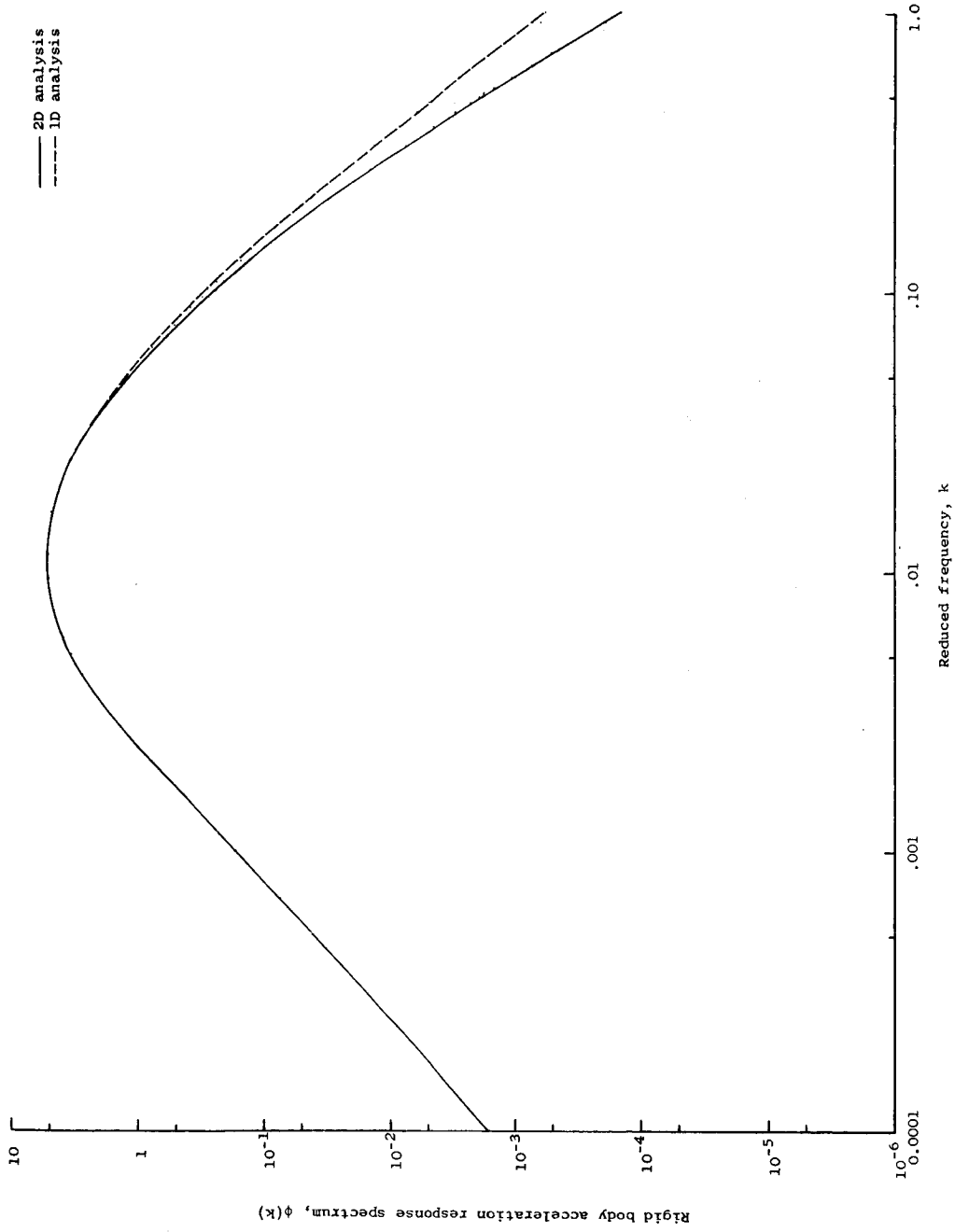

Figure 6.- Rigid body acceleration response spectra variation with reduced frequency (b/L = 0.05).

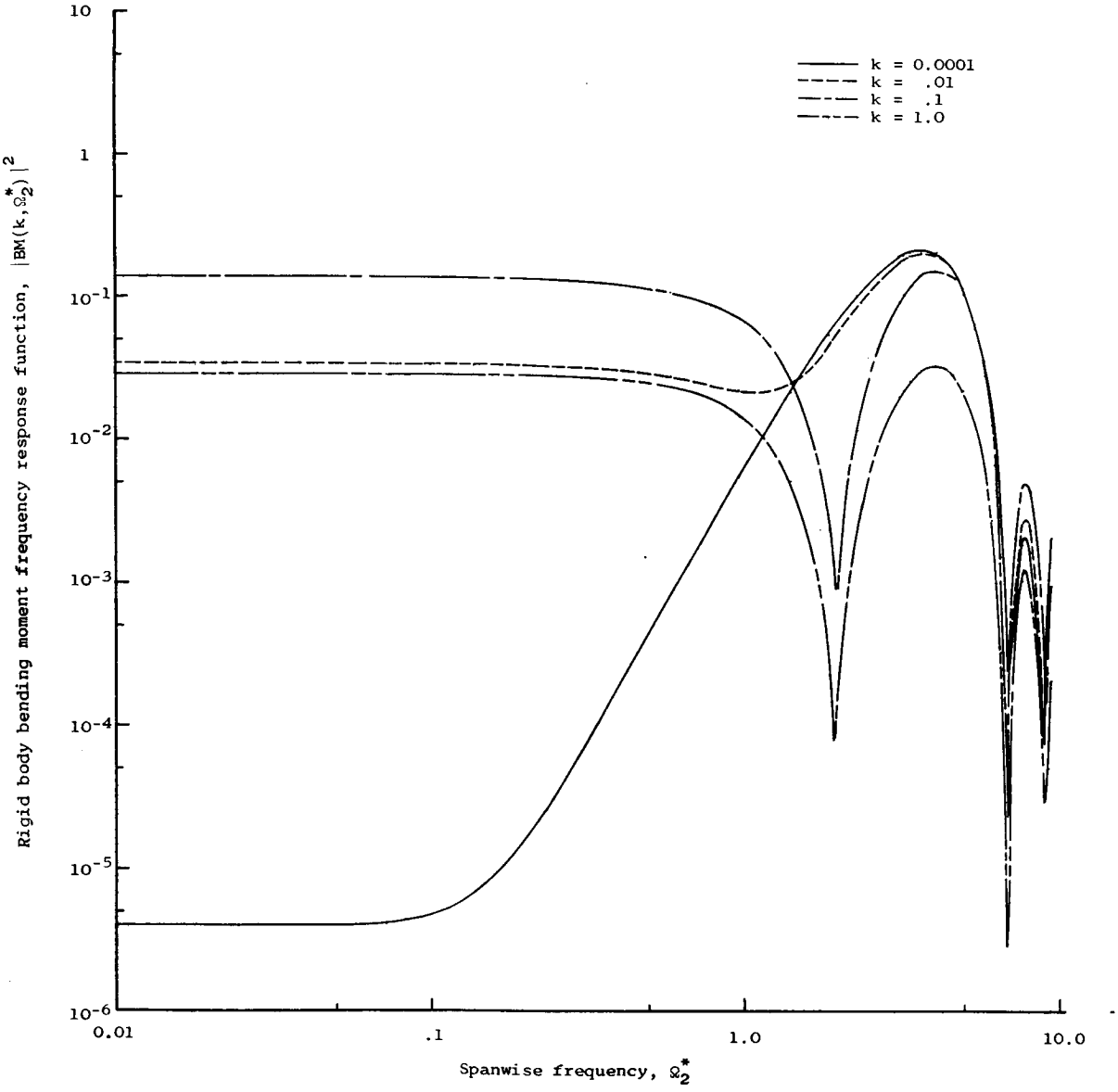

Figure 7.- Rigid body bending moment two-dimensional frequency response function variation with spanwise frequency (mass ratio = 0.585).

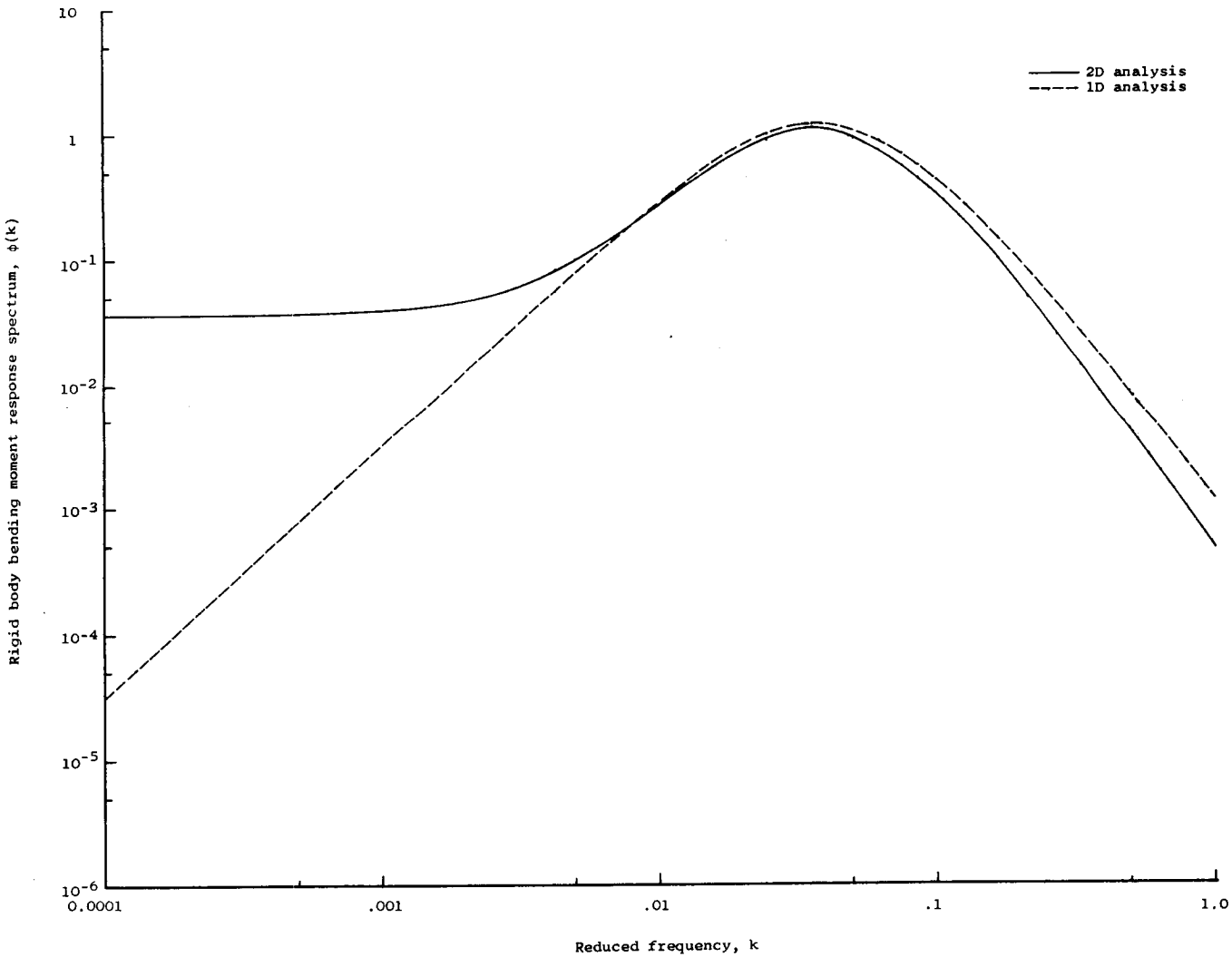

Figure 8.- Rigid body bending moment response spectra variation with reduced frequency (b/L = 0.5, mass ratio = 0.585).

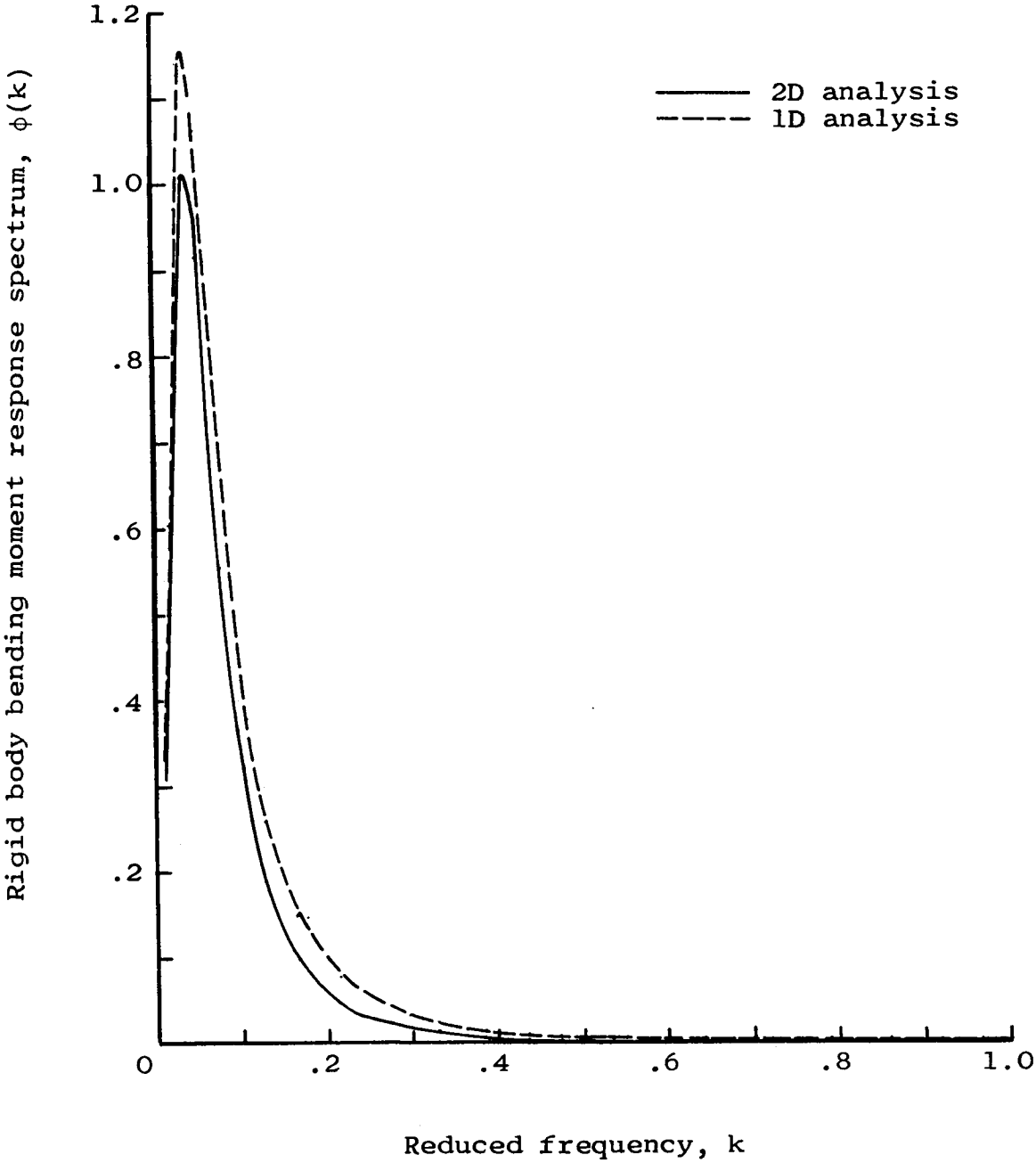

Figure 9.- Comparison of rigid body bending moment response spectra calculated by the one- and two-dimensional analyses (b/L = 0.5, mass ratio = 0.585).

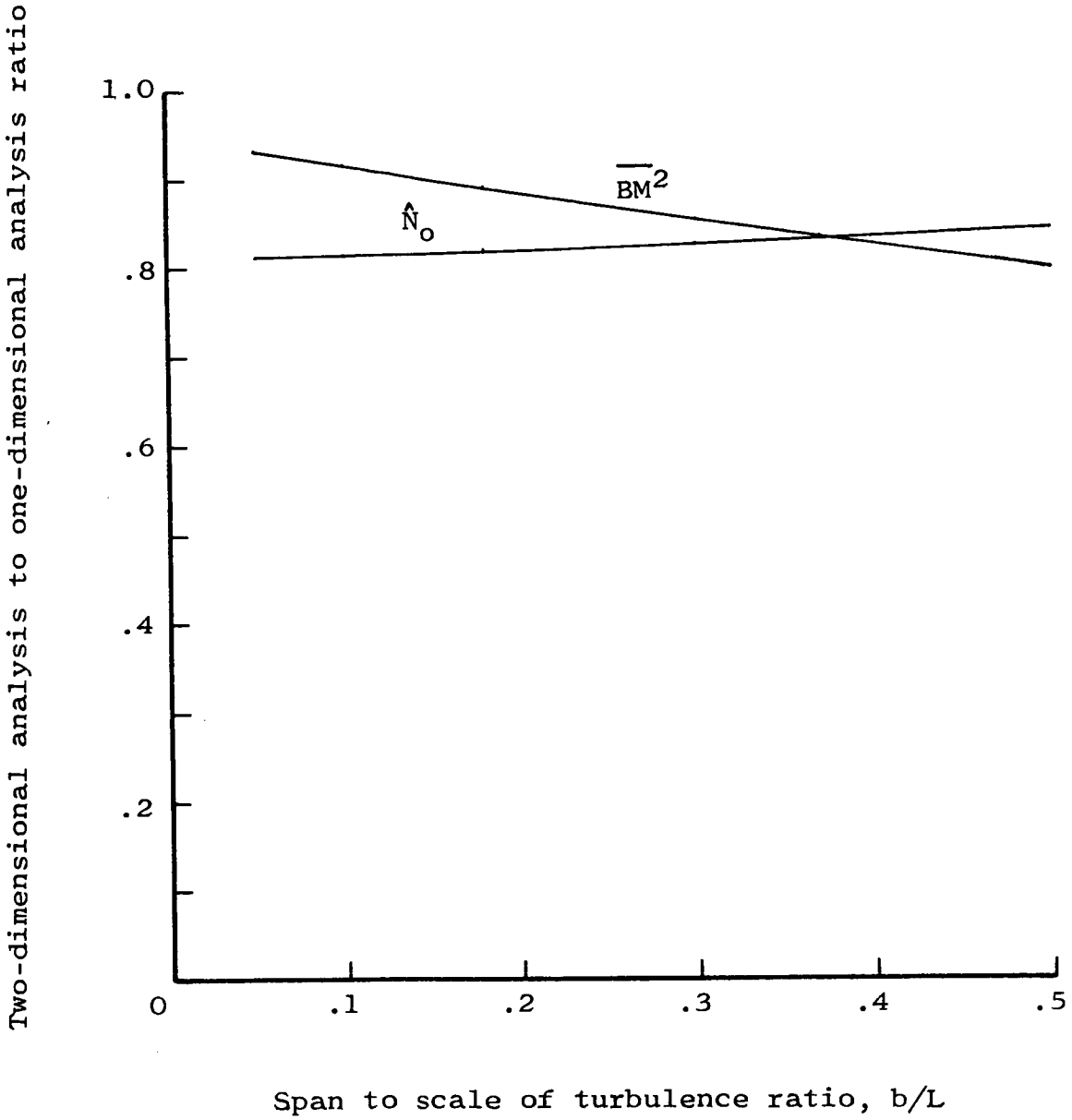

Figure 10.- Reduction of rigid body bending moment mean square value and $\hat{N}_o$ given by two-dimensional analysis variation with b/L (mass ratio = 0.585).

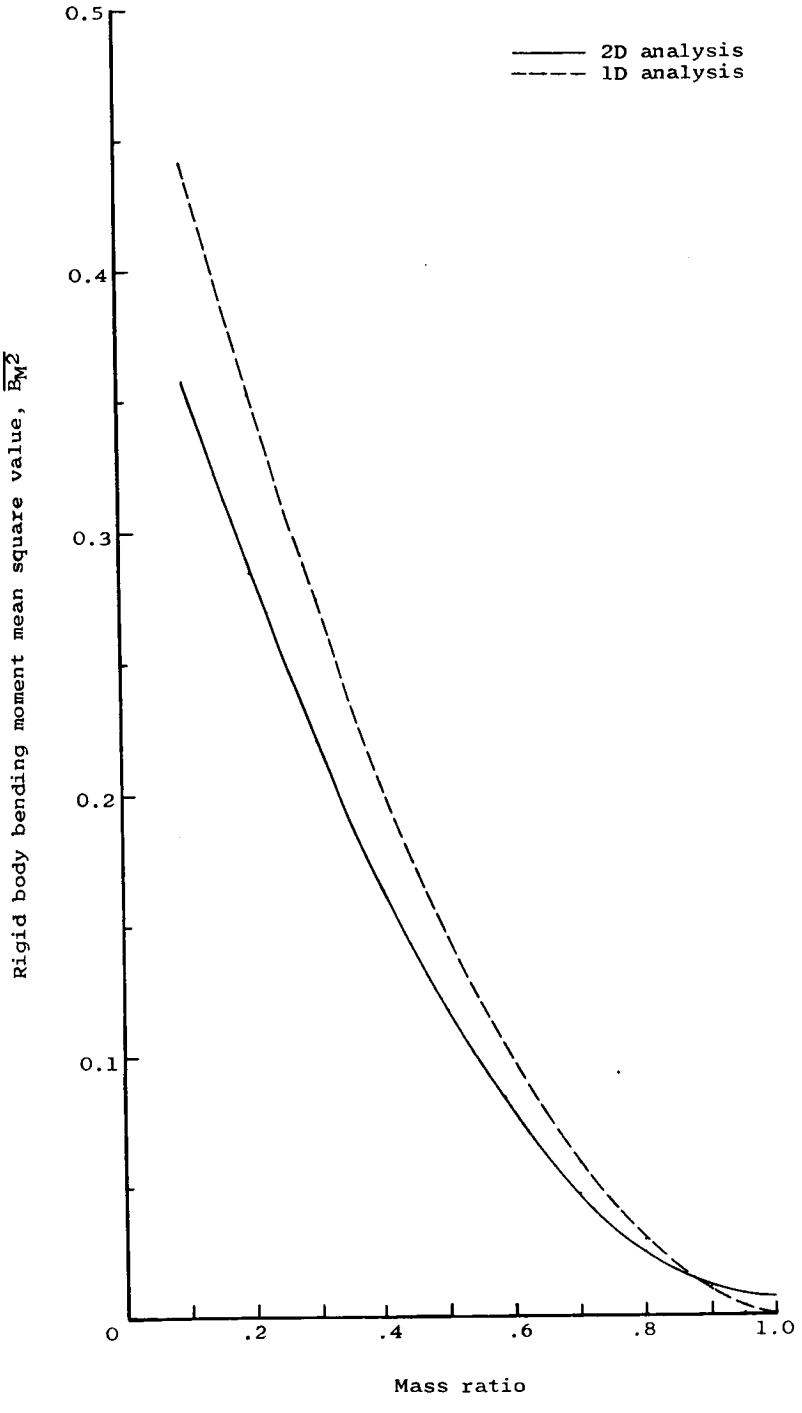

Figure 11.- Comparison of rigid body bending moment mean square value calculated by one- and two-dimensional analyses variation with mass ratio (b/L = 0.5).

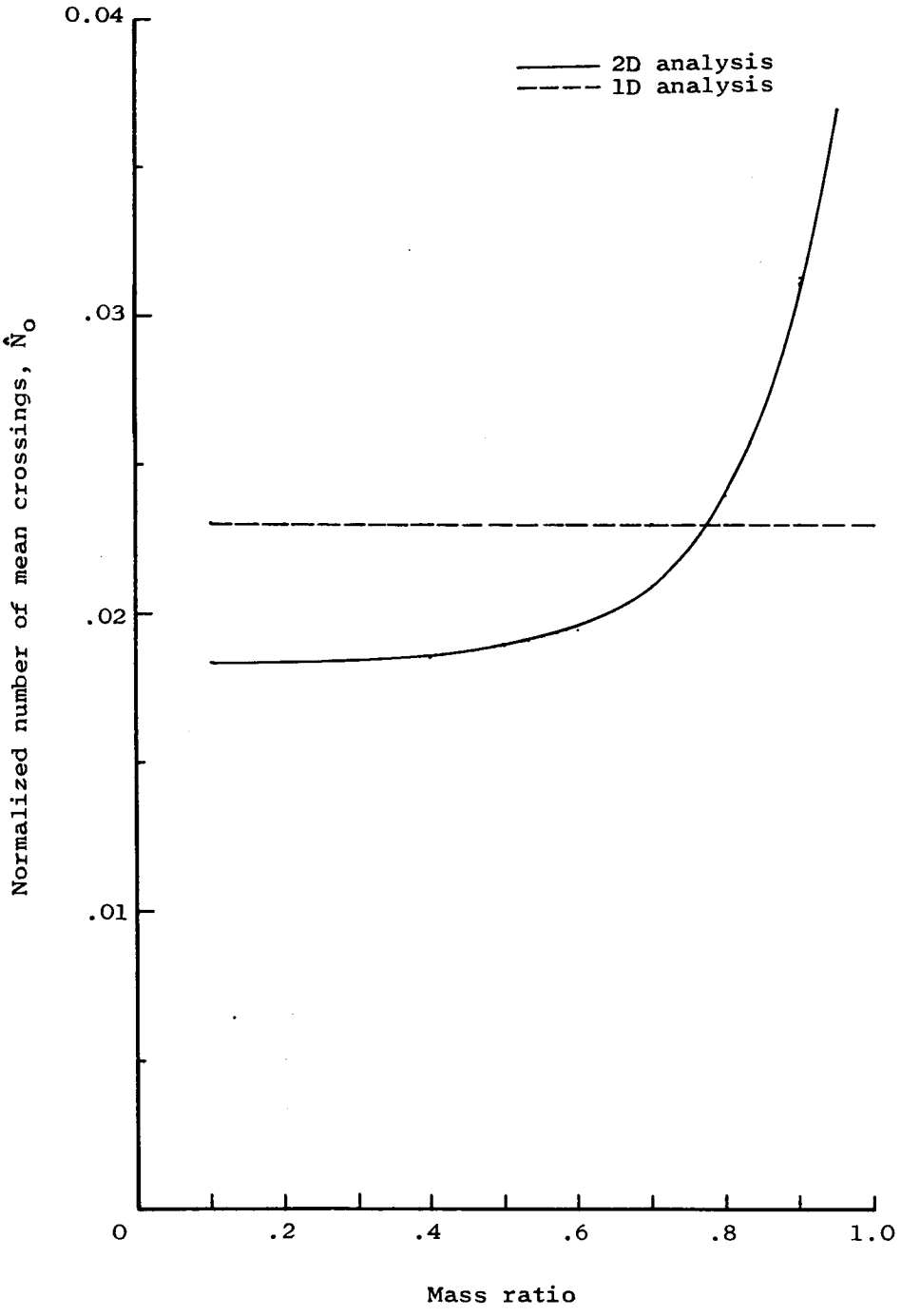

Figure 12.- Comparison of rigid body bending moment $\hat{N}_o$ calculated by one- and two-dimensional analyses variation with mass ratio (b/L = 0.5).

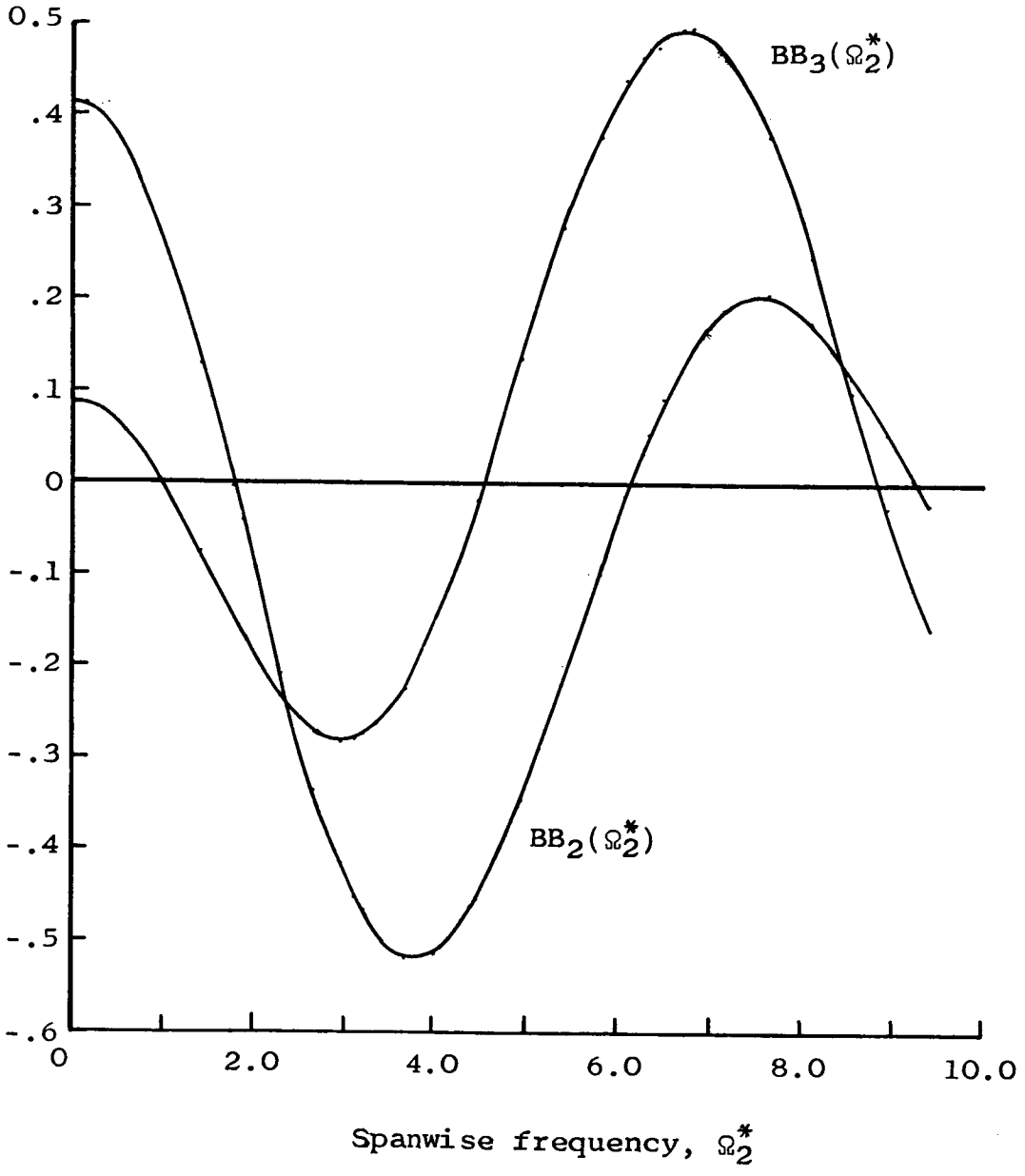

Figure 13.- Two-dimensional flexible gust force variation with spanwise frequency.

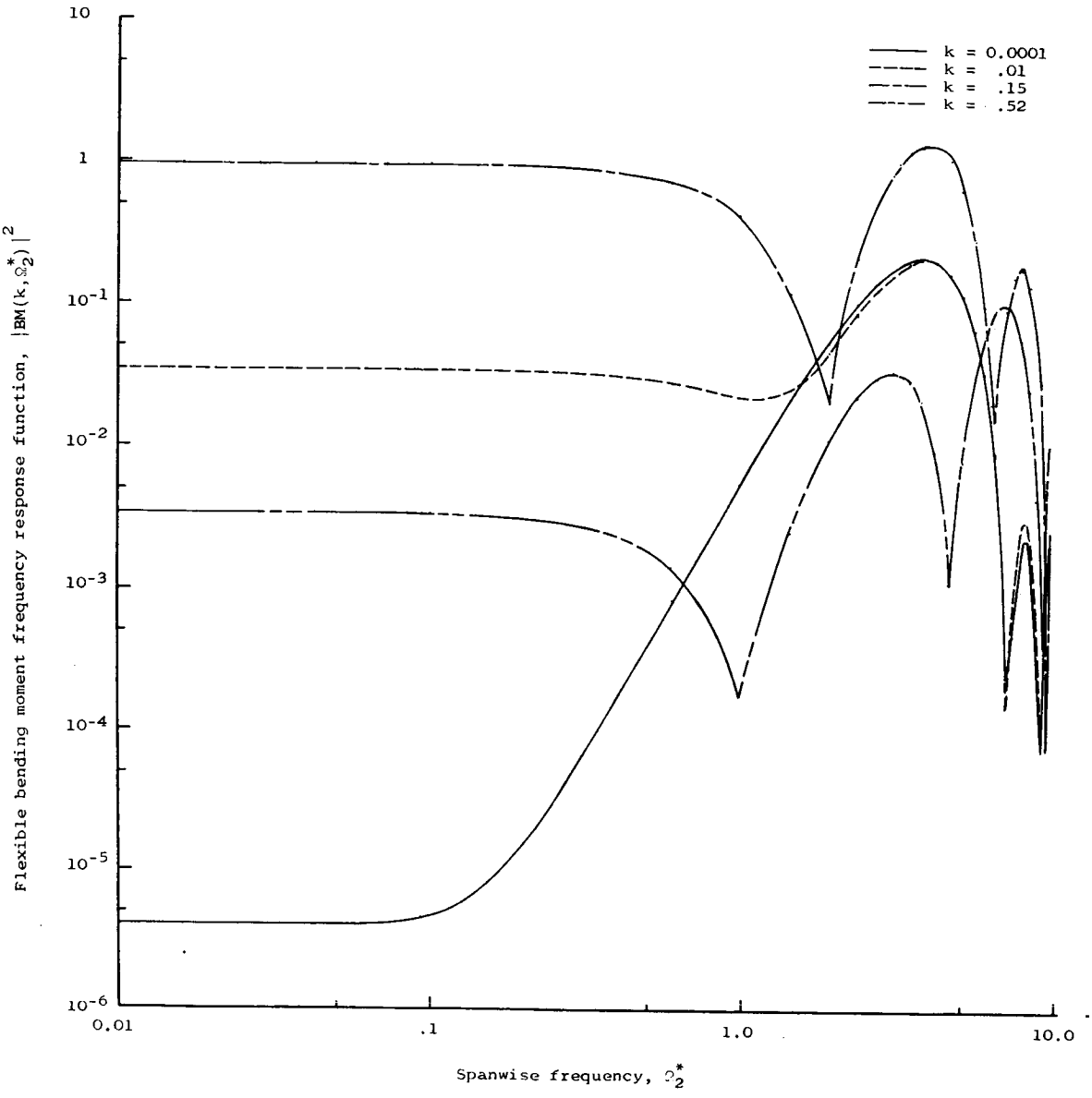

Figure 14.- Flexible bending moment two-dimensional frequency response function variation with spanwise frequency (mass ratio = 0.585).

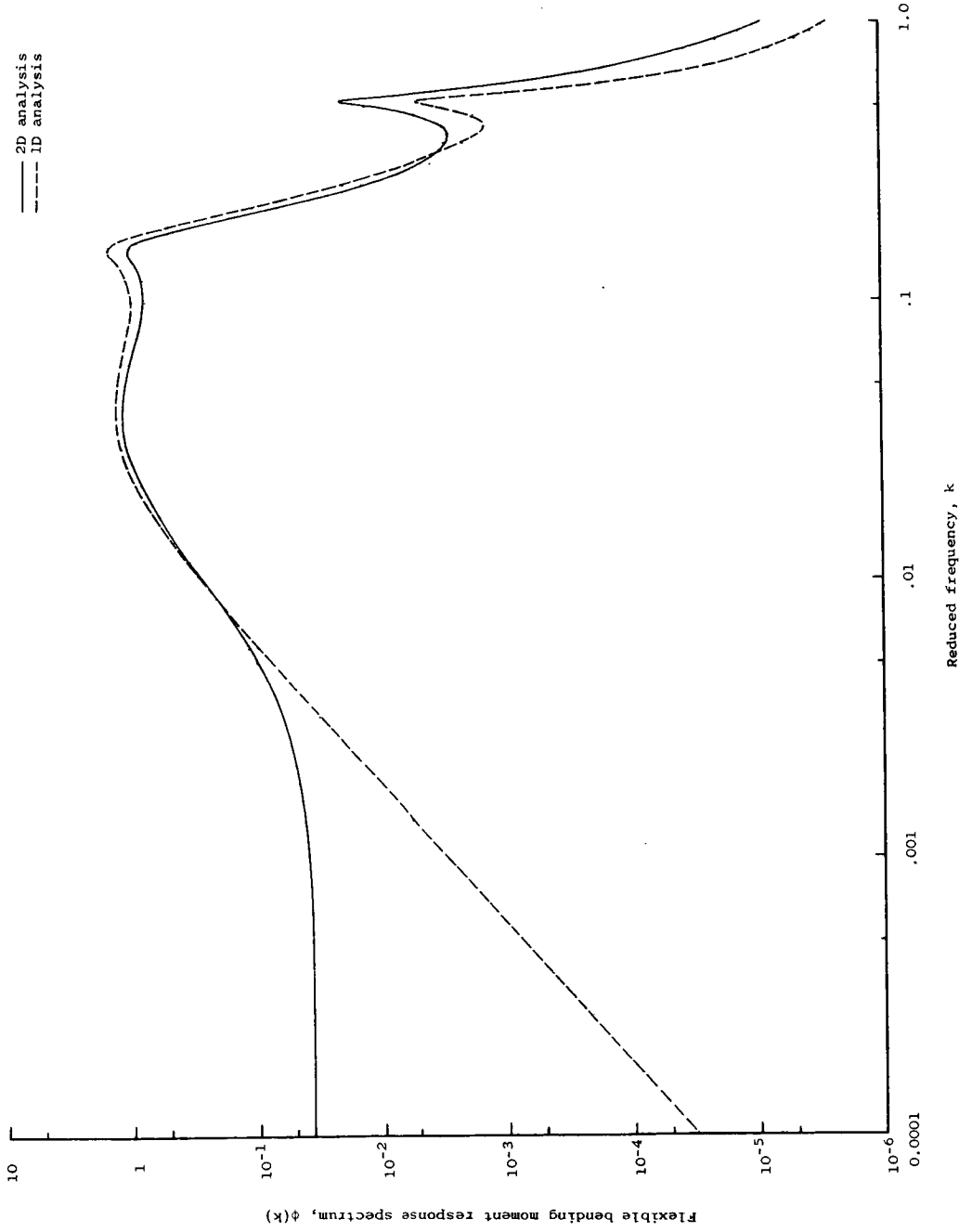

Figure 15.- Flexible bending moment response spectra variation with reduced frequency (b/L = 0.5, mass ratio = 0.585).

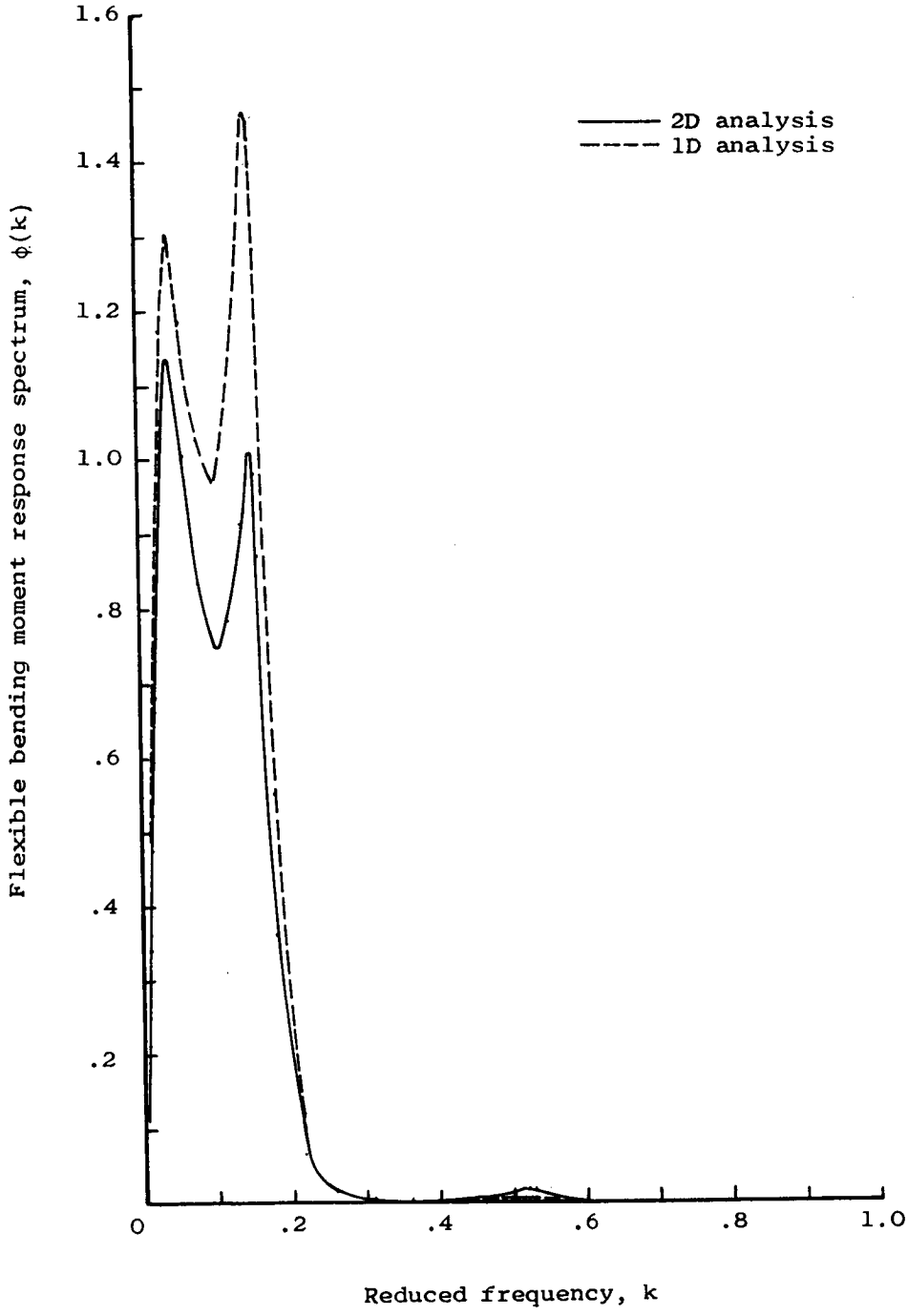

Figure 16.- Comparison of flexible bending moment response spectra calculated by one- and two-dimensional analyses (b/L = 0.5, mass ratio = 0.585).

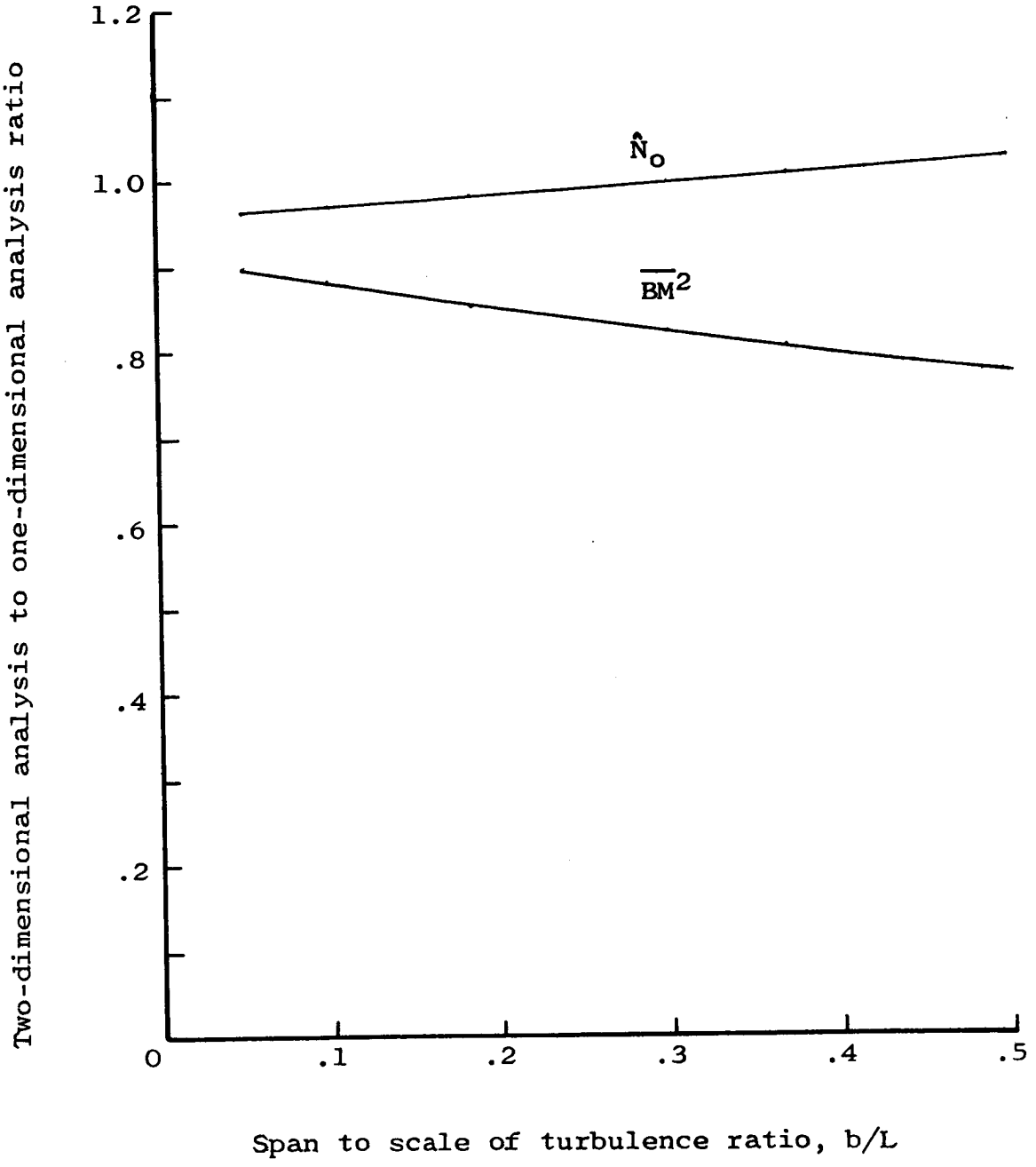

Figure 17.- Reduction of flexible bending moment mean square value and $\hat{N}_o$ given by two-dimensional analysis variation with b/L (mass ratio = 0.585).

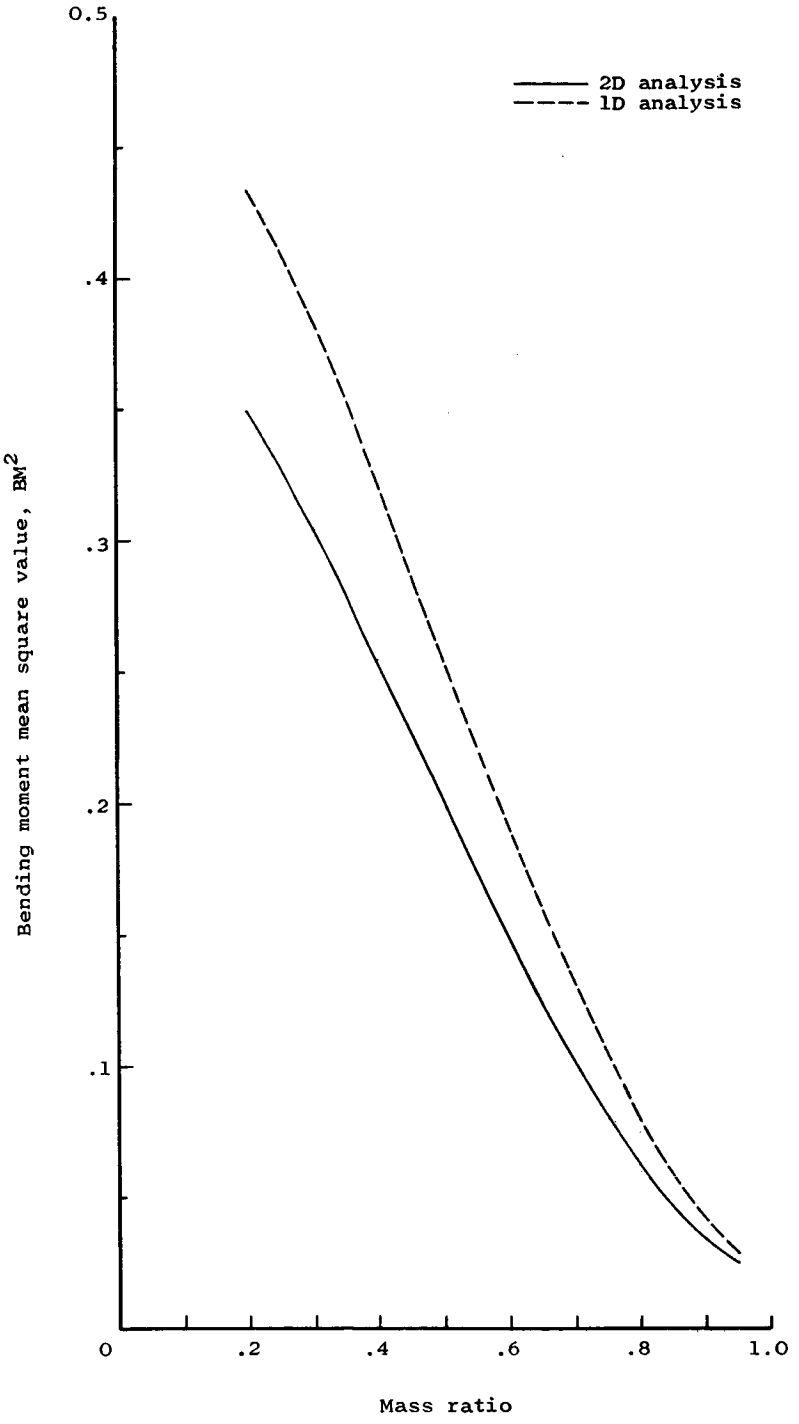

Figure 18.- Comparison of flexible bending moment mean square value calculated by one- and two-dimensional analyses variation with mass ratio (b/L = 0.5).

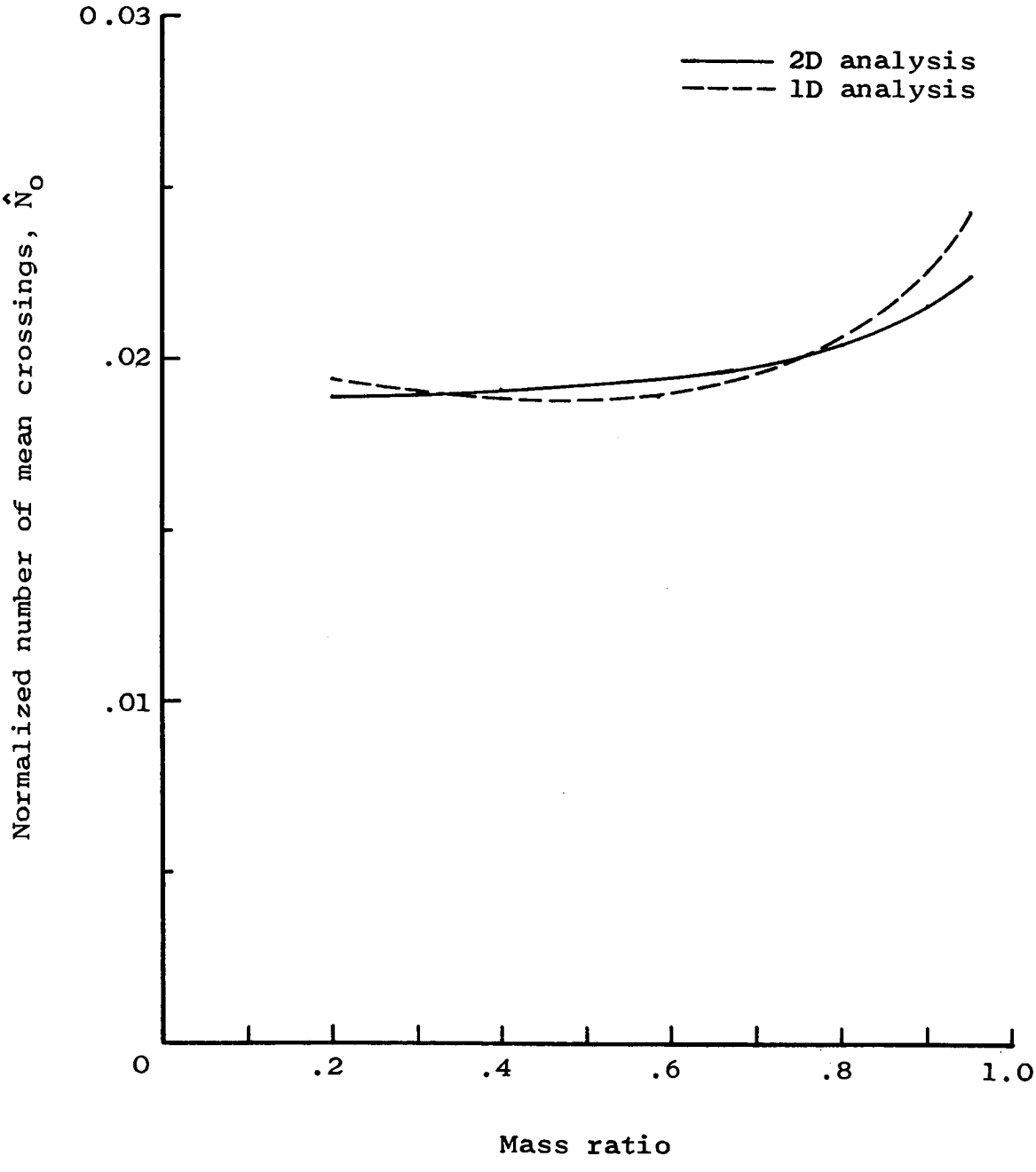

Figure 19.- Comparison of flexible bending moment $\hat{N}_o$ calculated by one- and two-dimensional analyses variation with mass ratio (b/L = 0.5).

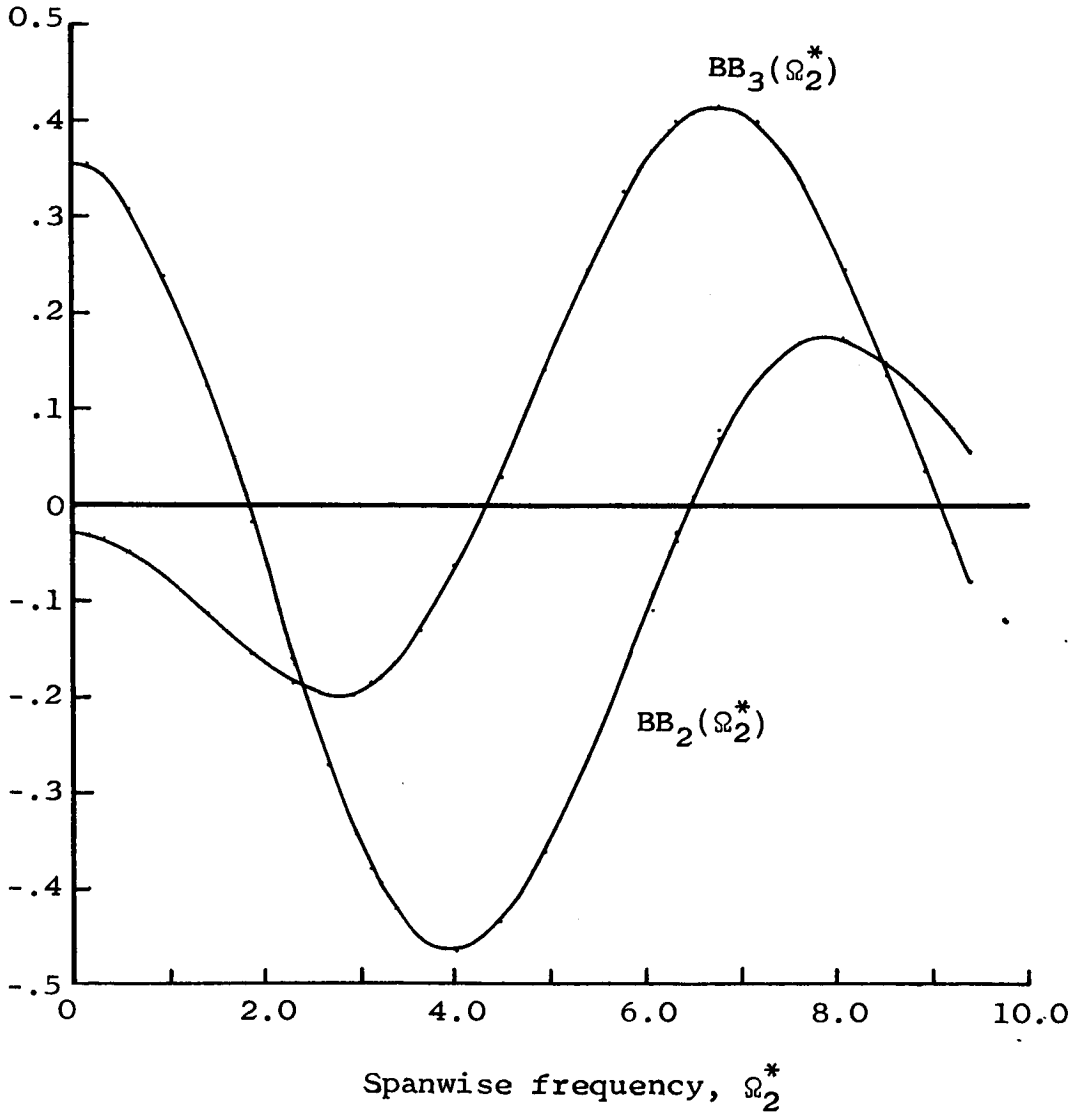

Figure 20.- Modified strip analysis two-dimensional flexible gust force variation with spanwise frequency.

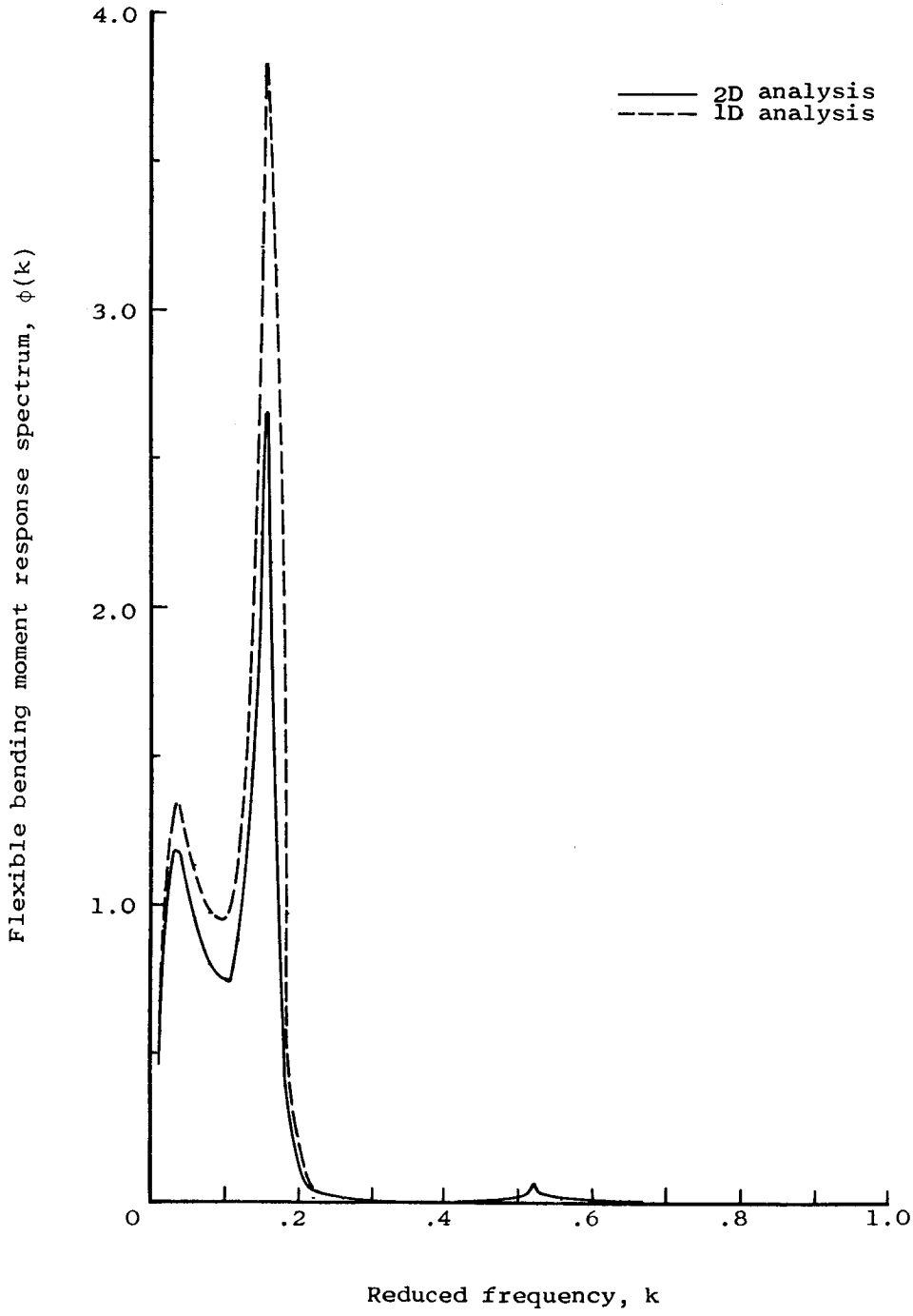

Figure 23.- Modified strip analysis comparison of flexible bending moment respose spectra calculated by the one- and two-dimensional analyses (mass ratio = 0.585, b/L = 0.5).

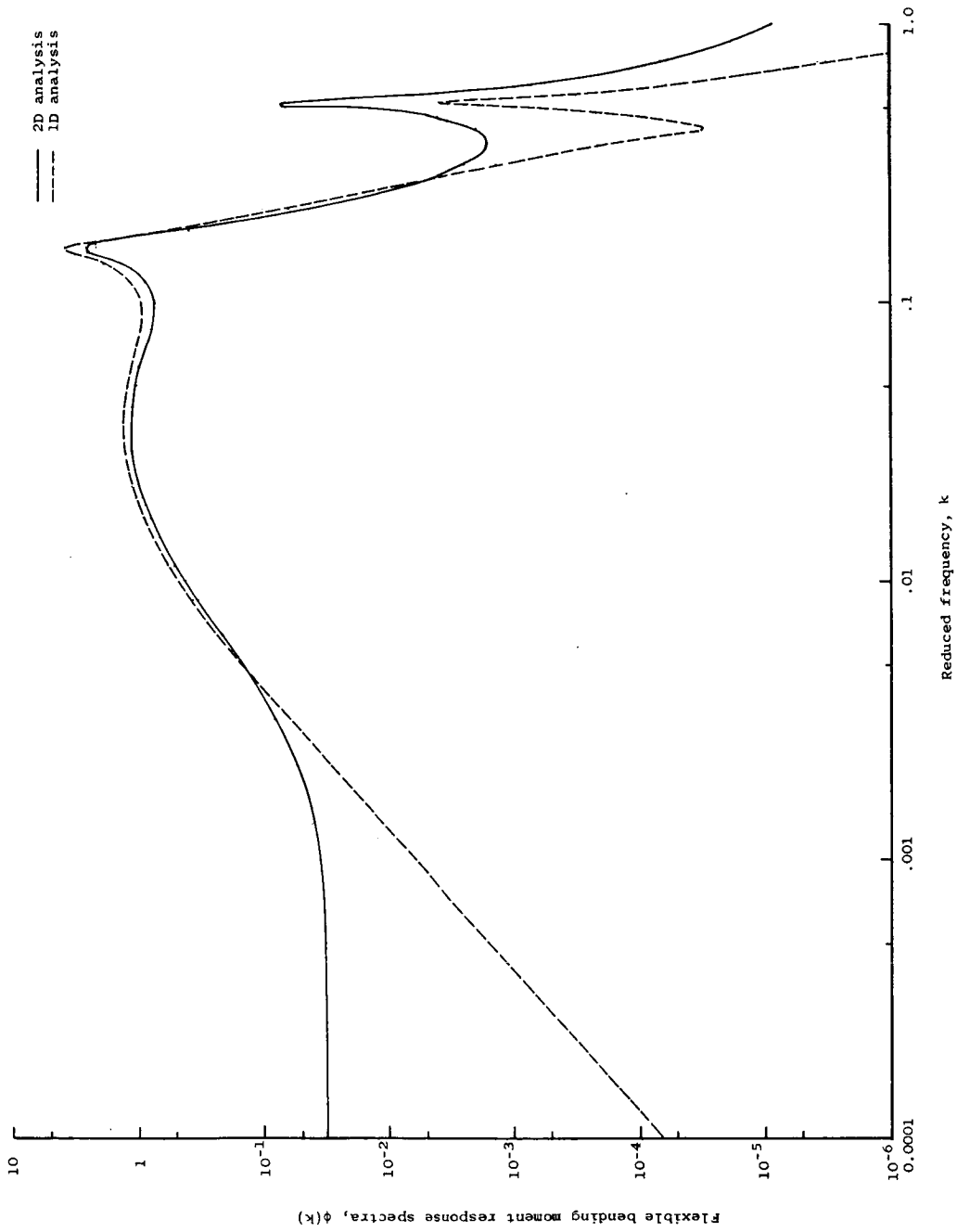

Figure 22.- Modified strip analysis flexible bending moment response spectra variation with reduced frequency (mass ratio = 0.585, b/L = 0.5).

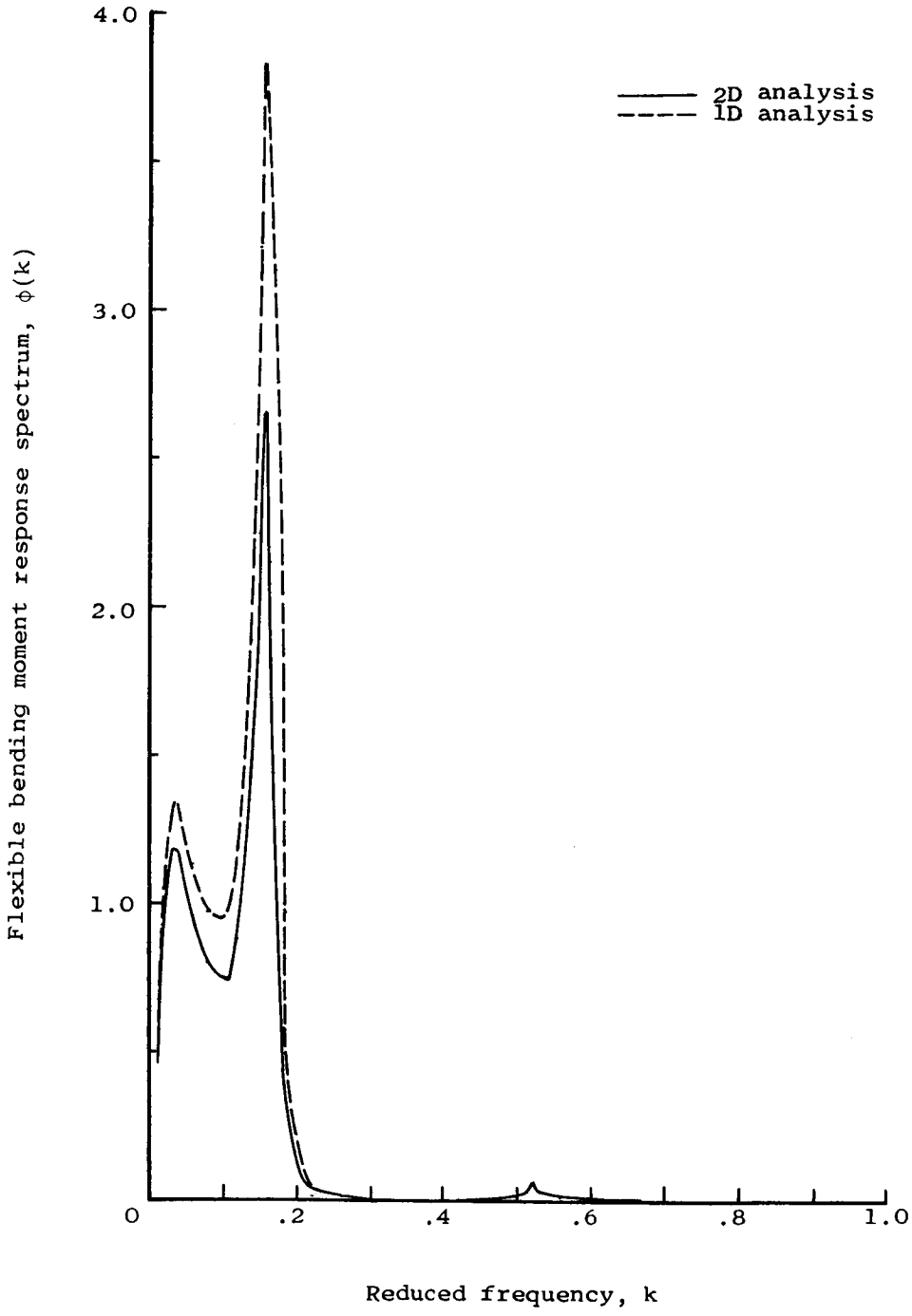

Figure 23.- Modified strip analysis comparison of flexible bending moment respose spectra calculated by the one- and two-dimensional analyses (mass ratio = 0.585, b/L = 0.5).

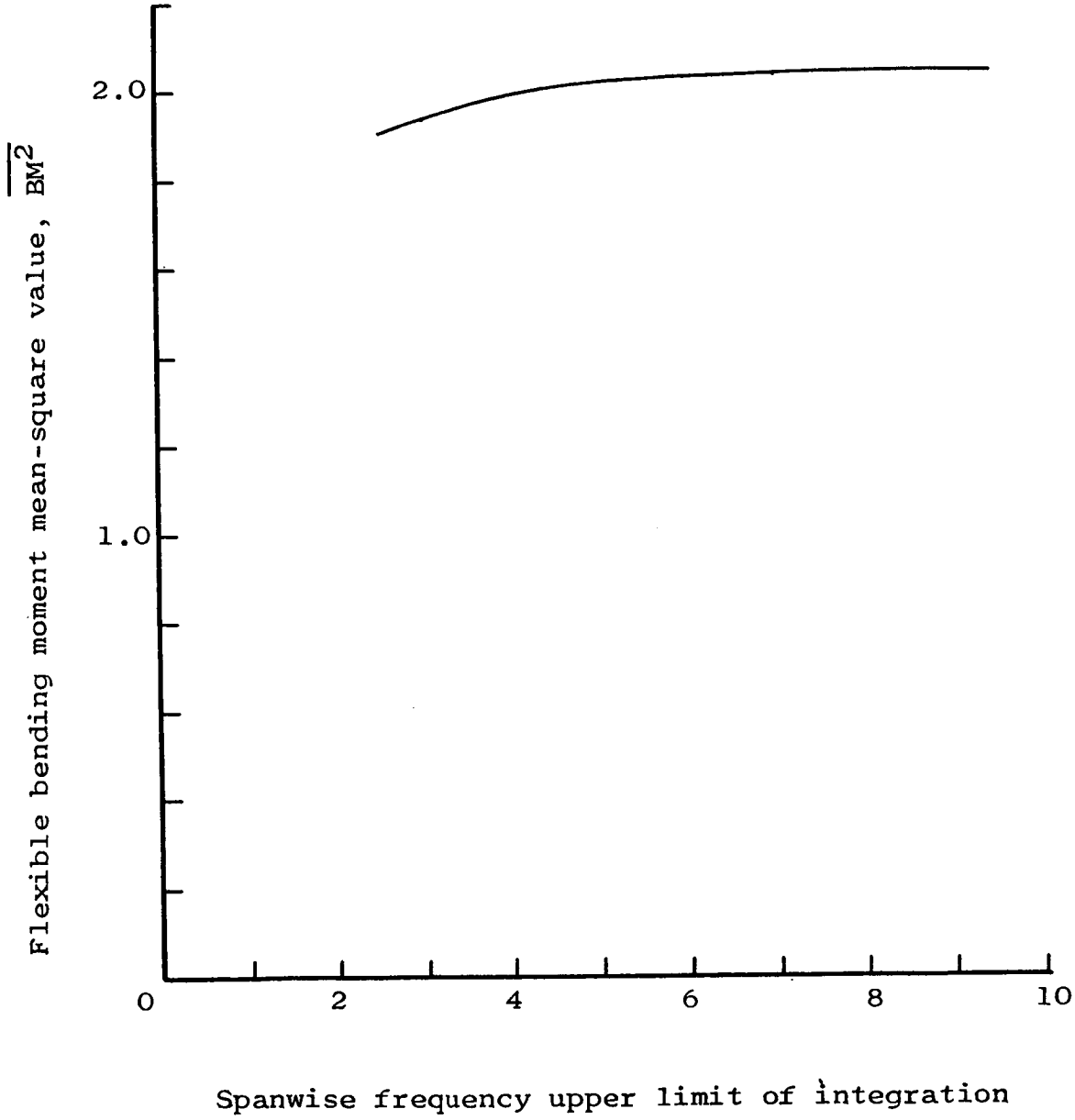

Figure 24.- Modified strip analysis flexible bending moment mean square value variation with upper limit of integration (mass ratio = 0.585, b/L = 0.5).